

## ABSTRACT

ALNASER, MAHMUD J. Polarimetric Vector Receivers for CDMA Multipath Signals. (Under the direction of Prof. Brian L. Hughes.)

In this dissertation, we investigate the design and performance of receivers for vector antenna systems on multipath fading channels. Vector antennas are co-located antennas that can detect or excite more than one component of the received electromagnetic field. We study the design and implementation of vector antenna receivers for code-division multiple-access (CDMA) signals in the presence of multipath signal propagation. The use of antenna arrays in CDMA systems has been widely investigated in wireless communications, due to the significant gain of capacity relative to a single antenna systems. Multiuser space-time detection schemes which utilize antenna arrays (e.g., the beamformer-RAKE) have also been proposed for CDMA systems to exploit space and time and to combat multiuser interference. Most of this previous work has focused on the use of linear arrays of single- or dual-polarized antennas, which typically measure one or two components of the received electromagnetic (EM) field in several locations. The use of vector antennas (arrays of antennas that measure multiple components of the EM field in one location) for CDMA systems has not been addressed in the literature.

We first consider space-time receivers for a single-user, direct-sequence CDMA (DS-SS) system. Using electromagnetic theory, we derive a channel model that describes joint multipath propagation of the electric and magnetic fields in space and time. Using this model, we derive vector antenna receivers which are optimal for various performance criteria, such as maximum-likelihood (ML), minimum mean-square error (MMSE), matched filter (MF), and zero-forcing or decorrelator (ZF). The performance of these receivers is measured in terms of the bit-error-rate (BER) as a function of the signal-to-noise ratio (SNR). Comparing the BER for various number

of antennas, we find that the diversity improvement obtained, for a fixed number of multipaths  $L$ , increases with the number of elements in the vector antenna. For example, three mutually orthogonal electric dipoles (known as a tripole antenna) offers more diversity gain than a dual-polarized antenna. Similarly, a six-element vector antenna provides more diversity gain than a tripole antenna.

Next we compare the performance of multiuser detection schemes for vector antennas and a uniform linear array (ULA). A space-time MMSE (ST-MMSE) receiver is derived for  $n$  users and  $L$  discrete multipath fading channels, assuming that the multipath coefficients and spreading codes of all users are known at receiver. When channel information is not available, an adaptive implementation of the MMSE receiver is considered, in which training data bits are used to estimate the channel coefficients. Simulations of BER suggest that the vector antenna achieves significantly higher diversity gain than the ULA for a fixed number of multipaths. We next consider vector antennas employed at the base station for a DS-SS systems with  $M$ -ary orthogonal modulation. Here  $M$ -ary orthogonal modulation is used at mobile station for data transmission and a beamformer-RAKE receiver is implemented at base station. The capacity in terms of the number of users as a function of number of antennas employed at the base station is evaluated. Simulations suggest that a vector antenna can achieve a higher capacity than a uniform linear array (ULA) at given SNR.

For multi-input multi-output (MIMO) channels, spatial multiplexing schemes such as V-BLAST and adaptive transmission are considered. Using V-BLAST, the BER of the normalized empirical data measurement for a single tripole antenna (i.e. three mutually orthogonal dipoles) at the transmitter and the receiver is simulated. An adaptive transmission scheme for the same antenna system is also simulated.

Finally, we investigate and analyze the signal-to-interference plus noise ratio (SINR)

of minimum variance (MV) beamforming at the receiver. An expression for the SINR is derived as a function of the direction-of-arrival (DOA) and polarization of both the desired signal and one interference signal in a multipath fading channel. Furthermore, the beampattern of the vector antenna steered toward the DOA is compared with a ULA. The vector antenna beampattern shows maximum gain in direction of desired signal while ULA have many side loops in other directions.

**Polarimetric Vector Receivers for CDMA Multipath Signals**

by

**Mahmud J. Al-Naser**

A dissertation submitted to the Graduate Faculty of  
North Carolina State University  
in partial fulfillment of the  
requirements for the Degree of  
Doctor of Philosophy

**Electrical Engineering**

Raleigh

2006

**Approved By:**

---

Dr. Gianluca Lazzi

---

Dr. Hamid Krim

---

Dr. Brian L. Hughes  
Chair of Advisory Committee

---

Dr. Stephen Schecter

*To my family*

## **Biography**

Mahmud Jawad AL-Naser received his B.S. degree in Electrical Engineering from University of Miami in January 1989 and in 1997, he received his Master degree in Electrical Engineering from Kuwait University. In January 2000, he started working toward his PhD degree in Electrical Engineering at North Carolina State University under the guidance of Prof. Brian Hughes.

## Acknowledgements

I would like to express my sincere thanks to Prof. Brian Hughes, who has enlightened me to knowledge and learning. Through his constructive discussion and positive feedback, he has helped me greatly in research. A man is known by the company he keeps.

I also would like to thank the committee members, Dr. Gianluca Lazzi, Dr. Hamid Krim and Dr. Stephen Schecter for their helpful remarks.

I am very proud of my wife and family support during my research years. Also I appreciate the support of my friends.

I would like to thank Xinying Yu, Anand Konanur, Chris Mary James and Ajith Kamath for their willingness to help and support.

Finally I would like to thank Kuwait Government (PAAET) for sponsoring my research.

# Contents

<b>List of Figures</b>	<b>vii</b>
<b>1 Introduction</b>	<b>1</b>
1.1 Diversity . . . . .	2
1.1.1 Fading Channels . . . . .	2
1.1.2 Diversity Techniques . . . . .	5
1.1.3 Diversity Combining . . . . .	6
1.1.4 Evolution of Wireless Communications . . . . .	6
1.2 Code-Division Multiple-Access . . . . .	7
1.3 Antenna Arrays . . . . .	10
1.3.1 Space-Time Processing . . . . .	13
1.3.2 Space-Time CDMA Receivers . . . . .	14
1.4 Multiple-Input Multiple-Output Systems . . . . .	14
1.4.1 Capacity . . . . .	15
1.4.2 Spatial Multiplexing . . . . .	16
1.5 Contribution of this Work . . . . .	16
<b>2 Beamforming Techniques For Vector-Antenna Receivers</b>	<b>20</b>
2.1 Introduction . . . . .	21
2.2 Channel Model . . . . .	23
2.3 Space-Time Receivers . . . . .	27
2.3.1 Maximum-Likelihood Receiver . . . . .	28
2.3.2 Linear Suboptimal Space-Time Receivers . . . . .	29
2.3.3 Decorrelating Detector (DD) . . . . .	30
2.3.4 Minimum Mean-Square Error (MMSE) . . . . .	31
2.3.5 Matched-Filter Receiver (MF) . . . . .	32
2.4 Numerical Examples . . . . .	33
2.5 Conclusions . . . . .	38

<b>3</b>	<b>Multiuser Detection for Vector Antennas</b>	<b>40</b>
3.1	Introduction . . . . .	41
3.2	A Space-Time MMSE Detector . . . . .	43
3.2.1	Space-Time Multiuser Detector . . . . .	45
3.2.2	Adaptive ST-MMSE Detector . . . . .	47
3.3	Simulation Results . . . . .	48
3.4	M-ary Orthogonal Modulation . . . . .	52
3.4.1	Adaptive Beamforming for CDMA . . . . .	53
3.4.2	System Model . . . . .	55
3.4.3	BER Analysis . . . . .	62
3.4.4	Numerical Results . . . . .	66
3.5	Conclusions . . . . .	69
<b>4</b>	<b>MIMO Systems based on Vector Antennas</b>	<b>71</b>
4.1	V-BLAST . . . . .	72
4.1.1	Transmission Algorithm . . . . .	73
4.1.2	Simulation . . . . .	75
4.2	Channel Inversion . . . . .	77
4.2.1	Simulation . . . . .	79
4.3	Conclusions . . . . .	80
<b>5</b>	<b>SINR Limitations of Vector Antenna Arrays</b>	<b>82</b>
5.1	Introduction . . . . .	83
5.2	Channel Model . . . . .	85
5.3	Beampattern of Certain Vector Antennas . . . . .	87
5.4	Numerical Results . . . . .	88
5.5	Conclusions . . . . .	90
<b>6</b>	<b>Conclusions</b>	<b>96</b>
	<b>Bibliography</b>	<b>99</b>

# List of Figures

1.1	Multipath fading environment . . . . .	4
1.2	Multipath RAKE Receiver . . . . .	11
2.1	A 3-element vector antenna consisting of two electric dipoles and a loop ( Courtesy of Dr. Lazzi [42]) . . . . .	22
2.2	The orthonormal triad indicating the spherical coordinates $(r, \theta, \varphi)$ and the unit vectors $\mathbf{u}_r$ , $\mathbf{u}_\theta$ and $\mathbf{u}_\varphi$ . . . . .	24
2.3	ML, MMSE, DD and MF-receivers for the “tripole” antenna (3-dipole) for $L=2$ equal-energy multipaths. . . . .	32
2.4	BER of the MF receiver for the “tripole” antenna (3-dipoles) versus dual-polarized antenna (2-dipoles) for $L = 1, 2, 4, 8$ multipaths. . . . .	35
2.5	BER of the MF receiver for the “tripole” antenna versus the 3-element vector in Fig. 2.1 for $L = 1, 2, 4, 8$ multipaths. . . . .	37
2.6	BER of the MF receiver for a 6-element vector antenna with $L = 1, 2, 4, 8$ multipaths. . . . .	38
3.1	BER of ST-MMSE and ST-DD for a single tripole antenna with $L = 2, 4, 8$ multipaths and $n = 5$ users. . . . .	49
3.2	BER of adaptive ST-MMSE for a single tripole antenna with $L = 2, 4$ multipaths, $n = 5$ users, and adaptive step size $\mu = 0.001$ . . . . .	50
3.3	BER of ST-MMSE for a single tripole antenna (3-elements) and a linear antenna array (3-elements) for $L = 2, 4$ multipaths and $n = 5$ users. . . . .	51
3.4	Receiver block diagram . . . . .	59
3.5	Beamforming and noncoherent RAKE . . . . .	61
3.6	BER of 3- and 6-element vector antennas compared with linear antenna arrays with 3 and 6 elements for $L=3$ multipaths. . . . .	64
3.7	BER of the tripole and the 2-dipole and loop vector antenna from [42] for $L=3$ multipaths. . . . .	65
3.8	BER of a linear array of 3 tripoles and a 9-element ULA for $L=3$ multipaths. . . . .	66
3.9	BER of tripole antenna for $\alpha = 0.1$ and 1 and $L=3$ multipaths. . . . .	67

4.1	Measured and theoretical BER for a V-BLAST system with tripoles at the transmitter and receiver. . . . .	76
4.2	Measured BER for a V-BLAST system with tripoles at the transmitter and receiver for all 46 channel realizations. . . . .	77
4.3	Measured and theoretical BER for a BPSK with channel Inversion (CI) for tripole at the transmitter and dual-polarized antenna at receiver. . . . .	79
4.4	Measured and theoretical BER for a Channel Inversion (CI) for tripole at the transmitter and 2-element antenna at receiver. . . . .	80
5.1	The expected SINR as a function of the desired signal polarization, $0 \leq \alpha_d \leq 1$ , for a nearly linearly polarized interference ( $\alpha_u = 0.1$ ). . . . .	90
5.2	The expected SINR as a function of the desired signal polarization, $0 \leq \alpha_d \leq 1$ , for an interference with equal energy in the horizontal and vertical polarizations ( $\alpha_u = 1$ ). . . . .	91
5.3	The expected SINR as a function of the interference signal polarization, $0 \leq \alpha_u \leq 1$ , for a nearly linearly polarized desired signal ( $\alpha_d = 0.1$ ). . . . .	92
5.4	The expected SINR as a function of the interference signal polarization, $0 \leq \alpha_u \leq 1$ , for an desired signal with equal energy in the horizontal and vertical polarizations ( $\alpha_d = 1$ ). . . . .	93
5.5	Beampattern of the 6-element vector antenna . . . . .	94
5.6	Beampattern of the 6-element ULA with spacing $d = \lambda/2$ . . . . .	95

# Chapter 1

## Introduction

Wireless communications technology is developing rapidly to meet the increasing demand for high quality mobile services. The wireless channel is a challenging communications medium since it is plagued by major impairments, such as multipath fading and spreading of the transmitted signal. Advanced signal processing techniques can significantly reduce these impairments, leading to improved capacity and better quality of service. Two particular signal processing techniques, array processing and interference cancelation, have proved to be very effective in improving the performance of commercial cellular systems.

The challenge in wireless communication arises in the reliable design of transmitter and receiver architectures that have low complexity and at the same time ensure good quality of communication. The need for high data rate, mobility and security on the one hand, and the simplicity of transmitter-receiver architecture on the other, has led to the development of a variety of simple communication techniques to improve performance over wireless channels. In this chapter, we briefly overview some of the most important techniques for coping with fading: diversity, code-division multiple-access, array processing and multiple-input multiple-output systems.

## 1.1 Diversity

### 1.1.1 Fading Channels

The performance of a wireless channel depends on both large-scale and small-scale fading effects. The large-scale effects occur when there is separation of a few kilometers between the transmitter and receiver. As the mobile moves a large distance away from the transmitter, the received signal average power decreases. The average power can also be reduced by shadowing from large structures such as buildings. These changes in average received power are called large-scale fading. However, the rapid fluctuations of the received signal strength over short distances (a few wavelengths) is termed small-scale (or multipath) fading. Since large-scale fading does not lead to rapid variations of received signal strength, it is not generally as serious an impairment as small-scale fading.

One of the main challenges to reliable wireless communications is multipath fading, which arises in many different environments, such as indoor and cellular radio communications. Multipath fading is caused by reflection, diffraction and scattering of the transmitted signal. These multipath signals can add constructively or destructively at the received antenna, resulting in a received signal with a time-varying amplitude and phase which is called fading (see Fig. 1.1).

For a large number of scatterers, the central limit theorem implies that the impulse response of a fading channel can be modeled as a zero-mean complex-valued Gaussian random process. Since the envelope of this process is Rayleigh distributed, the channel is called a Rayleigh fading channel. The Rayleigh distribution has a probability distribution function (pdf)

$$f(a) = \begin{cases} \frac{2a}{\sigma^2} \exp\left(-\frac{a^2}{\sigma^2}\right), & a \geq 0; \\ 0, & a < 0. \end{cases} \quad (1.1)$$

where  $a$  is the envelope of the received signal and  $\sigma^2$  is the time-averaged power of the received signal.

Multipath propagation can cause the transmitted signal to spread in time, frequency and space. The time spread leads to several replicas of the transmitted signal arriving at the receiver with different time delays, which is characterized by the delay spread of the signal. The time dispersion, which is the delay spread caused by multipath, will affect the degree to which the received signal fading varies with frequency. If the delay spread is small compared to the inverse signal bandwidth, then all frequencies present in the transmitted signal fade in the same way. This is called flat fading. If delay spread is large compared to the inverse signal bandwidth, then the amplitude and phase of the channel vary significantly over the signal bandwidth, which results in frequency-selective fading. The large delay spread will also result in intersymbol interference (ISI), which requires more complex signal processing techniques at the receiver.

The frequency spread refers to the changes occurring over time due to movement of objects between the transmitter and receiver, or objects surrounding the receiver, causing a Doppler shift in the received multipaths. The coherence time of the channel  $T_c$ ,  $T_c \simeq \frac{1}{f_d}$  ( $f_d$  is the channel Doppler bandwidth) is a measure of frequency dispersion in the channel. Frequency dispersion causes the signal amplitude and phase to vary with time. Slow fading occurs when the symbol duration is less than the coherence time and fast fading when the symbol time is greater than the coherence time. For slow fading, several successive symbols tend to fade simultaneously which results in burst errors.

The spatial spread refers to signal changes caused by the spreading of the multipaths in space at the receiver. In general, the signal amplitude and phase depend on the location of the received antenna. The spatial spreading can be character-

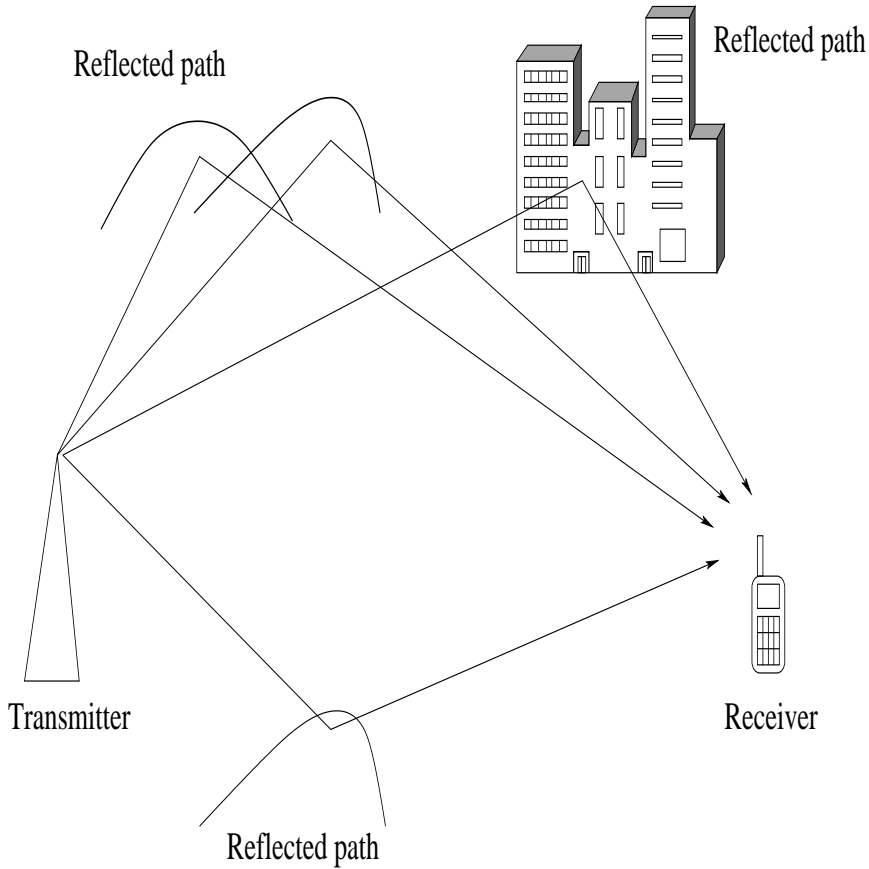


Figure 1.1: Multipath fading environment

ized by the coherence distance  $d_c$  between antenna elements, which is the minimum distance required between antennas in order to obtain independently fading amplitudes. A larger spread typically means a smaller  $d_c$ , and thus more diversity paths are available at the receiver.

In order to combat the effects of channel variations and multipath fading, diversity techniques are often used at the transmitter or receiver or both. In principle, diversity techniques provide the receiver with independently faded replicas of the same transmitted signal.

### 1.1.2 Diversity Techniques

The aim of diversity techniques is to combine multiple independently fading copies of the transmitted signal in order to reduce the overall probability of a deep fade. Diversity techniques generally exploit some form of signal dispersion, which results either from multipath propagation or else is deliberately introduced by the transmitter. These techniques are generally classified by the type of dispersion they exploit:

- Frequency diversity: Exploits time dispersion (frequency-selective fading). Frequency diversity can be exploited by spread-spectrum techniques or forward error correction (FEC) in conjunction with multicarrier modulation. In spread spectrum, the signal bandwidth exceeds the coherence bandwidth of the channel resulting in resolvable multipath signals which can be exploited by a RAKE receiver.
- Time diversity: Exploits frequency dispersion caused by Doppler shifts (time selective fading). Interleaving, FEC and automatic repeat requests are forms of time diversity.
- Space diversity: Exploits the dispersion of the signal in space by employing a multi-antenna system. The spatial separation between antennas is usually chosen so that diversity branches experience uncorrelated fading. This diversity technique is attractive since it does not require extra bandwidth. Other forms of diversity such as angle spread and polarization diversity are another form of space diversity. For polarization diversity, vertical and horizontal polarization are detected at the receiver and transmitter, where scatterers tend to affect the polarization state and result in different polarized plane waves at the receiver.

### 1.1.3 Diversity Combining

The techniques used at the receiver to combine multiple received signals from diversity branches are known as diversity combining. There are three main combining methods :

- Maximal-Ratio Combining (MRC): Diversity branches are weighted with respect to their complex fading path gains and then added. In the absence of interference, MRC is an optimal combining scheme in the sense of minimizing the probability of error in the presence of i.i.d. Gaussian noise.
- Equal-Gain Combining (EGC) : The diversity branches are equally weighted and combined. This scheme is less complex than MRC since the branch weights are not required at receiver. This scheme is useful for modulation techniques having equal energy symbols (e.g.,  $M$ -ary phase-shift keying).
- Selection Combining (SC) : Selecting from  $L$  branches the one with largest signal-to-noise ratio (SNR) value at the receiver.

### 1.1.4 Evolution of Wireless Communications

Mobile communication began with the first generation (1G) in the 1980s which used frequency-division multiple-access (FDMA), in which the channel is divided into disjoint frequency bands and each user is assigned one fixed band. Since analog systems were not able to cope with the increasing demand for wireless services, in the second-generation (2G) systems, analog modulation was replaced by digital modulation, which can achieve higher bandwidth and power efficiency. The use of error-control coding and advanced signal processing methods make digital systems more reliable and robust to changing channel conditions. In 1990, a combination of time-division multiple-access (TDMA) and FDMA was introduced for second-generation

systems. In the late 1990s, another multiple-access system called direct-sequence code-division multiple-access (DS-CDMA) was introduced. In DS-CDMA, all users share the same frequency spectrum, but each user is assigned a unique spreading code. Third-generation (3G) systems also provide support for multimedia services, such as the Internet and data communication [2]. Fourth-generation (4G) systems aim to integrate cellular communication with wireless local area networks (WLAN), thus providing access to multimedia services such as voice, data and video.

The main focus of this dissertation is DS-CDMA systems, which are described in the next section.

## 1.2 Code-Division Multiple-Access

In a multiple-access system, many users share a common communication channel. One of the most widely used multiple-access techniques is code-division multiple-access (CDMA), in which users transmit in the same frequency band and are distinguished at the receiver by unique spreading codes. The spreading codes can be categorized as either orthogonal codes (such as Walsh codes) or non-orthogonal codes. The Shift Register, Gold and Kasami codes are considered to be non-orthogonal. These four types of code are defined as follows:

- Shift Register codes: These codes [3] are generated by an  $m$ -stage digital linear shift register with feedback (LFSR) and the output is periodic with length  $j = 2^m - 1$ .
- Gold codes: These codes [4] are generated by modulo-2 addition of two  $m$ -shift register codes and characterized by a low cross-correlation which makes them attractive for interference cancellation.

- Kasami codes: Like Gold codes, Kasami codes are generated from two LFSR sequences; however, the second sequence is derived from the first by decimating it and repeating  $N$  times.
- Walsh-Hadamard codes : These codes [1] are generated by using Hadamard sequences. Each Walsh code consist of a 64-ary Hadamard sequence. These codes are used in the downlink to specify a particular user and in the uplink to modulate information.

For an  $n$  user system, each of the  $i$ -th user's spreading code waveform can be given by

$$c_i(t) = \sum_{r=1}^{N_c} c_{i,r} p(t - rT_c)$$

where  $p(\cdot)$  is a rectangular chip pulse and the code sequence  $c_{i,r}$  of chip elements  $(-1, +1)$  which are assumed to be independent, identically distributed random variables with equal probability. The spreading code  $c_i(t)$  is periodic with period equal to the processing gain  $N_c = \frac{T}{T_c}$ , where  $T$  and  $T_c$  are the information bit duration and chip duration, respectively. The transmitted signal is obtained by multiplying the data by the spreading code waveform. The spreading code waveform has higher bandwidth than the data signal, which results in a higher transmission bandwidth. The transmitted signal of the  $i$ -user can be written as

$$S_i(t) = \sum_{m=1}^M \sqrt{P_i} b_i(m) c_i(t - mT)$$

where  $P_i$  denotes the power of the  $i$ -th user's signal and  $b_i(m)$  is the sequence of transmitted information bits for the  $i$ -th user. For frequency-selective multipath fading, the channel impulse response can be written as a linear filter [1]

$$h(t) = \sum_{\ell=1}^L a_\ell e^{-j\theta_\ell} \delta(t - \tau_\ell)$$

where  $L$  is the number of resolvable multipaths and  $a_\ell, \theta_\ell, \tau_\ell$  are the amplitude, phase, and delay of the  $\ell$ -th path. Without loss of generality, we consider  $\tau_1 = 0$  to be the reference path and order the delays  $\tau_1 < \tau_2 \dots < \tau_L$ .

In a multiuser system, the signal detected at the receiver is the superposition of the signal of all the users and noise

$$Y(t) = \sum_{i=1}^n \sum_{\ell=1}^L \sqrt{P_i} \alpha_{i,\ell} S_i(t - \tau_{i,\ell}) + n(t)$$

where  $\alpha_{i,\ell} = a_\ell e^{-j\theta_\ell}$  is a complex Gaussian random variable and  $n(t)$  is complex zero-mean AWGN noise with variance  $\sigma^2$ .

To counter the effects of multipath fading the receiver is equipped with  $L$  branches where each branch is synchronized to a distinct multipath component. At each branch or finger, the received signal is despread at one chip delay and therefore the energy of one multipath component is captured and other multipath components arriving at different delays will be suppressed. Each of these fingers are referred to as RAKE fingers. This type of receiver is known as a RAKE [43]. Assuming the spreading codes, time delays and channel coefficients are known at the receiver, then each RAKE finger is multiplied by the path gain of the corresponding multipath component. The post-correlation signal of the first user for the  $m$ -th bit and  $\ell$ -th multipath is given by [47]

$$\begin{aligned} \mathcal{Y}_{1,\ell}(m) &= \frac{1}{\sqrt{T}} \int_{(m-1)T+\tau_{1,\ell}}^{mT+\tau_{1,\ell}} c_1^*(t - mT - \tau_{1,\ell}) Y(t) dt \\ &= \sqrt{TP_1} \alpha_{1,\ell} b_1(m) + i_{1,\ell} + n_{1,\ell} \end{aligned}$$

where  $c_1(t - \tau_{1,\ell})$  is the spreading code of the first user delayed by  $\tau_{1,\ell}$ ,  $b_1(m)$  is the  $m$ -th data bit for the first user, and  $n_{1,\ell}$  is the thermal noise. The multiple-access interference (MAI) contributed from other users and self-interference is given by

$$i_{1,\ell} = \sum_{k=1, k \neq \ell}^L \sqrt{P_1} \alpha_{1,k} I_{1,\ell,1,k} + \sum_{i=2}^n \sum_{k=1}^L \sqrt{P_i} \alpha_{i,k} I_{1,\ell,i,k}$$

where the first term corresponds to self-interference due to multipath, and the second term is due to multiple-access interference and

$$I_{1,\ell,i,k} = \frac{1}{\sqrt{T}} \int_{(m-1)T+\tau_{1,\ell}}^{mT+\tau_{1,\ell}} b_i(m)c_i(t-mT-\tau_{i,k})c_1^*(t-mT-\tau_{1,\ell})dt.$$

Now on each RAKE finger, the corresponding multipath component is weighted and multiplied by the conjugate of the fading path gain. The combining of the RAKE output is referred to as maximal-ratio combining (MRC), since it maximizes the signal-to-noise ratio (SNR) at the combiner output (see Fig. 1.2). However, this form of combining is not optimal in the presence of MAI. Therefore, the performance is degraded when MAI is high at the receiver [1].

In order to suppress MAI, more complex receivers have been derived. For DS-SS-CDMA systems, a minimum-mean square-error (MMSE) receiver has been proposed by Madhow and Honig [70], and a decorrelator receiver has been proposed by Zvonar and Brady [9].

### 1.3 Antenna Arrays

Spatial processing with antenna arrays can significantly improve the performance of wireless communications systems [22, 23, 24]. The promising performance of antenna arrays have led researchers to develop various new array signal processing techniques to utilize the signals induced on different antenna elements. Array signal processing can be considered as spatial filtering where gain is maximized in the direction of the desired signal and interference from other directions is nulled.

The increase in wireless services and number of users in multipath environments has resulted in an increase in interference in both the spatial and temporal domains. For antenna arrays, the ability to steer nulls in the direction of the interference enables the receiver to increase the gain in the direction of the desired signal and thus increases

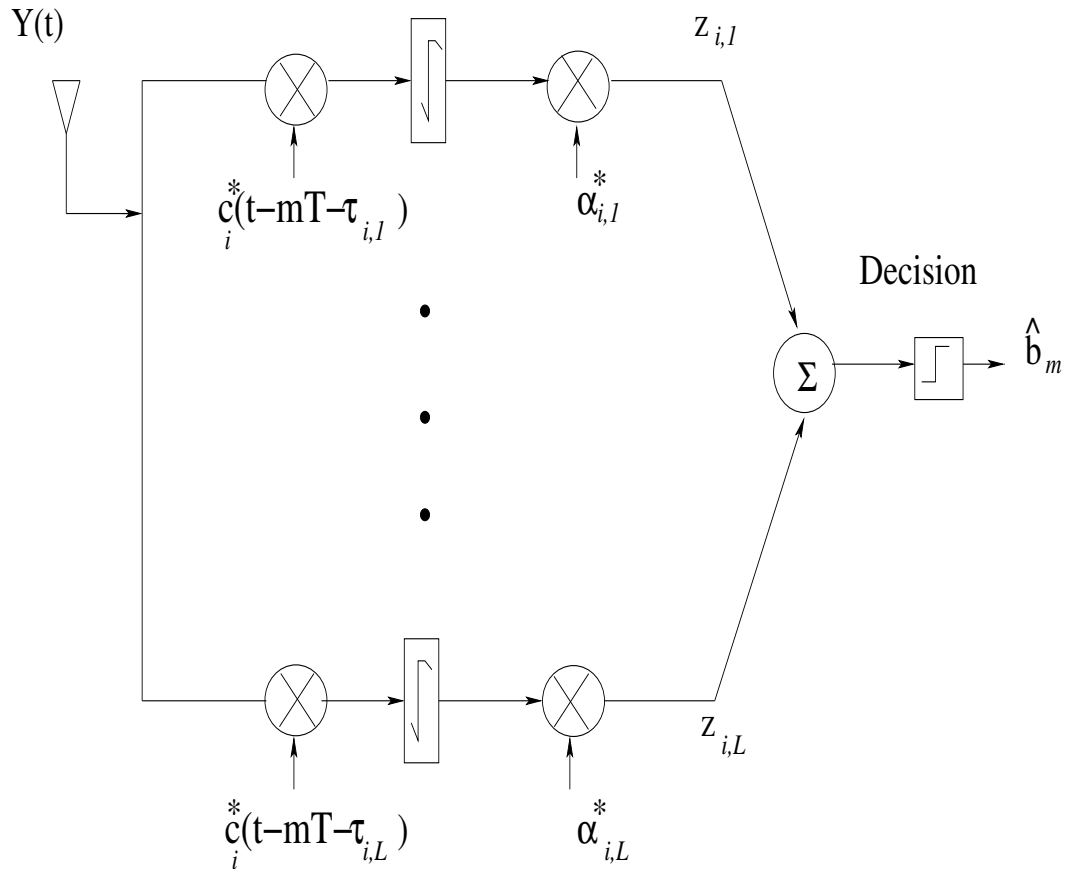


Figure 1.2: Multipath RAKE Receiver

the signal-to-interference-plus-noise ratio (SINR). Antenna array performance may be optimized by adapting the gains and phases of antenna elements. Beamforming with antenna arrays has become a good solution for canceling interference. Since multipath signals usually vary with time, the receiver needs to adjust to these changes. Consequently, adaptive beamforming will often enhance the quality of the received signal.

Antenna arrays using adaptive beamforming techniques have been investigated by Bogachev and Kiselev [7] for a flat fading channel with a single user and later by Winters [8], who extended it to the multiuser case. This work showed that optimum multiuser combining can outperform MRC when MAI is present.

Several criteria have been considered to optimize the beamforming weights, such as maximum likelihood (ML), MMSE, and maximization of the signal-to-interference-plus-noise ratio (MSINR). The derivation of adaptive forms of the ML, MMSE and MSINR beamformers are presented in [47]. For each of these criteria, the optimum weights are scalar multiples of one another, since MMSE and ML for Gaussian measurements result in the same estimator [10]. Also, all three beamforming techniques can be used either with a reference signal or training data bits.

In the adaptive antenna array, direction-of-arrival (DOA) estimation techniques achieve improvement in the quality of the signal at the demodulator. Several algorithms for directional-finding have been developed in the literature, such as MUSIC (multiple signal classification), ESPRIT (estimation of signal parameters via rotational invariant techniques) and WSF (weighted subspace fitting) [11, 12, 13, 14, 15] combined with optimum beamforming. These are considered to be eigenstructure methods. Nevertheless, the complexity of the propagation channel and the large number of signals (users) received will limit application of these techniques. For mobile communications, where the number of users exceeds the number of antennas, Naguib [47] has proposed a code-filtering approach that requires an estimate of the channel covariance of the received signals.

For adaptive implementation, the least-mean-squared (LMS) algorithm, proposed by Widrow *et al* [16], is a computationally simple algorithm to adaptively calculate the weight vector that satisfies the MMSE beamforming criterion. LMS is widely used in practice and has been the subject of considerable research. There are different variations of the LMS algorithm: the constrained/unconstrained LMS [17, 18, 19, 20, 21]; the sign algorithm LMS [25]; and the normalized LMS [26, 27].

A simulation study of adaptive antenna arrays with co-channel interference has shown the recursive least-squares algorithm (RLS) algorithm to be superior to the

LMS and the SMI (sample matrix inversion) algorithms for flat fading in a mobile communications environment [28].

### 1.3.1 Space-Time Processing

The overwhelming majority of papers on antenna arrays for fading channels deal with linear arrays of dipoles antennas which are separated by a distance  $d > \lambda/2$  ( $\lambda$  is the wavelength) which is sufficient to ensure that fading signals received on different elements are uncorrelated. When multiple users are present, then interference tends to be spatially and temporally distributed, so that processing the received signal in one dimension (e.g., the time domain) is suboptimal. In this case the optimal beamforming weights are a function of the signal strengths of the desired and undesired signals, their directions-of-arrival and their covariances. As a result, the optimal receiver should exploit the space and time domains in order to reliably estimate the desired data and simultaneously suppress the interference. Therefore, space-time processing can reduce multiple-access interference and intersymbol interference (ISI).

The propagation conditions present in wireless communication will also require advanced processing techniques to estimate the desired channel parameters. For example, in a rich scattering environment, the angle-of-arrival will often have a large angle spread, resulting in uncorrelated fading at antenna elements. Consequently, a scalar representation of the fading channel will not adequately describe the multipath component. Instead, these components are generally modeled in the literature by random vectors (e.g., see [31, 32, 33]) and statistics signal processing techniques are needed at the receiver to effectively use the space-time domain to capture the necessary information, suppress interference and therefore enhance performance.

### 1.3.2 Space-Time CDMA Receivers

In DS-CDMA systems, the autocorrelation of spreading codes can be exploited by the receiver to resolve multipath signals which are separated in time. Using antenna arrays combined with DS-CDMA enables the receiver to distinguish signals which are separated in either space or time. This combination is currently used in the second-generation cellular standard IS-95, which employs DS-CDMA modulation together with antenna arrays at the base station.

Several space-time receivers have been proposed specifically for CDMA in the presence of multipath fading. A receiver consisting of a beamformer combined with a RAKE receiver was proposed in [34, 36]. Performance studies show that this space-time receiver can support more users at the base station than a conventional temporal RAKE receiver. For a single-user system, Naguib [47] proposed the space-time matched receiver for frequency-selective Rayleigh fading and derived an ML receiver for DS-CDMA signals.

## 1.4 Multiple-Input Multiple-Output Systems

Over the last decade, research on multiple-input multiple-output (MIMO) systems have shown that deploying multiple antennas at both the transmitter and receiver can significantly improve the capacity of wireless channels with multipath fading. In particular the seminal work of Telatar [37] and Foschini and Gans [78] has shown that, at high signal-to-noise ratios and in the presence of rich multipath, capacity grows linearly with the minimum of the number of transmit and receive antennas. In recent years, MIMO technologies have been incorporated into several new and emerging wireless standards, such as wideband CDMA, IS-95 and IEEE 802.11n.

### 1.4.1 Capacity

The benefits of MIMO systems over conventional single-input single-output (SISO) systems are often illustrated by considering the ergodic capacity. From information theory [1], the capacity of a communications channel is given by

$$C = \max_{p(\mathbf{x})} I(X; Y),$$

where  $X$  and  $Y$  are random variables representing the channel input and output, respectively, and  $I(X; Y)$  is the mutual information between  $X$  and  $Y$ . The mutual information is maximized over all possible probability distributions  $p(\mathbf{x})$  of  $\mathbf{x}$ . For  $t$  transmit and  $r$  receive antennas the discrete time baseband equivalent channel model is given by

$$\mathbf{y} = H\mathbf{x} + \mathbf{n}$$

where  $H$  is an  $r \times t$  complex channel matrix with Gaussian-distributed elements having zero mean and unit variance denoted as  $\mathcal{CN}(0, 1)$ . The noise  $\mathbf{n}$  is modeled as i.i.d. circularly symmetric complex Gaussian entries with zero mean and variance  $\sigma^2$ , denoted by  $\mathcal{CN}(0, \sigma^2)$ .

If  $H$  is known at the receiver, the ergodic capacity is achieved with i.i.d. Gaussian inputs at the transmitter and is given by [37]

$$C(\rho) = \mathbb{E}_H \log \det(I_r + (\gamma_r/t)HH^\dagger)$$

where  $\gamma_r$  is the signal-to-noise power ratio (SNR) at each receive antenna,  $I_r$  denotes the identity matrix of size  $r$ ,  $\log$  is the base-2 logarithm,  $\mathbb{E}_H$  denotes the expectation with respect to the distribution of  $H$ ,  $\det$  denotes the determinant operation, and  $H^\dagger$  denotes the conjugate-transpose of  $H$ .

### 1.4.2 Spatial Multiplexing

MIMO systems can achieve high spectral efficiencies by transmitting multiple, resolvable data streams in the same bandwidth. This approach is known as “spatial multiplexing” or BLAST (Bell Labs Layered Space-Time) [77]. In vertical BLAST (V-BLAST), data streams are demultiplexed and transmitted on an array of  $M_t$  antennas. At the receiver, these data streams are detected by  $M_r \geq M_t$  using sequential nulling to eliminate co-channel interference. The main advantage of this system is that data rates increase by a factor  $M_t$ . Wolniansky *et al* [79] have shown that V-BLAST can achieve a spectral efficiency of 20-40 bps/Hz at SNR from 24 dB to 34 dB in rich scattering environments.

## 1.5 Contribution of this Work

We now give an overview of the topics considered in this work and an outline of the main ideas and approaches used.

In cellular communications, base stations typically employ uniform linear arrays (ULA) which consist of a collection of equally spaced dipoles. These dipoles are usually placed such that they respond to vertical or horizontal polarization. Since dipoles sample only one component of the electric field, some potentially useful data may be neglected at the receiver.

In this work, we investigate the use of antenna elements that are capable of measuring multiple components of the electromagnetic field in one location. These elements, called vector antennas, are often constructed by combining up to three co-located electric dipoles with up to three magnetic loops. The use of vector antennas to estimate direction-of-arrival in line-of-sight propagation has been extensively studied [50, 53, 55]. However, the applications of these antennas to wireless communication

has received considerably less attention.

In Chapter 2, we consider the application of vector antennas to a CDMA system with multipath fading. We first present a model that describes the complete electromagnetic field detected at the receiver. Using this model, we derive maximum-likelihood (ML), minimum mean-squared error (MMSE), matched filter (MF) and decorrelator space-time receivers for the case of a single vector antenna in multipath fading. We further plot the bit-error-rate (BER) as a function of signal-to-noise ratio (SNR) for various numbers of antennas. These plots show that vector antennas achieve larger diversity gains than conventional single-antenna systems. We also compare and contrast the performance of several types of vector antennas: a dual-polarized antenna comprising two orthogonal dipoles; a “tripole” antenna that consists of three mutually orthogonal dipoles; and an ideal vector antenna capable of measuring all six components of the incident electromagnetic (EM) field. These results suggest that vector antennas with more elements can achieve greater diversity gains, even in the presence of sparse multipath.

In Chapter 3, we extend the analysis of Chapter 2 to the multiuser scenario. We consider a fading multipath channel that is shared by multiple transmitters, who communicate to a common receiver which employs a vector antenna. Since interference from other users can limit the capacity of wireless communication, using a vector antenna at the receiver provides more signaling dimensions which can be used to suppress interference and therefore increase capacity. We present a space-time model in which multiple users transmit to a common receiver via  $L$  discrete multipath components. Using this model, we consider the use of a linear space-time MMSE multiuser detector at the receiver. We further consider an adaptive implementation of this receiver suitable when the channel coefficients are not available at the receiver. We use the LMS algorithm, which uses training bits to learn the channel. A decorrelator

receiver for the multiuser system is also implemented at the receiver. We compare the performance of the vector antenna receiver with a ULA having the same number of dipoles. These results suggest that vector antennas can often achieve higher diversity gains than ULAs, even in the presence of multiple interfering users. Finally, we present  $M$ -ary orthogonal modulation for data transmission at mobile station and a beamformer-RAKE receiver at base station. This receiver employ a non-coherent combining method. We compare the performance of vector antennas to ULA for the number of users that each antenna system can accommodate. The results suggest that for various number of antenna elements, vector antennas can accommodate more users than ULAs.

In Chapter 4, we consider the use of vector antennas in a single-user MIMO system. Previous work by Konanur *et al* [80] has shown that deploying vector antennas at the transmitter and receiver can provide capacity gains comparable to that of ULAs with the same number of antennas. In this chapter, we consider a MIMO system consisting of tripole antennas at both the transmitter and receiver, which employs V-BLAST combined with a zero-forcing detector at the receiver. Empirical measurements of the channel fading path gains, obtained from Konanur *et al* [80], are used to evaluate the bit-error-rate performance. We further evaluate the performance of adaptive transmission, in which the MIMO channel is decomposed into parallel channels. The transmitter adapts to the channel by the power allocation method. Simulations of the BER of V-BLAST and adaptive transmission are compared with the i.i.d. case. The BER of both schemes have shown that empirical data vary from i.i.d. case. To verify this variation a confidence test is performed on the mean value.

In Chapter 5, we study the signal-to-interference-plus-noise ratio (SINR) limitation for the purpose of analyzing the tripole and 6-element vector antennas. To derive an expression for the SINR, we consider one user and one interference source received

by a vector antenna in a multipath fading channel. The expression for SINR is a function of the direction-of-arrival (DOA) and the polarization of the received signal. Our results suggest that the vector antenna is able to limit interference and adjust to the polarization state and DOA of the desired transmitted signal. The beampattern of the vector antenna is calculated and compared to that of ULA, which reveals that vector antennas are plagued by fewer nulls and side lobes than conventional linear arrays.

# Chapter 2

## Beamforming Techniques For Vector-Antenna Receivers

Most wireless receivers currently employ single- or dual-polarized antennas, which measure one or two components of the received electromagnetic (EM) signal. In rich scattering environments, however, it may be possible to improve performance by using “vector antennas” that can detect up to six independent components of the EM field. In this chapter we consider the design of vector-antenna receivers and analyze their performance for direct-sequence code-division multiple-access (DS-CDMA) signals. We present a simple model that describes joint multipath propagation of the electric and magnetic fields in space and time. The model is then used to derive maximum-likelihood (ML), minimum mean-square error (MMSE), decorrelator (DD), and matched-filter (MF) receivers for a fading multipath channel. Analysis and simulations of these receivers suggest that vector antennas can significantly improve the diversity and bit-error-rate (BER) performance of CDMA signals in the presence of rich multipath.

## 2.1 Introduction

It is well known that space and polarization diversity can significantly improve the reliability and reduce the power requirements of wireless communications systems (e.g., [38, 39, 40]). Most wireless systems currently employ single- or dual-polarized antennas, which can measure at most two components of the received electromagnetic (EM) signal. However, since the signal consists of six field components (three electric and three magnetic), some potentially useful information may be neglected. Andrews *et al* [41] have recently suggested that dramatic gains in wireless capacity might be possible by exploiting these extra components of the received signal. In principle, a “vector antenna” that can independently detect or excite all six EM field components enables the communication system to access additional signaling dimensions, which may enhance performance in the same way as antenna arrays. These extra dimensions can provide additional diversity to combat signal fading, allow the system to spatially-leverage bandwidth by transmitting multiple separable signals in the same bandwidth, and improve the suppression of interference in multiuser environments.

In principle, a six-element vector antenna might be constructed by combining three electric dipoles to detect the electric field components with three magnetic dipoles (i.e., loops) to detect the magnetic field components. In [1], Andrews *et al* propose a “tripole” antenna that consists of three mutually-orthogonal dipoles and show through simulation that this antenna improves on the capacity of scalar- and dual-polarized antennas for a simple propagation example involving a line-of-sight component and one reflected path. A similar study of a three-element antenna system consisting of a loop and two dipoles (see Fig. 2.1) was presented in [42]. Vector sensors that respond to all six EM field components have also been investigated [52], although these devices are large and unsuited to wireless applications. The use of such sensors to estimate the direction-of-arrival of electromagnetic signals in line-of-

sight propagation has been extensively investigated (see [50, 53, 55] and references therein); however, the possible use of these antennas for wireless communication in multipath propagation environments has received little attention.

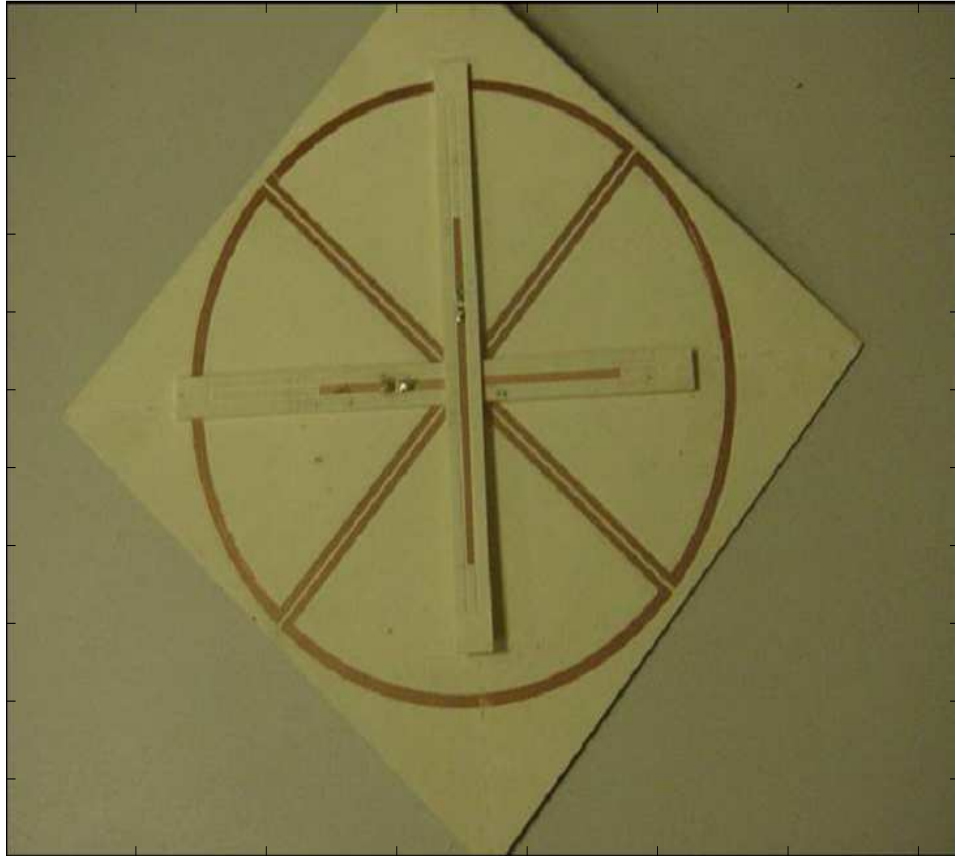


Figure 2.1: A 3-element vector antenna consisting of two electric dipoles and a loop ( Courtesy of Dr. Lazzi [42])

We consider the application of vector antennas to the problem of detecting code-division multiple-access (CDMA) signals in the presence of multipath. In the case of a single scalar receiving antenna, this problem was studied in Price and Green's classic work on the RAKE receiver [43]. Extensions to dual-polarized antennas have been considered in conjunction with multiuser detection in [45, 46]. More recently, uniform linear arrays of spatially-separated scalar antennas were investigated by Naguib [47],

who proposed a RAKE receiver in two dimensions (one spatial and one temporal dimension).

In this chapter, we consider the design and analysis of vector-antenna receivers for CDMA signals. We present a simple model that describes joint multipath propagation of the electric and magnetic fields in space and time, which is then used to derive maximum-likelihood, decorrelator, and matched-filter receivers for a fading multipath channel. These receivers lead to multi-dimensional polarimetric RAKE receivers in up to seven dimensions (six spatial and one temporal). Analysis and simulations of these receivers suggest that vector antennas can significantly improve the diversity and bit-error-rate performance of CDMA signals in the presence of rich multipath.

In the following sections, we first present a channel model to describe the propagation of DS-CDMA signals over a multipath channel. We then derive optimal and suboptimal receivers for a single-user system based on this model. Finally, we present numerical analysis and simulation results which characterize the performance of these receivers.

## 2.2 Channel Model

We now present a simple model for the complete electromagnetic signal detected by a vector antenna at the receiver. Consider a channel in which the signal propagates from the transmitter to the receiver by  $L$  dominant paths, each created by scattering and by reflection from physical objects in the environment. We assume that each of the dominant scatterers is sufficiently far from both the transmitting and receiving arrays to justify a far-field approximation. Thus, each multipath component arrives as a polarized plane wave at the receiver. The model is similar to the one considered by Nehorai and Paldi [50], but is here generalized to include the effects of fading,

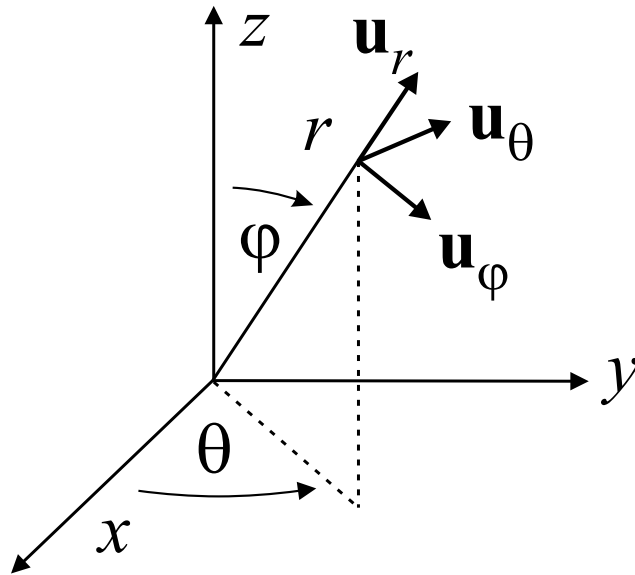


Figure 2.2: The orthonormal triad indicating the spherical coordinates  $(r, \theta, \varphi)$  and the unit vectors  $\mathbf{u}_r$ ,  $\mathbf{u}_\theta$  and  $\mathbf{u}_\varphi$ .

multipath, and delay spread.

Consider first a single vector antenna at the receiver. Each arriving multipath component is a two-dimensional vector  $\mathbf{R}(t)$ , consisting of the horizontally and vertically polarized components of the electric field. For narrowband sinusoidal signals, it is convenient to write the signal in terms of its complex envelope  $\mathbf{Z}$ , where  $\mathbf{R}(t) = \text{Re}\{\exp(j\omega_c t)\mathbf{Z}\}$ , and  $\omega_c$  is the carrier frequency. For any polarized signal, the complex envelope can be written as

$$\mathbf{Z} = Ae^{j\psi} \begin{bmatrix} \cos \alpha & \sin \alpha \\ -\sin \alpha & \cos \alpha \end{bmatrix} \begin{bmatrix} \cos \beta \\ j \sin \alpha \end{bmatrix}$$

where  $A, \psi, \alpha, \beta$  are the amplitude, phase, orientation angle, and ellipticity angle, respectively [50]. Since the signal is a function of the transmitted data, the amplitude, phase and polarization angles vary with time, and we write  $\mathbf{Z} = \mathbf{Z}(t)$ .

If the multipath component is reflected or scattered by an object in the far-field, then the signal can be approximated as a plane wave at the receiver. Let  $\mathbf{E}(t)$  and

$\mathbf{H}(t)$  denote the three-dimensional complex envelopes of the electric and magnetic field vectors at the receiver, and suppose that the multipath component arrives at the sensor from the direction

$$\mathbf{u}_r = \begin{bmatrix} \cos \theta \sin \varphi \\ \sin \theta \sin \varphi \\ \cos \varphi \end{bmatrix}$$

where  $\theta$  and  $\varphi$  are the azimuth and elevation, respectively, of the incoming signal in the receiver coordinates (see Fig. 2.1). For a narrowband plane wave propagating in a nonconductive, homogeneous, and isotropic medium, the received signal can be modeled by [50]

$$\mathbf{Y}(t) = \begin{bmatrix} \mathbf{E}(t) \\ \eta \mathbf{H}(t) \end{bmatrix} = B(\theta, \varphi) \mathbf{Z}(t) + \mathbf{N}(t)$$

where  $\mathbf{N}(t)$  represents thermal noise,  $\eta$  is the intrinsic impedance of the propagation medium, and

$$B(\theta, \varphi) = \begin{bmatrix} -\sin \theta & \cos \theta \cos \varphi \\ \cos \theta & \sin \theta \cos \varphi \\ 0 & -\sin \varphi \\ \cos \theta \cos \varphi & \sin \theta \\ \sin \theta \cos \varphi & -\cos \theta \\ -\sin \varphi & 0 \end{bmatrix}. \quad (2.1)$$

We are interested in using the antenna system described above to detect CDMA signals in the presence of rich multipath. We assume that the transmitted signal is a complex baseband signal of the form

$$S(t) = \sum_{m=1}^M b_m c(t - mT)$$

where  $c(t)$  is a unit-energy spreading waveform that vanishes outside the interval  $[0, T)$ , and  $b_m$  is a sequence of transmitted information bits. When  $S(t)$  is transmitted, the horizontally and vertically polarized components of each multipath component consist of  $S(t)$  with some amplitude and phase shift, so that  $\mathbf{Z}(t) = \mathbf{Z}S(t)$  for some fixed complex vector  $\mathbf{Z}$ .

Suppose now that the transmitted signal propagates to the receiver by multiple paths produced by  $L$  different scatterers. If the  $l$ -th path arrives at the receiver from direction  $\theta_l, \varphi_l$ , the superposition of these components at the receiver is given by

$$\mathbf{Y}(t) = \sum_{\ell=1}^L \sqrt{P_\ell} B(\theta_\ell, \varphi_\ell) \mathbf{Z}_\ell S(t - \tau_\ell) + \mathbf{N}(t) , \quad (2.2)$$

where  $P_\ell$  is the signal power in  $\ell$ -th multipath,  $\tau_\ell$  is the propagation delay of the  $\ell$ -th path, and  $\mathbf{Z}_\ell$  reflects the change in amplitude, phase, and polarization experienced by the  $l$ -th multipath component as it propagates from the transmitter to the receiver.

Thus far, we have considered only six-element vector antennas at the receiver. A vector antenna with  $t_{em} \leq 6$  elements can be modeled by

$$\mathbf{Y}(t) = \sum_{\ell=1}^L \sqrt{P_\ell} \mathbf{G}_\ell S(t - \tau_\ell) + \mathbf{N}(t) , \quad (2.3)$$

where  $\mathbf{G}_\ell$  consists of the appropriate  $t_{em}$  components of  $B(\theta_\ell, \varphi_\ell) \mathbf{Z}_\ell$ . This model is also easily generalized to arrays that consist of multiple spatially-separated, non-interacting vector antennas: Suppose that the receive array consists of  $r$  spatially-separated vector antennas located at positions  $\mathbf{x}_1, \dots, \mathbf{x}_r$  in receiver coordinates, that  $\mathbf{Y}_i(t)$  is the signal detected at the  $i$ -th receiver antenna, and that

$$\mathbf{Y}(t) = \begin{bmatrix} \mathbf{Y}_1(t) \\ \vdots \\ \mathbf{Y}_r(t) \end{bmatrix} .$$

A simple model for the resulting space-polarimetric channel is given with  $\mathbf{G}_\ell = [A_r(\theta, \varphi) \otimes B(\theta, \varphi)]\mathbf{Z}_\ell$ , where

$$B_r(\theta, \varphi) = A_r(\theta, \varphi) \otimes B(\theta, \varphi) ,$$

$\otimes$  is the Kronecker product,  $A_r(\theta, \varphi)$  is the classical narrowband array response

$$A_r(\theta, \varphi) = \begin{bmatrix} \exp(-j\omega_c d_1) \\ \vdots \\ \exp(-j\omega_c d_r) \end{bmatrix} , \quad d_i = -\frac{\mathbf{u}_r \cdot \mathbf{x}_i}{c} ,$$

and  $c$  denotes the speed of light.

## 2.3 Space-Time Receivers

We now consider the design of optimal receivers for the system model in eq. 2.3. While the polarimetric model is new, to the best of our knowledge, this model is mathematically similar to models of arrays of spatially separated scalar antennas, which have been already been studied in the literature by Naguib [51]. We assume that the channel coefficient and multipath delays are perfectly estimated at the receiver. The components of vector  $\mathbf{Z}_\ell$  are modeled as i.i.d. zero-mean complex Gaussian random variables and therefore the elements of  $\mathbf{G}_\ell$  are also zero-mean complex Gaussian random variables. The vector  $\mathbf{N}(t)$  is additive-white-Gaussian noise (AWGN) with zero mean and covariance  $\sigma^2\mathbf{I}$ . It is well-known that sufficient statistics for detecting the  $b_m, m = 1, \dots, M$  are the quantities [51]

$$z_\ell(m) = \int_{-\infty}^{\infty} c^*(t - mT - \tau_\ell) \mathbf{G}_\ell^\dagger \mathbf{Y}(t) dt , \quad \ell = 1, \dots, L.$$

Let  $\mathbf{z}(m) = [z_1(m), \dots, z_L(m)]^T \in \mathcal{C}^{L \times 1}$ , and  $\mathbf{n}(m) = [n_1(m), \dots, n_L(m)]^T$  where

$$n_\ell(m) = \int_{-\infty}^{\infty} \mathbf{G}_\ell^\dagger c^*(t - mT - \tau_\ell) \mathbf{N}(t) dt , \quad \ell = 1, \dots, L.$$

Note that the correlation between  $c(t - mT - \tau_\ell)$  and  $c(t - m'T - \tau_i)$  is given by

$$\rho_\Delta(\tau_\ell - \tau_i) = \int_{-\infty}^{\infty} c^*(t - mT - \tau_\ell) c(t - m'T - \tau_i) dt$$

where  $\Delta = m' - m$ . Let  $R_{\ell i}(\Delta) = \rho_\Delta(\tau_\ell - \tau_i)$ , and note that  $\rho_\Delta(\tau_\ell - \tau_i) = \rho_{-\Delta}(\tau_i - \tau_\ell)$ , where  $|\tau| > T$  and  $\Delta = 0, \pm 1$ . With this notation, the sufficient statistics of the received data can be written as

$$\mathbf{z}(m) = \mathcal{H}(1)b_{m-1} + \mathcal{H}(0)b_m + \mathcal{H}(-1)b_{m+1} + \mathbf{n}(m), \quad m = 1, \dots, M \quad (2.4)$$

where  $b_0 = b_{M+1} = 0$ , and

$$\mathcal{H}(\Delta) = [\underline{\mathbf{G}}^\dagger \underline{\mathbf{G}} \odot \mathbf{R}(\Delta)] \underline{\mathbf{A}} \in \mathcal{C}^{L \times 1},$$

where

$$\begin{aligned} \underline{\mathbf{G}} &= [\mathbf{G}_1 : \dots : \mathbf{G}_L] \in \mathcal{C}^{tem \times L}, \\ \mathbf{R}(\Delta) &= [\rho_\Delta(\tau_\ell - \tau_i)], \quad 1 \leq i, \ell \leq L, \\ \underline{\mathbf{A}} &= [\sqrt{P_1}, \sqrt{P_2}, \dots, \sqrt{P_L}]^T \in \mathcal{R}^{L \times 1}, \end{aligned}$$

where  $\odot$  is the Schur product (element-wise product), and  $\mathbf{n}(m)$  is a Gaussian noise vector with zero mean and covariance  $\mathbf{R}_n = \sigma^2 \underline{\mathbf{G}}^\dagger \underline{\mathbf{G}}$ .

We now present maximum-likelihood, minimum mean-squared error, decorrelating, and matched-filter receivers for the detection of  $b_m$ . Since the vector antenna channel model in eq. 2.3 is similar in form to the ULA models in Naguib [47], the corresponding receivers will also be similar. However, the characteristics of the  $\mathbf{G}_\ell$  are in general different, which will lead to different performance characteristics.

### 2.3.1 Maximum-Likelihood Receiver

For equally-likely data bits, the maximum-likelihood (ML) receiver minimizes the probability of an error in the transmitted data sequence. For channel in eq. 2.3, ML

sequence estimation can be efficiently implemented by the Viterbi algorithm (VA) [48]. To see this, the maximum-likelihood receiver can be written as

$$\begin{aligned} \hat{\mathbf{b}} &= \arg \min_{\mathbf{b} \in \{-1, +1\}^M} \sum_{m=1}^M \left\| \mathbf{z}(m) - \right. \\ &\quad \left. \mathcal{H}(1)b_{m-1} - \mathcal{H}(0)b_m - \mathcal{H}(-1)b_{m+1} \right\|_{\mathbf{R}_n}^2 \end{aligned} \quad (2.5)$$

where  $\| \mathbf{z} \|_{\mathbf{R}_n}^2 = \mathbf{z}^\dagger \mathbf{R}_n^{-1} \mathbf{z}$ . Let us assume that  $\mathbf{R}_n^{-1}$  exists and that  $\mathbf{R}_n^{-1/2}$  is the inverse square root of  $\mathbf{R}_n$ . Multiplying both sides of eq. 2.4 by  $\mathbf{R}_n^{-1/2}$ , we get

$$\begin{aligned} \tilde{\mathbf{z}}(m) &= \mathbf{R}_n^{-1/2} [\mathcal{H}(1)b_{m-1} + \mathcal{H}(0)b_m + \mathcal{H}(-1)b_{m+1} + \mathbf{n}(m)] \\ &= \mathbf{R}_n^{-1/2} [\mathcal{H}(1)b_{m-1} + \mathcal{H}(0)b_m + \mathcal{H}(-1)b_{m+1}] + \tilde{\mathbf{n}}(m) \end{aligned}$$

where the noise  $\tilde{\mathbf{n}}(m)$  has zero mean and covariance  $\mathbf{I}$  [51]. The ML receiver can then be written as

$$\begin{aligned} \hat{\mathbf{b}} &= \arg \min_{\mathbf{b} \in \{-1, +1\}^M} \sum_{m=1}^M \left\| \tilde{\mathbf{z}}(m) - \right. \\ &\quad \left. \mathbf{R}_n^{-1/2} [\mathcal{H}(1)b_{m-1} - \mathcal{H}(0)b_m - \mathcal{H}(-1)b_{m+1}] \right\|^2 \end{aligned} \quad (2.6)$$

where  $\| \mathbf{z} \|^2 = \mathbf{z}^\dagger \mathbf{z}$ . This detector is easily implemented recursively via the Viterbi algorithm using a four-state trellis. Since the complexity of ML will grow exponentially with the number of states, a suboptimal receivers may be desirable in some circumstances.

### 2.3.2 Linear Suboptimal Space-Time Receivers

For large number of states, the optimal ML receiver introduced in the previous section has a prohibitive computational complexity. In order to reduce complexity, we consider suboptimum linear space-time receivers for vector antennas. In particular, we derive the MMSE, decorrelator and space-time RAKE receivers for a single-user system where the spreading waveform and the channel parameters are known at the receiver.

### 2.3.3 Decorrelating Detector (DD)

The first suboptimum receiver we consider is the decorrelating (i.e., zero forcing) filter, which completely eliminates the MAI at the possible expense of enhancing the noise. Now the outputs of the  $L$  matched-filter banks for the  $j$ -th receiving antenna element can be written in a vector form as

$$\begin{aligned}\bar{\mathbf{z}}^j(m) &= \bar{\mathcal{H}}^j(-1)b_{m+1} + \bar{\mathcal{H}}^j(0)b_m + \bar{\mathcal{H}}^j(1)b_{m-1} \\ &+ \bar{\mathbf{n}}^j(m)\end{aligned}\quad (2.7)$$

where

$$\bar{\mathcal{H}}^j(\Delta) = \mathbf{R}(\Delta)\bar{\mathbf{G}}^j\mathbf{A} \in \mathcal{C}^{L \times 1}$$

and  $\bar{\mathbf{G}}^j = \text{diag}(\mathbf{G}_1^j, \dots, \mathbf{G}_L^j) \in \mathcal{C}^{L \times L}$  is the channel coefficients matrix where  $\mathbf{G}_\ell^j$  is the  $j$ -th element of  $\mathbf{G}_\ell$ . The covariance of noise  $\bar{\mathbf{n}}^j(m)$  is given by  $E[\bar{\mathbf{n}}^j(m)\bar{\mathbf{n}}^{j\dagger}(m')] = \sigma^2\mathbf{R}(m' - m)$ .

This decorrelating receiver is given by the time-invariant matrix inverse filter  $\mathcal{G}_d$  [56], whose  $z$ -transform is given by

$$\mathcal{G}_d(z) = [\mathbf{R}(-1)z + \mathbf{R}(0) + \mathbf{R}(1)z^{-1}]^{-1},$$

which is essentially the inverse of the CDMA channel response, which depends on the correlations among the delayed versions of the spreading waveform that appear in each multipath component. This detector will cancel the correlations between the multipath components but may also enhance the noise at low SNR. The  $z$ -transform of the decorrelator output at the  $j$ -th receiving antenna element is given by

$$\bar{\mathbf{z}}_d^j(z) = [\bar{\mathbf{G}}^j\mathbf{A}b](z) + \bar{\mathbf{n}}_d^j(z)$$

where  $\bar{\mathbf{n}}_d^j(z)$  is  $z$ -transform of Gaussian noise vector whose covariance has  $z$ -transform  $\sigma^2\mathcal{G}_d(z)$ .

Assuming knowledge of the channel coefficients at the receiver, the maximal-ratio combiner (MRC) output is the scalar statistic

$$\hat{\mathbf{z}}_d(m) = \sum_{j=1}^{tem} \underline{\mathbf{G}}^j \bar{\mathbf{z}}_d^j(m) \quad (2.8)$$

where  $\underline{\mathbf{G}}^j = [\mathbf{G}_1^j, \dots, \mathbf{G}_L^j]^T \in \mathcal{C}^{L \times 1}$

### 2.3.4 Minimum Mean-Square Error (MMSE)

We now consider the MMSE receiver for a single-user direct-sequence transmission in a multipath environment. Here intersymbol interference arises from the multipath delays, which cause successive bits to overlap. The aim of the MMSE receiver is to minimize the mean-square error between the transmitted data and the receiver output. In other words, the MMSE is a linear transformation that operates on the entire received data block (which is optimal in this case) or on a one-data-bit interval, which is called a one-shot MMSE detection (proposed by Honig *et al* [61]). In our scenario, MMSE is applied to the entire received block of  $M$  data bits. We assume knowledge of the channel coefficients and multipath delays at the receiver.

The output of the  $L$  matched-filter banks for the  $j$ -th receiving antenna element is given in eq. 2.7. The MMSE receiver minimizes the cost function between the transmitted user data and the output of the linear transformation, i.e.,  $E \|\mathcal{G}_{MMSE}^\dagger(z) \bar{\mathbf{z}}^j - b\|^2$ . The corresponding MMSE linear detector is the  $L$ -input,  $L$ -output filter with transfer function

$$\mathcal{G}_{MMSE}^\dagger(z) = (\bar{\mathbf{G}}^j \underline{\mathbf{A}})^\dagger [\tilde{\mathcal{H}}^j(-1)z + \tilde{\mathcal{H}}^j(0) + \tilde{\mathcal{H}}^j(1)z^{-1} + \sigma^2 \bar{\mathbf{A}}]^{-1}, \quad (2.9)$$

where

$$\tilde{\mathcal{H}}^j(\Delta) = [\mathbf{R}(\Delta) \bar{\mathbf{G}}^j \bar{\mathbf{G}}^{j\dagger}] \in \mathcal{C}^{L \times L},$$

and the matrix  $\bar{\mathbf{A}} = \text{diag}(P_1^{-1}, P_2^{-1}, \dots, P_L^{-1})$ .

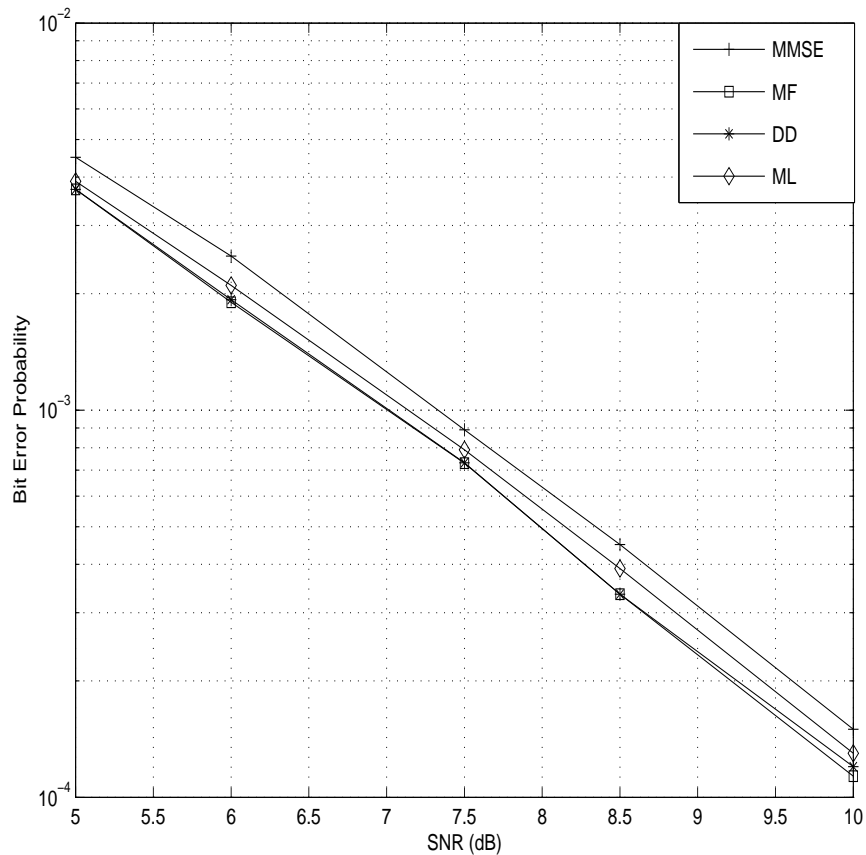


Figure 2.3: ML, MMSE, DD and MF-receivers for the “tripole” antenna (3-dipole) for  $L=2$  equal-energy multipaths.

### 2.3.5 Matched-Filter Receiver (MF)

The space-time RAKE is a conventional receiver that treats multipath interference as Gaussian noise. We can write the output of the space-time matched filter or sufficient statistic vector at the output of space-time RAKE receiver as [47]

$$\mathbf{z}(m) = \mathcal{H}(0) b_m + \tilde{\mathbf{n}}(m) \in \mathcal{C}^{L \times 1} \quad (2.10)$$

where  $\tilde{\mathbf{n}}(m)$  is the undesired multipath interference plus thermal noise with mean zero and covariance  $\mathbf{R}_u = \mathcal{H}(-1)\mathcal{H}^\dagger(-1) + \mathcal{H}(1)\mathcal{H}^\dagger(1) + \sigma_n^2 \mathbf{I}$ . The decision statistics

is the scalar output

$$\hat{b} = \text{sgn} \left( \sum_{\ell=1}^L z_{\ell}(m) \right).$$

For a single-user system with low interference, the MF receiver may be of interest since it is less complex than the other receivers considered here, such as ML and MMSE. However, for a large number of multipaths the orthogonality of the components may be degraded, and more efficient receivers may be useful to efficiently detect the signal.

## 2.4 Numerical Examples

In this section we numerically plot the BER of the ML, MMSE, MF and DD receivers for a vector antenna array at the receiver. Our main focus is to determine the diversity gain that a vector antenna can capture in a multipath environment when various numbers of antenna elements are used.

We start by assuming that the multipath components are uniformly distributed on a sphere where the azimuth angle  $\theta_{\ell}$  is i.i.d. and uniform on  $\in [0, 2\pi]$ , and the elevation angle  $\varphi_{\ell}$  is i.i.d. with probability density function

$$P(\varphi_{\ell}) = \begin{cases} \frac{1}{2} \sin(\varphi_{\ell}), & 0 \leq \varphi_{\ell} \leq \pi \\ 0, & \text{otherwise} \end{cases}$$

and the polarizations  $\mathbf{Z}_{\ell}$  are i.i.d.  $\mathcal{CN}(\mathbf{0}, I)$ . The noise  $\mathbf{N}(t)$  is spatially and temporally white and Gaussian (i.e.  $E[\mathbf{N}(t)\mathbf{N}^{\dagger}(t + \tau)] = \sigma^2\mathbf{I}$ ). The fading channel is assumed to be a frequency-selective, slowly Rayleigh fading channel, and the multipath delays  $\tau_{\ell}$  are set at discrete intervals, which is equivalent to one chip duration ( $T_c$ ).

We now consider the simulated performance of the ML, MMSE, DD, and MF given in eqs. 2.6, 2.9, 2.8, 2.10, respectively. We will evaluate the performance of four

different vector antennas: a 6-element vector antenna, where  $B(\theta_\ell, \varphi_\ell)$  is given by eq. 2.1; the 3-element “tripole” antenna proposed by Andrews *et al* [41] consisting of three mutually orthogonal dipoles, where  $B(\theta_\ell, \varphi_\ell)$  are given by

$$B(\theta_\ell, \varphi_\ell) = \begin{bmatrix} -\sin \theta_\ell & \cos \theta_\ell \cos \varphi_\ell \\ \cos \theta_\ell & \sin \theta_\ell \cos \varphi_\ell \\ 0 & -\sin \varphi_\ell \end{bmatrix},$$

the 3-element vector antenna proposed by Konanur *et al* [42] which consists of two dipoles and a loop (see Fig 2.1), where the elements of  $B(\theta_\ell, \varphi_\ell)$  are given by

$$B(\theta_\ell, \varphi_\ell) = \begin{bmatrix} -\sin \theta_\ell & \cos \theta_\ell \cos \varphi_\ell \\ \cos \theta_\ell & \sin \theta_\ell \cos \varphi_\ell \\ \cos \theta \cos \varphi & \sin \theta \end{bmatrix},$$

and a dual-polarized antenna consisting of two orthogonal dipoles, where the elements of  $B(\theta_\ell, \varphi_\ell)$  are given by

$$B(\theta_\ell, \varphi_\ell) = \begin{bmatrix} -\sin \theta_\ell & \cos \theta_\ell \cos \varphi_\ell \\ \cos \theta_\ell & \sin \theta_\ell \cos \varphi_\ell \end{bmatrix}.$$

We first consider the case of two multipath components with delays  $\tau_1$  and  $\tau_2$ , respectively, such that  $\tau_2$  is delayed by one chip relative to  $\tau_1$ . At the transmitter we assume BPSK modulation and Gold spreading sequences of length 31 [49] and a unit-energy spreading waveform. The autocorrelation matrix  $\mathbf{R}(\Delta)$  for  $\Delta = -1, 0, 1$  is then given by

$$\begin{aligned} \mathbf{R}(-1) &= \begin{pmatrix} 0 & \rho_{-1}(\tau_1 - \tau_2) \\ 0 & 0 \end{pmatrix} = \begin{pmatrix} 0 & -0.0303 \\ 0 & 0 \end{pmatrix} \\ \mathbf{R}(0) &= \begin{pmatrix} 1 & \rho_0(\tau_1 - \tau_2) \\ \rho_0(\tau_2 - \tau_1) & 1 \end{pmatrix} \end{aligned}$$

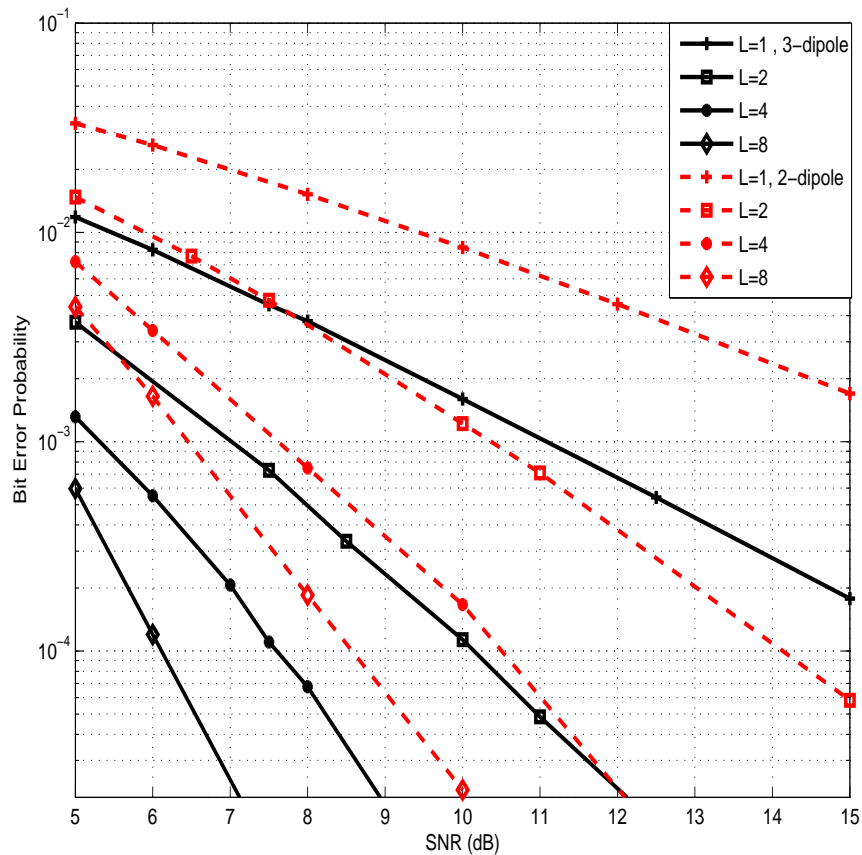


Figure 2.4: BER of the MF receiver for the “tripole” antenna (3-dipoles) versus dual-polarized antenna (2-dipoles) for  $L = 1, 2, 4, 8$  multipaths.

$$\begin{aligned}
 &= \begin{pmatrix} 1 & 1 \times 10^{-17} \\ 1 \times 10^{-17} & 1 \end{pmatrix} \\
 \mathbf{R}(1) &= \begin{pmatrix} 0 & 0 \\ \rho_1(\tau_2 - \tau_1) & 0 \end{pmatrix} = \begin{pmatrix} 0 & 0 \\ -0.0303 & 0 \end{pmatrix}.
 \end{aligned}$$

In Fig. 2.3, the performances of the ML, MMSE, DD and MF detectors for equal-energy multipaths are plotted. Note that the performance of all three receivers are very close in terms of BER, since the low autocorrelation of the Gold sequence enables the receiver to resolve the two multipath components. When the multipath components are fully resolved, a closed-form formula can be given for the BER of

the MF receiver for the tripole and 6-element vector antenna. In these two cases, the performance is determined by the post-processing signal-to-noise ratio (SNR), which is given by

$$\gamma_b = \sum_{\ell=1}^L \gamma_\ell = \frac{\gamma_r}{L} \sum_{\ell=1}^L \mathbf{G}_\ell^\dagger \mathbf{R}_n^{-1} \mathbf{G}_\ell$$

where  $\gamma_r$  is signal-to-noise ratio per receive antenna. If the noise is white ( $\mathbf{R}_n = I$ ) and  $\mathbf{G}_\ell$  is a zero-mean complex Gaussian random variable, then  $\gamma_b$  has a  $\chi^2$  probability density function (pdf) with  $4L$  degrees of freedom [1]:

$$f_{\gamma_b}(\gamma) = \frac{\gamma^{2L-1}}{(\bar{\gamma})^{2L}(2L-1)!} e^{-\gamma/\bar{\gamma}}$$

where  $\bar{\gamma} = \frac{\rho}{L\sigma^2}$  is the average SNR-per-path-per-antenna. The average BER of BPSK modulation is therefore given by Proakis [1, page 825]

$$\begin{aligned} P_b &= \int_0^\infty Q(\sqrt{2\gamma}) f_{\gamma_b}(\gamma) d\gamma \\ &= \left(\frac{1-u}{2}\right)^{2L} \sum_{\ell=0}^{2L-1} \binom{2L-1+\ell}{\ell} \left(\frac{1+u}{2}\right)^\ell \end{aligned}$$

where for the tripole antenna

$$u = \sqrt{\frac{\bar{\gamma}}{1+\bar{\gamma}}}$$

and for the 6-element vector antenna

$$u = \sqrt{\frac{2\bar{\gamma}}{1+2\bar{\gamma}}}.$$

In Fig. 2.4, the BER of the “tripole” antenna is compared with the BER of a dual-polarized antenna (two orthogonal dipoles) for the MF receiver. Fig. 2.5 compares the BER of the tripole antenna to the BER of the vector antenna proposed in Konanur *et al* [42] and depicted in Fig. 2.1. Fig. 2.6 plots the BER of a 6-element vector antenna capable of detecting all 6 components of the EM field at the receiver.

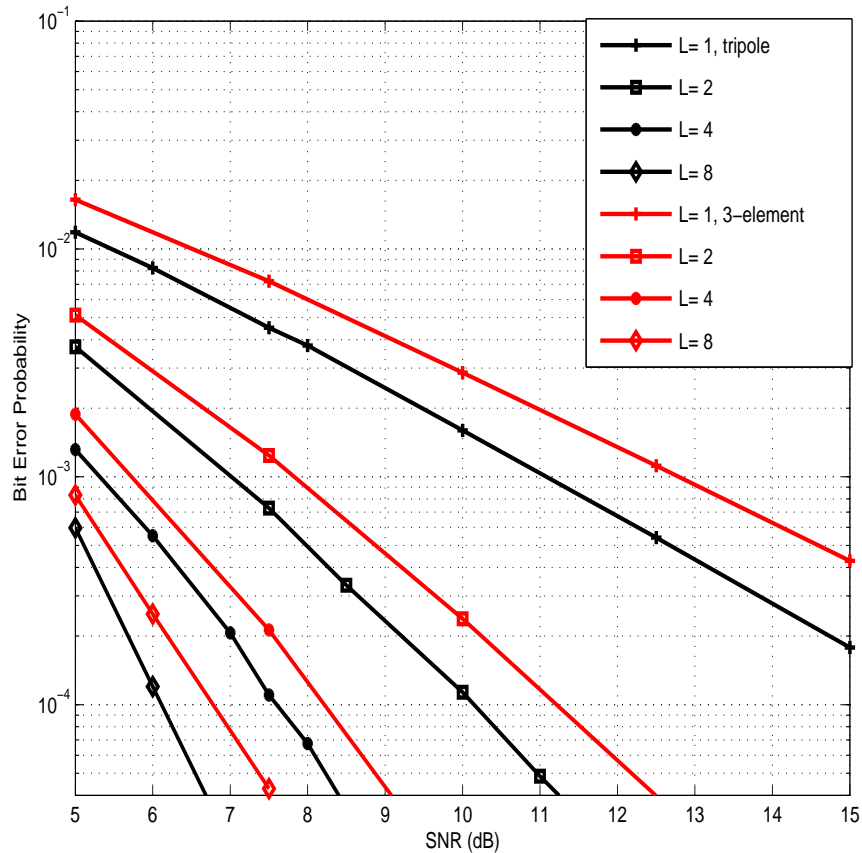


Figure 2.5: BER of the MF receiver for the “tripole” antenna versus the 3-element vector in Fig. 2.1 for  $L = 1, 2, 4, 8$  multipaths.

Comparing these figures, we see that for each  $L$ , the three-element antennas offer a 2-5 dB improvement in BER relative to dual-polarized antennas, while the six-element antenna offers a 4-12 dB improvement. Fig. 2.5 further illustrates that the geometry of the antenna elements has a significant impact on performance, since the tripole antenna outperforms the antenna in Fig. 2.1 by about 0.5-1 dB. This performance difference can be explained by the presence of “blind spots” in the antenna system of Fig. 2.1 (i.e., directions along which the antenna is unreceptive). For example, observe that a plane wave that arrives with electric field vector perpendicular to the loop and magnetic field in the plane of the loop will produce no response. This cannot

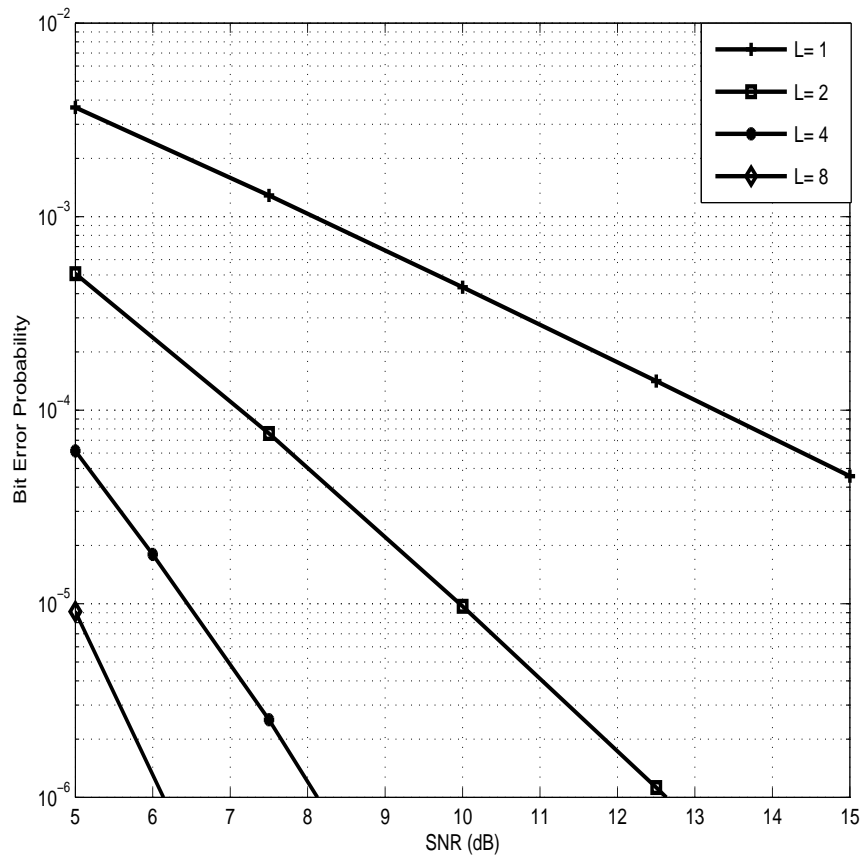


Figure 2.6: BER of the MF receiver for a 6-element vector antenna with  $L = 1, 2, 4, 8$  multipaths.

happen with the tripole antenna.

## 2.5 Conclusions

In this chapter, we presented a simple model for single vector antenna that describes the joint multipath propagation of EM field components. This model is generalized to array that consist of multiple spatially-separated vector antennas. Based on single vector antenna model, we derived ML, MMSE, decorrelator, and MF receivers for DS-CDMA signals in a multipath environment. The simulation results of these receivers for various vector antennas showed improvement of diversity and

BER. The impact of antenna geometry on performance is simulated for tripole and the two dipole and loop. The tripole showed improvement in BER over 2 dipole and loop antenna.

## Chapter 3

# Multiuser Detection for Vector Antennas

In Chapter 2, we have considered the performance of vector-antenna receivers for a single-user system and a CDMA multipath channel. In this chapter, we again consider the performance of vector-antenna receivers in a multiuser environment. We first present space-time minimum-mean square error (ST-MMSE) and decorrelator (ST-DD) detectors, for both vector-antenna systems and uniform linear arrays (ULA) in a multiuser environment. We then present the adaptive implementation of these receivers and investigate their performance in the presence of multipath fading. We will use a trained adaptive algorithm based on the stochastic gradient method, which does not require knowledge of the channel coefficients at the receiver. Analysis and simulations of these receivers suggest that vector antennas can significantly improve the diversity and bit-error-rate performance of CDMA signals in the presence of rich multipath. They further suggest that vector antennas can outperform the uniform linear arrays with the same number of antenna elements.

Next we consider a vector-antenna receiver structure at the base station for DS-

CDMA signals with  $M$ -ary orthogonal modulation. The proposed receiver is a vector antenna beamformer-RAKE that employs non-coherent combining. The BER as a function of the number of users is studied. Simulation results suggest that, for a given BER, a vector antenna can accommodate more users than a uniform linear array (ULA) with the same number of elements.

### 3.1 Introduction

For single-antenna systems, it is well known that multiuser detection [56] can improve the performance of CDMA systems by exploiting the cross-correlations between the spreading sequences of the users to reduce the effects of multi-access interference (MAI). This reduced interference can, in turn, be traded for a higher CDMA system capacity. In recent years, Wang and Poor [71] have shown that performance can be further improved on fading multipath channels by deploying multiple antennas at the receiver and using space-time processing to combat fading and exploit the cross-correlations among the fading path gains (Analogous results for single-antenna receivers were presented by Naguib and Paulraj [60].) Optimal maximum-likelihood space-time multiuser detectors were derived for flat fading by Miller and Schwartz [66] and Kandala *et al* [65], and for multipath fading by Nagatsuka [67]. Since these ML detectors are often prohibitively complex to implement for a large number of users, less complex linear detectors, such as the decorrelator (DD) and MMSE receivers have been derived in [68], [69] and [57].

Both the DD and MMSE detector require knowledge of the user's spreading waveforms at the receiver. The DD seeks to null multiple-access interference, which can enhance the background noise. In contrast, the MMSE detector seeks to minimize the mean-square error between the user's signal and the detector output, and thereby

minimizes the sum of MAI and noise. As a consequence, the MMSE receiver usually outperforms the DD receiver at low signal-to-noise ratio (SNR), however, as the background noise decreases, the performance of the MMSE detector converges to that of the DD. The MMSE multiuser detector was introduced in [70] for single-antenna systems and extended to multiple antennas and multipath fading channels in [57] and [71].

In this chapter, we consider the application of vector antennas to the problem of detecting synchronous code-division multiple-access (CDMA) signals in the presence of multipath channels that result in multiple access interference. The advantages of the vector antenna have been considered for single-user systems in Chapter 2; however, the benefits of these antennas have not been considered for multiuser receivers. We will investigate the performance benefits of vector antennas and how they depend on channel parameters, such as the number, type, and geometry of the antenna elements. The impact on performance of the polarization states and propagation delays of the multipath components will also be studied.

This chapter is organized as follows. In Section 3.2, we describe the channel model for a vector-antenna system in a multiuser fading environment. In Section 3.2.1, we present a space-time MMSE multiuser detector. This receiver requires knowledge of the desired user's spreading code, propagation delays and fading path gains at the receiver. We then describe an adaptive implementation of this receiver in Section 3.2.2 and compare its simulated performance to that of a uniform linear array in Section 3.3. In Section 3.4.2 we describe the channel model for  $M$ -ary orthogonal modulation for a CDMA system in which  $n$  users transmit to a common single vector antenna receiver. Then the beamformer-RAKE receiver is described and the receiver design for multiuser environment is presented. In Section 3.4.3, we derive the decision statistics of the receiver and analyze the BER. Simulation results for vector antennas

and ULAs are compared in Section 3.4.4. Finally, our conclusions are summarized in Section 3.5.

## 3.2 A Space-Time MMSE Detector

We consider a collection of  $n$  users transmitting to a single vector-antenna receiver using CDMA signaling. The transmitted signal of user  $i$  is a complex baseband signal of the form

$$S_i(t) = \sum_{m=1}^M b_i(m)c_i(t - mT),$$

where  $c_i(t)$  is a unit-energy spreading waveform that vanishes outside the interval  $[0, T)$ , and  $b_i$  is a sequence of transmitted information bits for user  $i$ . When  $S_i(t)$  is transmitted, the horizontally and vertically polarized components of each multipath component consist of  $S_i(t)$  with some amplitude and phase shift, so that  $\mathbf{Z}_i(t) = \mathbf{Z}_i S_i(t)$  for some fixed complex vector  $\mathbf{Z}_i$  as defined in Chapter 2.

As in Chapter 2, we assume that each user's transmitted signal propagates to the receiver by multiple paths produced by  $L$  different scatterers. If the  $l$ -th path for user  $i$  arrives at the receiver from direction  $(\theta_{i,l}, \varphi_{i,l})$ , the superposition of the multipaths of all  $n$  users and noise at the receiver is given by

$$\mathbf{Y}(t) = \sum_{i=1}^n \sum_{\ell=1}^L \sqrt{P_i} B(\theta_{i,\ell}, \varphi_{i,\ell}) \mathbf{Z}_{i,\ell} S_i(t - \tau_{i,\ell}) + \mathbf{N}(t), \quad (3.1)$$

where  $P_i$  is the signal power of the  $i$ -th user,  $B(\theta, \varphi)$  is the  $6 \times 2$  antenna response given in eq. 2.1,  $\tau_{i,\ell}$  is the propagation delay of the  $l$ -th path of user  $i$ , and  $\mathbf{Z}_{i,\ell}$  reflects the change in amplitude, phase, and polarization experienced by the  $l$ -th multipath component as it propagates from the transmitter of user  $i$  to the receiver. The noise  $\mathbf{N}(t)$  is a zero-mean complex Gaussian vector with covariance  $\sigma^2 \mathbf{I}$ .

A  $t_{em}$ -element vector antenna with  $t_{em} \leq 6$  can sense only  $t_{em}$  components of

$\mathbf{Y}(t)$ . With a slight abuse of notation, we can therefore rewrite eq. 3.1 as

$$\mathbf{Y}(t) = \sum_{i=1}^n \sum_{\ell=1}^L \sqrt{P_i} \mathbf{G}_{i,\ell} S_i(t - \tau_{i,\ell}) + \mathbf{N}(t), \quad (3.2)$$

where  $\mathbf{G}_{i,\ell}$  consists of the appropriate  $t_{em}$  components of  $B(\theta_{i,\ell}, \varphi_{i,\ell}) \mathbf{Z}_{i,\ell}$ . The components of the vector  $\mathbf{Z}_{i,\ell}$  are modeled as i.i.d. zero-mean complex Gaussian random variables and therefore the elements of  $\mathbf{G}_{i,\ell}$  are also zero-mean complex Gaussian random variables.

Since the system is chip and symbol synchronous, we can sample  $\mathbf{Y}(t)$  at the chip frequency to obtain a discrete-time vector  $\mathbf{Y}$  given by

$$\mathbf{Y} = \mathbf{C} \mathbf{G} \mathbf{A} \mathbf{b} + \mathbf{N}. \in \mathcal{C}^{N_c t_{em} \times 1}.$$

The spreading code matrix is given by

$$\mathbf{C} = \begin{bmatrix} \mathbf{C}^1 & 0 & \cdots & 0 \\ 0 & \mathbf{C}^2 & \cdots & 0 \\ 0 & 0 & \ddots & 0 \\ 0 & 0 & 0 & \mathbf{C}^{t_{em}} \end{bmatrix} \in \mathcal{R}^{N_c t_{em} \times n L t_{em}}$$

where  $N_c$  is the processing gain. For the  $j$ -th receiving antenna,  $\mathbf{C}^j$  is given by

$$\mathbf{C}^j = [\mathbf{c}_{1,1}, \dots, \mathbf{c}_{1,L}, \dots, \mathbf{c}_{n,1}, \dots, \mathbf{c}_{n,L}] \in \mathcal{R}^{N_c \times n L}$$

where  $\mathbf{c}_{i,\ell}$  is the sampled spreading code for user  $i$  at  $\tau_{i,\ell}$  given by

$$\mathbf{c}_{i,\ell} = [c_i(T_c - \tau_{i,\ell}), \dots, c_i(N_c T_c - \tau_{i,\ell})]^T \in \mathcal{R}^{N_c \times 1}$$

and the channel coefficients at the  $t_{em}$  receiving antenna elements are given by

$$\mathbf{G} = \begin{bmatrix} \mathbf{G}^1 \\ \mathbf{G}^2 \\ \vdots \\ \mathbf{G}^{t_{em}} \end{bmatrix} \in \mathcal{C}^{n L t_{em} \times n}$$

where  $\mathbf{G}^j$  is a block-diagonal matrix of channel coefficients at the  $j$ -th receiving antenna element given by

$$\mathbf{G}^j = \begin{bmatrix} \mathbf{G}_1^j & 0 & \cdots & 0 \\ 0 & \mathbf{G}_2^j & \cdots & 0 \\ 0 & 0 & \ddots & 0 \\ 0 & 0 & 0 & \mathbf{G}_n^j \end{bmatrix} \in \mathcal{C}^{nL \times n}$$

and the matrix of channel coefficients for the multipaths of the  $i$ -th user is

$$\mathbf{G}_i^j = \begin{bmatrix} \mathbf{G}_{i,1}^j \\ \mathbf{G}_{i,2}^j \\ \vdots \\ \mathbf{G}_{i,L}^j \end{bmatrix} \in \mathcal{C}^{L \times 1}$$

where  $\mathbf{G}_{i,\ell}^j$  is the  $j^{\text{th}}$  element of  $\mathbf{G}_{i,\ell}$ . The matrix  $\mathbf{A} = \text{diag}(\sqrt{P_1}, \sqrt{P_2}, \dots, \sqrt{P_n})$  is an  $n \times n$  block-diagonal matrix of the user's signal power. The transmitted data of the  $n$  users at time  $m$  is given by the vector  $\mathbf{b} = [b_1(m), b_2(m), \dots, b_n(m)]^T \in \mathcal{R}^{n \times 1}$ , and the noise vector  $\mathbf{N}$  is AWGN with zero-mean and covariance  $\sigma^2 \mathbf{I}$ .

### 3.2.1 Space-Time Multiuser Detector

Assuming knowledge of the channel coefficients, delay spread and user's spreading waveforms at the receiver, we can write the output of a space-time matched filter by

$$\begin{aligned} \tilde{\mathbf{Y}} &= \mathbf{G}^\dagger \mathbf{C}^T \mathbf{Y} \\ &= \mathbf{G}^\dagger \mathbf{C}^T \mathbf{C} \mathbf{G} \mathbf{A} \mathbf{b} + \mathbf{G}^\dagger \mathbf{C}^T \mathbf{N} \\ &= \mathcal{T} \mathbf{A} \mathbf{b} + \mathbf{N}_{\tilde{\mathbf{Y}}}, \end{aligned}$$

where  $\mathcal{T} = \mathbf{G}^\dagger \mathbf{C}^T \mathbf{C} \mathbf{G} = \mathbf{G}^\dagger \mathbf{R} \mathbf{G}$  is the space-time correlation matrix. Here  $\mathbf{R} = \mathbf{C}^T \mathbf{C}$  is the block-diagonal correlation matrix of the user's spreading waveforms. The noise

$\mathbf{N}_{\tilde{\mathbf{Y}}}$  is a zero-mean complex Gaussian vector with covariance matrix  $\mathcal{T} = \mathbf{G}^\dagger \mathbf{R} \mathbf{G}$ . We assume the delay spread is small compared to the symbol period, so intersymbol interference can be ignored.

The MMSE receiver takes the form  $\mathbf{z} = \mathbf{W}^\dagger \tilde{\mathbf{Y}}$ , where  $\mathbf{W}$  is a weight vector chosen to minimize the cost function  $E\{\|\mathbf{W}^\dagger \tilde{\mathbf{Y}} - \mathbf{b}\|^2\}$ . As shown by Wiener, the optimal weight vector is given by

$$\begin{aligned} \mathbf{W}^\dagger &= E[\mathbf{b} \tilde{\mathbf{Y}}^\dagger] (E[\tilde{\mathbf{Y}} \tilde{\mathbf{Y}}^\dagger])^{-1} \\ &= \mathbf{A}^{-1} (\mathbf{G}^\dagger \mathbf{R} \mathbf{G} + \sigma^2 \mathbf{A}^{-2})^{-1}. \end{aligned}$$

The output of the space-time MMSE receiver is therefore

$$\begin{aligned} \mathbf{z} &= \mathbf{W}^\dagger \tilde{\mathbf{Y}} \\ &= \mathbf{A}^{-1} (\mathbf{G}^\dagger \mathbf{R} \mathbf{G} + \sigma^2 \mathbf{A}^{-2})^{-1} \tilde{\mathbf{Y}} \\ &= \mathbf{W}^\dagger \mathcal{T} \mathbf{A} \mathbf{b} + \mathbf{W}^\dagger \mathbf{N}_{\tilde{\mathbf{Y}}}. \end{aligned} \tag{3.3}$$

Since we assume a BPSK data sequence, the decision statistic for the  $i$ -th user's data bit is

$$\hat{b}_i = \text{sgn}[\text{Re}(\mathbf{z}_i)]$$

where  $\mathbf{z}_i$  is the  $i$ -th component of  $\mathbf{z}$  and  $\text{sgn}(x)$  is

$$\text{sgn}(x) = \begin{cases} +1, & x \geq 0 \\ -1, & x < 0. \end{cases}$$

The conditional bit-error probability for the  $i$ -th user given the fading path gains  $\mathbf{G}$  is given by

$$P_i = Q\left(\frac{(\mathbf{W}^\dagger \mathcal{T} \mathbf{A} \mathbf{b})_i}{\sigma \sqrt{(\mathbf{W}^\dagger \mathcal{T} \mathbf{W})_{ii}}}\right)$$

where  $(\cdot)_i$  and  $(\cdot)_{ii}$  denote the  $i$ -th element of a vector and the  $ii$ -th element of a square matrix, respectively.

Note that the MMSE detector in eq. 3.3 depends explicitly on the amplitudes  $\mathbf{A}$  of the  $n$  users. When a user's amplitude is not available at the receiver, an alternative receiver which does not require knowledge of the signal amplitudes is the decorrelator given by [71]

$$\mathbf{z}_d = (\mathbf{G}^\dagger \mathbf{R} \mathbf{G})^{-1} \tilde{\mathbf{Y}}. \quad (3.4)$$

The decorrelator is essentially a zero-forcing detector which nulls MAI. When the channel coefficients are unavailable at the receiver, then the adaptive MMSE can also be used to estimate the channel parameters. The adaptive MMSE usually outperforms the decorrelator receiver for slowly varying channel coefficients.

### 3.2.2 Adaptive ST-MMSE Detector

The ST-MMSE detector can be implemented adaptively when the channel coefficients are not known to the receiver or vary with time. Similar to single-user adaptive filtering, the weight matrix  $\mathbf{W}$  can be computed iteratively with the use of a training sequence of data bits that is known by all users. We consider the stochastic-gradient type algorithm known as the least-mean square (LMS) algorithm [74]. In particular, we use LMS to choose a weight  $\mathbf{W}$  to adaptively minimize the MMSE criterion of

$$\begin{aligned} \arg \min_{\mathbf{W}} J(\mathbf{W}) &= E \|\mathbf{b}(m) - \mathbf{W}(m)^\dagger \bar{\mathbf{Y}}(m)\|^2 \\ &= E \|\mathbf{b}(m) - \mathbf{z}(m)\|^2 \\ &= E \left[ \sum_{i=1}^n |b_i(m) - z_i(m)|^2 \right] \end{aligned}$$

where  $\bar{\mathbf{Y}}$  is the vector of the code-matched filter output given by

$$\bar{\mathbf{Y}} = \mathbf{C}^T \mathbf{Y} = \mathbf{R} \mathbf{G} \mathbf{A} \mathbf{b} + \mathbf{N}_{\bar{\mathbf{Y}}},$$

and the weight is adapted using the multiuser LMS algorithm [57]

$$\mathbf{W}(m+1) = \mathbf{W}(m) + \mu \bar{\mathbf{Y}}(m) [\mathbf{b}(m) - \mathbf{z}(m)]. \quad (3.5)$$

The performance of this adaptive algorithm will depend on the step size parameter  $\mu$ , which controls the speed of convergence and the variations of the learning curve. Here  $\mu$  is optimized in an *ad hoc* manner, where at each simulation,  $\mu$  is selected such that the BER converges to the vicinity of the BER of the non-adaptive MMSE receiver. After training of the algorithm, the adaptive algorithm will switch to a decision-directed mode

$$\mathbf{W}(m+1) = \mathbf{W}(m) + \mu \bar{\mathbf{Y}}(m) [\hat{\mathbf{b}}(m) - \mathbf{z}(m)], \quad (3.6)$$

where  $\hat{\mathbf{b}}(m) = [\hat{b}_1(m), \hat{b}_2(m), \dots, \hat{b}_n(m)]$  are the detected bits for the  $n$  users.

To compare the performance of the vector-antenna array to a uniform linear array (ULA), we present the equivalent ULA model. The ULA [72] is modeled as a collection of dipole antenna elements that are spatially and uniformly distributed in a plane containing array elements. The antenna response for a uniform linear array parallel to the  $z$ -axis and centered on the  $x$ -axis can be modeled as

$$B(\theta, \varphi) = \sin \varphi \begin{bmatrix} e^{-j2\pi x_1 \cos \theta / \lambda} & 0 \\ \vdots & \vdots \\ e^{-j2\pi x_M \cos \theta / \lambda} & 0 \end{bmatrix} \quad (3.7)$$

where  $x_i, i = 1, 2, \dots, M$  corresponds to the  $x$ -coordinates of the antennas. This uniform antenna system can respond to one polarization component, horizontal or vertical.

### 3.3 Simulation Results

We now present simulations of the performance of the vector-antenna system described in the previous section for a variety of propagation conditions. These results will also be compared to the performance obtained with uniform linear arrays.

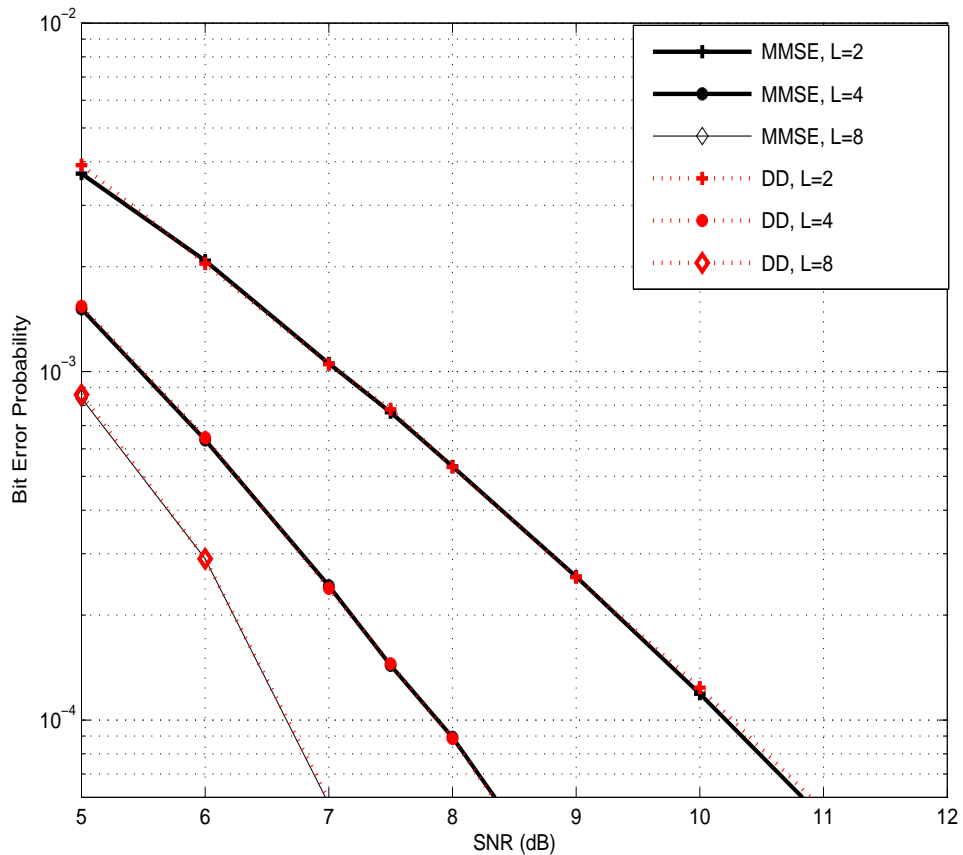


Figure 3.1: BER of ST-MMSE and ST-DD for a single tripole antenna with  $L = 2, 4, 8$  multipaths and  $n = 5$  users.

We consider the performance of the space-time receivers for a multiuser system in a multipath fading channel for BPSK modulation and a Gold code spreading sequence. Each user is assigned a unique Gold spreading sequence of length 31. In each plot, the multipath component of the desired and interference signals are uniformly distributed on a sphere where the azimuths angles  $\theta_{i,\ell}$  are i.i.d. and uniform on  $\in [0, 2\pi]$ , and the elevation angles  $\varphi_{i,\ell}$  are i.i.d. with probability density function

$$P(\varphi_{i,\ell}) = \begin{cases} \frac{1}{2} \sin(\varphi_{i,\ell}), & 0 \leq \varphi_{i,\ell} \leq \pi \\ 0, & \text{otherwise} \end{cases}$$

and the polarizations  $\mathbf{Z}_{i,\ell}$  are i.i.d.  $\mathcal{CN}(\mathbf{0}, \mathbf{I})$ . The noise is spatially and temporally

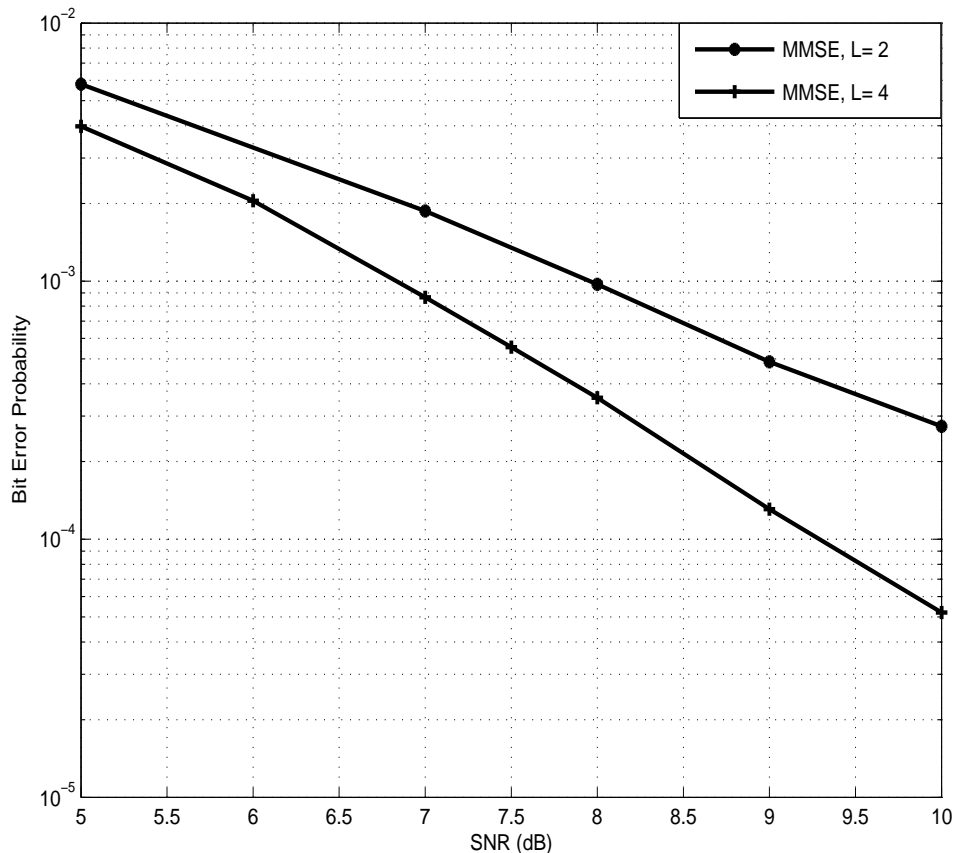


Figure 3.2: BER of adaptive ST-MMSE for a single tripole antenna with  $L = 2, 4$  multipaths,  $n = 5$  users, and adaptive step size  $\mu = 0.001$ .

Gaussian with covariance  $\sigma^2\mathbf{I}$ . The fading channel is assumed to be a frequency-selective slowly Rayleigh fading channel, and the multipath delays are set at discrete intervals equivalent to chip duration. The scenario of synchronous users is assumed here with the number of users taken to be  $n = 5$  for all simulations. The number and values of the multipath delays  $L$  are equal for all users, so that all users arrive with same delays at the receiver. The amplitudes of all users are equal at the receiver and we assume the detection of first user.

In Fig. 3.1, we consider the tripole antenna proposed in [41] consisting of three mutually orthogonal electrical dipoles for ST-MMSE receiver. The ST-MMSE re-

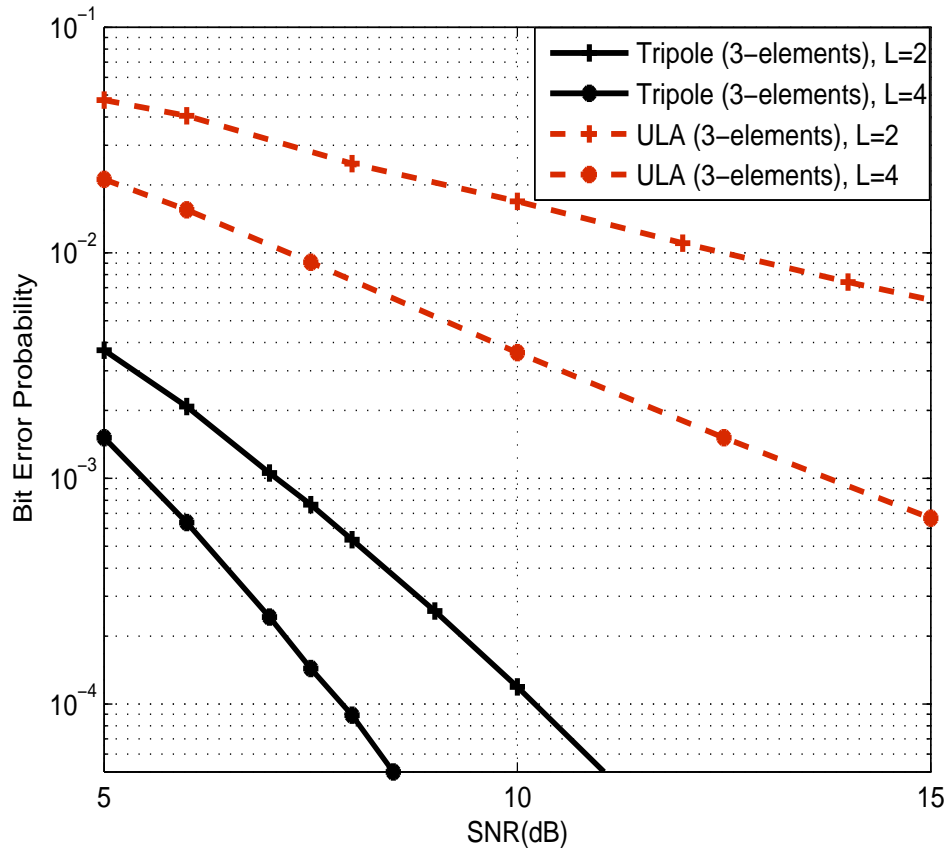


Figure 3.3: BER of ST-MMSE for a single tripole antenna (3-elements) and a linear antenna array (3-elements) for  $L = 2, 4$  multipaths and  $n = 5$  users.

ceiver is given in eq. 3.3, assuming the channel coefficients, spreading waveforms and delay spread are known at the receiver. On the same figure, the performance of the decorrelator, given by eq. 3.4, is plotted for  $L = 2, 4, 8$  equal-energy multipaths for both the desired and interference signals. From the plot, we see that both detectors give comparable performance for this situation, and are capable of exploiting the additional diversity provided by the time spread of the desired user.

In Fig. 3.2, the adaptive implementation of the ST-MMSE receiver is simulated for  $L = 2, 4$  multipaths and the tripole antenna. Using eq. 3.5, the LMS algorithm is implemented to estimate the channel coefficients with a step size of  $\mu = 0.001$ . For

each data block, the algorithm runs for 800 iterations then switches to the decision-directed mode given by eq. 3.6 for another 100 iterations. Again, we see that the tripole antenna is capable of exploiting the additional diversity provided by  $L = 4$  multipaths; however, the adaptive algorithm suffers a 1-1.5 dB performance loss relative to the non-adaptive case plotted in Fig. 3.1.

In Fig. 3.3, we compare the performance of the non-adaptive ST-MMSE receiver with a tripole antenna to the performance of a linear array with 3-elements. From the figure, the tripole antenna attains a considerable gain over the linear antenna array. For example, for  $L = 4$  paths and SNR=5.5 dB, the tripole antenna attains BER= $10^{-3}$  where as the ULA would require SNR=13.8 dB to achieve the same BER. This performance difference is most likely due to the fact that the ULA can sense only one polarization of the incident electric field, where as the tripole can detect all three components.

### 3.4 M-ary Orthogonal Modulation

We now consider the use of vector antennas in a multiuser setting, in which many transmitters communicate to a single receiver using  $M$ -ary orthogonal modulation. A channel model is presented for a beamformer-RAKE receiver for an uplink (mobile to base) CDMA system in multipath fading. This model is then used to compare the performance of vector antennas to that of uniform linear arrays that respond to single polarization. In this study, performance is measured by the number of users that each system can support. We compare the performance of vector antennas and ULAs in terms of capacity at given BER.

In direct-sequence code-division multiple-access (DS-CDMA), each user is assigned a unique spreading sequence with a low cross correlation, and bandwidth is shared by

all users. At the base station, since different users are distinguished by their spreading sequences, detection of the desired user is highly affected by multi-access interference (MAI) experienced from other users in the same cell and in neighboring cells. Also, multipath fading can result in intersymbol interference (ISI) at the receiver. Since CDMA is interference limited, the effects of MAI and fading typically limit the user capacity. Consequently, more sophisticated signal processing methods have to be used either at the base station or the mobile station to reduce interference and boost capacity.

In recent years, antenna arrays have been investigated at the base station to provide diversity and enhance interference cancelation in order to efficiently utilize the available capacity [35]. One way to increase capacity is adaptive beamforming with an antenna array to suppress co-channel interference by suppressing signals which occupy the same frequency band but are separated in the spatial domain.

The presence of multiuser interference can limit performance over fading multipath channels. However, space-time processing at the receiver can reduce the effects of multipath fading and interference by optimally combining the output of an antenna array to maximize signal-to-interference-plus-noise ratio (SINR). Naguib *et al* [36] have recently proposed a space-time RAKE receiver for linear antenna arrays in multiuser environments. This receiver employs adaptive beamforming to estimate the channel fading coefficients and multipath delays. This receiver is a 2-dimensional (space and time) extension of the classic 1-dimensional RAKE receiver (time only).

### 3.4.1 Adaptive Beamforming for CDMA

In the space-time RAKE receiver proposed by Naguib *et al* [36], signals are tracked in space and time by implementing a space-time correlator for each path. The space-time correlator consists of a spatial beamformer matched to the  $\ell$ -th multipath,

followed by a separate correlation in time. The outputs of the correlators are then summed by a conventional RAKE receiver. Other, blind adaptive beamforming techniques have been proposed for CDMA linear antenna arrays by both Naguib and Paulraj [36] and by Zoltowski and Ramos [64]. The adaptive beamformer-RAKE receiver in [36] is used to estimate the optimum weights that maximizes the SINR. A technique called code-filtering to estimate the channel fading path gains and MAI was implemented. This technique is based on finding the eigenvector corresponding to the largest eigenvalue by solving the generalized eigenvalue problem for the pre-correlation and post-correlation covariance matrices. This technique is considered to be blind since no training sequence is needed to estimate the unknown parameters, such as the channel fading gains. Details of this method are presented later in this chapter.

In this section, we consider the application of the space-time RAKE to receivers which employ vector antennas instead of uniform linear arrays. In particular, we consider the performance of CDMA signals in multiuser environments for an adaptive beamformer-RAKE receiver with  $M$ -ary orthogonal modulation for the uplink case. A mathematical derivation similar to that used by Naguib [60] is given, except that we consider an antenna with a different geometry. In the linear array case, only the azimuth angle of a multipath is detected; in vector antennas, both the azimuth and elevation of an incident multipath can be exploited. In outdoor rural environments, the distinction between these antennas may not be significant, since the variation in elevation among multipaths is probably not significant. However, in indoor or urban environments, where elevation varies more widely, vector antennas and linear antenna arrays may yield very different performance.

Adaptive beamforming for the vector antenna has previously been considered by Compton [85] for the case of a narrowband system with three mutually-orthogonal

dipoles. The polarization states of the desired user and one interfering user at the receiver were studied. An analytical expression for the SINR was derived based on the least-mean-square (LMS) criterion. In contrast, our work focuses on the adaptive detection of CDMA signals, where performance is measured by BER.

### 3.4.2 System Model

For coherent detection, a pilot signal is usually required to estimate the channel. Coherent detection is usually used only in the downlink (base to mobile), since the base station uses a pilot signal for identification, while for the uplink each user would need a pilot signal to allow the base station to separate users in the cell. The absence of carrier phase and amplitude information on the uplink therefore makes  $M$ -ary orthogonal modulation with noncoherent reception or differential detection (e.g., DPSK) desirable. We will assume that users have time synchronization, but signal phase and amplitude are not available at the base station.

For noncoherent detection in the uplink, a beamformer-RAKE receiver was proposed by Naguib *et al* [60]. In this paper, the authors consider an uplink scenario in which many users transmit to a single base station which employs a multi-element antenna array. Each user sends an  $M$ -ary orthogonal Walsh code for data modulation followed by a long code sequence. The output of the long code spreading sequence is further spread by an in-phase and quadrature short code sequence. At the base station, the beamformer-RAKE receiver tracks the signal for a specific user in space and time and the optimum weights are estimated by the code-filtering approach. Analytical results were given for the system capacity in terms of the number of users in multipath environment.

In this section, we consider a DS-CDMA uplink employing  $M$ -ary orthogonal modulation similar to the one in [60], in which vector antennas are used at the base

station rather than linear arrays. Our aim is to compare the performance of linear antenna arrays that respond to only one polarization component to that of vector antennas.

We assume the channel to be a frequency-selective, Rayleigh fading channel. User  $i$ 's signal arrives at the base station from  $L_i$  different multipaths, where the multipath delays follow a uniform distribution over  $[0, \tau_{max}]$ , and  $\tau_{max}$  is the maximum delay spread of the channel. At the mobile, a sequence of  $J = \log_2 M$  data bits is used to select one of  $M$  orthogonal Walsh codes to be used for transmission. The Walsh code is then spread by a long pseudonoise (PN) spreading waveform sequence  $c_i(t)$ . Following the direct spreading, the channel is spread in quadrature. The in-phase and quadrature components are spread by short sequences denoted by  $a^I(t)$  and  $a^Q(t)$ , respectively, with a shorter period than  $c_i(t)$ . The transmitted signal for the  $i$ -th mobile can be written as

$$s_i^h(t) = \sqrt{P_i} [W^h(t)c_i(t)a^I(t) \cos(w_ct) + W^h(t)c_i(t)a^Q(t) \sin(w_ct)], \quad 0 \leq t \leq T_w$$

where  $P_i$  is the transmitted power for user  $i$  and  $W^h$  is the  $h^{th}$  orthogonal Walsh code,  $h = 1, \dots, M$ . The processing gain is  $N_c = \frac{T_w}{T_c}$ , where  $T_w$  is the symbol period and  $T_c$  is the chip period. For simplicity as in [60], the product of the user's PN code and the in-phase and quadrature component are represented as

$$c_i^I(t) = c_i(t)a^I(t) \quad \text{and} \quad c_i^Q(t) = c_i(t)a^Q(t).$$

To simplify our analysis, the in-phase and quadrature components can be represented by [62]

$$\begin{aligned} c_i^I(t) &= \sum_{r=-\infty}^{\infty} c_{i,r}^I p(t - rT_c) \\ c_i^Q(t) &= \sum_{r=-\infty}^{\infty} c_{i,r}^Q p(t - rT_c) \end{aligned}$$

where  $c_{i,r}^I$  and  $c_{i,r}^Q$  are assumed to be independent and identically distributed random variables which are equally likely to be  $-1$  or  $+1$ . Here the chip pulse  $p(t)$  is assumed to be a rectangular waveform.

At the base station, the signal detected at the vector antenna due to the  $\ell$ -th multipath component of the  $i$ -th user is

$$Y_{i,\ell}(t) = \mathbf{G}_{i,\ell} s_i^h(t - \tau_{i,\ell})$$

where  $\tau_{i,\ell}$  is the delay of the  $\ell$ -th multipath of the  $i$ -th user and  $\mathbf{G}_{i,\ell}$  is the  $t_{em} \times 1$  channel response. Here we assume that  $\mathbf{G}_{i,\ell}$  consists of the appropriate  $t_{em}$  ( $1 \leq t_{em} \leq 6$ ) components of  $B(\theta_{i,\ell}, \varphi_{i,\ell})\mathbf{Z}_{i,\ell}$  and

$$B(\theta_{i,\ell}, \varphi_{i,\ell}) = \begin{bmatrix} -\sin \theta_{i,\ell} & \cos \theta_{i,\ell} \cos \varphi_{i,\ell} \\ \cos \theta_{i,\ell} & \sin \theta_{i,\ell} \cos \varphi_{i,\ell} \\ 0 & -\sin \varphi_{i,\ell} \\ \cos \theta_{i,\ell} \cos \varphi_{i,\ell} & \sin \theta_{i,\ell} \\ \sin \theta_{i,\ell} \cos \varphi_{i,\ell} & -\cos \theta_{i,\ell} \\ -\sin \varphi_{i,\ell} & 0 \end{bmatrix}$$

is the antenna response (eq. 2.1). The complex vector  $\mathbf{Z}_{i,\ell}$  reflects the change in amplitude, phase, and polarization experienced by the  $\ell^{th}$  multipath component of the  $i$ -th user. The components of vector  $\mathbf{Z}_{i,\ell}$  are modeled as i.i.d. zero-mean complex Gaussian random variables and therefore the elements of  $\mathbf{G}_{i,\ell}$  are also zero-mean complex Gaussian random variables.

The total received signal at the base station will be a superposition of the multipaths due to all  $n$  users plus noise, which is given by

$$Y(t) = \sum_{i=1}^n \sum_{\ell=1}^{L_i} Y_{i,\ell}(t) + N(t) \quad (3.8)$$

where  $N(t)$  is AWGN. We will consider detecting the first user, where the multipath delays are assumed to be perfectly estimated at the receiver.

The block diagram of the receiver is shown in Fig. 3.4 where the received signal is fed into a bank of  $M$  orthogonal Walsh correlators at each path delay. The output of the post-correlation for the signal vector for the  $k^{th}$  tracked path for the first user and the  $m$ -th Walsh code is

$$\begin{aligned}\tilde{Y}_{1,k}^m &= \frac{1}{\sqrt{T_w}} \int_{\tau_{1,k}}^{\tau_{1,k}+T_w} Y(t) s_1^{m*}(t - \tau_{1,k}) dt \\ &= \begin{cases} d_{1,k}^m + u_{1,k}^m, & \text{if } m = h \\ u_{1,k}^m, & \text{if } m \neq h \end{cases}\end{aligned}$$

where

$$\begin{aligned}d_{1,k}^m &= \sqrt{T_w P_1} \mathbf{G}_{1,k} && \text{is the desired signal,} \\ u_{1,k}^m &= \text{mai}_{1,k}^m + s_{1,k}^m + n_{1,k}^m && \text{is total interference,}\end{aligned}$$

and  $\text{mai}_{1,k}^m$  is the multi-access interference from other users,  $s_{1,k}^m$  is a self-interference from multipath for the first user and  $n_{1,k}^m$  is due to the AWGN. The self- and multi-access interference (MAI) can be expressed as

$$\begin{aligned}s_{1,k}^m &= \sum_{\ell=1, \ell \neq k}^{L_1} \frac{1}{\sqrt{T_w}} \int_{\tau_{1,k}}^{\tau_{1,k}+T_w} Y_{1,\ell}(t) s_1^{m*}(t - \tau_{1,k}) dt \\ &= A_1 \sum_{\ell=1, \ell \neq k}^{L_1} I_{1,k,1,\ell}^m \mathbf{G}_{1,\ell} \\ &= A_1 \sum_{\ell=1, \ell \neq k}^{L_1} [(I_{1,k,1,\ell}^{m,II} + I_{1,k,1,\ell}^{m,QQ}) \\ &\quad + j(-I_{1,k,1,\ell}^{m,IQ} + I_{1,k,1,\ell}^{m,QI})] \mathbf{G}_{1,\ell} \\ \text{mai}_{1,k}^m &= \sum_{i=2}^n \sum_{\ell=1}^{L_i} \frac{1}{\sqrt{T_w}} \int_{\tau_{1,k}}^{\tau_{1,k}+T_w} Y_{i,\ell}(t) s_1^{m*}(t - \tau_{1,k}) dt \\ &= \sum_{i=2}^n \sum_{\ell=1}^{L_i} A_i I_{1,k,i,\ell}^m \mathbf{G}_{i,\ell} \\ &= \sum_{i=2}^n \sum_{\ell=1}^{L_i} A_i [(I_{1,k,i,\ell}^{m,II} + I_{1,k,i,\ell}^{m,QQ}) \\ &\quad + j(-I_{1,k,i,\ell}^{m,IQ} + I_{1,k,i,\ell}^{m,QI})] \mathbf{G}_{i,\ell}\end{aligned}$$

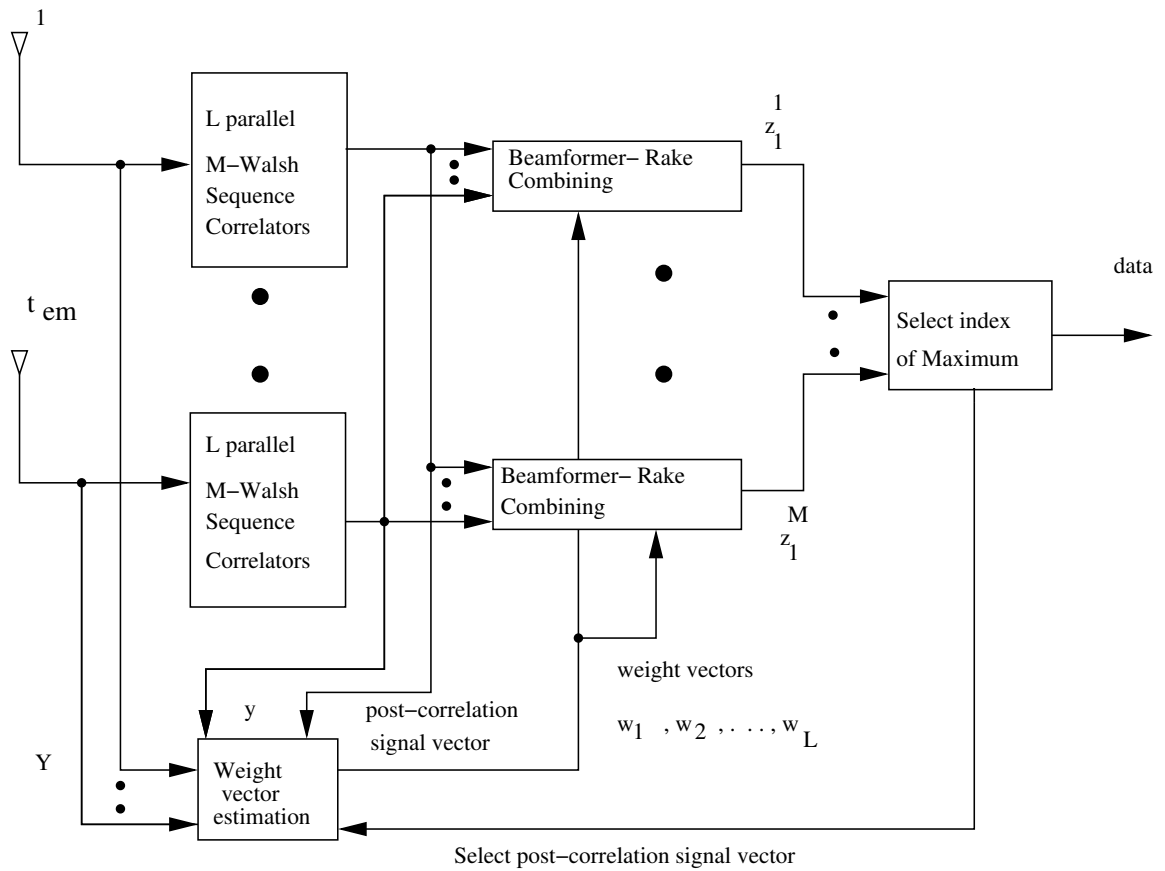


Figure 3.4: Receiver block diagram

where  $A_i = \sqrt{P_i}$  and  $I_{1,k,i,\ell}^{m,II}$ ,  $I_{1,k,i,\ell}^{m,QQ}$ ,  $I_{1,k,i,\ell}^{m,IQ}$ , and  $I_{1,k,i,\ell}^{m,QI}$  are defined as

$$I_{1,k,i,\ell}^{m,II} = \frac{1}{\sqrt{T_w}} \int_{\tau_{1,k}}^{\tau_{1,k}+T_w} W^h(t - \tau_{i,\ell}) c_i^I(t - \tau_{i,\ell}) \times W^m(t - \tau_{1,k}) c_1^I(t - \tau_{1,k}) dt$$

$$I_{1,k,i,\ell}^{m,QQ} = \frac{1}{\sqrt{T_w}} \int_{\tau_{1,k}}^{\tau_{1,k}+T_w} W^h(t - \tau_{i,\ell}) c_i^Q(t - \tau_{i,\ell}) \times W^m(t - \tau_{1,k}) c_1^Q(t - \tau_{1,k}) dt$$

$$I_{1,k,i,\ell}^{m,IQ} = \frac{1}{\sqrt{T_w}} \int_{\tau_{1,k}}^{\tau_{1,k}+T_w} W^h(t - \tau_{i,\ell}) c_i^I(t - \tau_{i,\ell}) \times W^m(t - \tau_{1,k}) c_1^Q(t - \tau_{1,k}) dt$$

$$\begin{aligned}
I_{1,k,i,\ell}^{m,QI} &= \frac{1}{\sqrt{T_w}} \int_{\tau_{1,k}}^{\tau_{1,k}+T_w} W^h(t - \tau_{i,\ell,i}) c_i^Q(t - \tau_{i,\ell}) \\
&\times W^m(t - \tau_{1,k}) c_1^I(t - \tau_{1,k}) dt.
\end{aligned}$$

Note that  $I_{1,k,i,\ell}^{m,II}$ ,  $I_{1,k,i,\ell}^{m,IQ}$ ,  $I_{1,k,i,\ell}^{m,QI}$ ,  $I_{1,k,i,\ell}^{m,QQ}$  are all zero-mean random variables.

In [63], it is shown analytically that, for large processing gain  $N_c$ , the total interference vector  $i_{1,k}^m = mai_{1,k}^m + s_{1,k}^m$  can be modeled as a zero-mean, complex Gaussian  $\mathcal{CN}(\mathbf{0}, \mathbf{I})$ . Simulation results presented in [60] also show that, for large  $n \times L$ , the total interference is spatially white. We therefore model  $i_{1,k}^m$  as a zero-mean Gaussian vector in this work, independent of  $m$ .

To estimate the optimum beamformer weights using the code-filtering approach [60], the pre-correlation and post-correlation covariance matrices  $R_{YY}$  and  $R_{\tilde{Y}\tilde{Y}}$  are estimated from the received signal pre- and post-correlation, respectively. The covariance of the pre-correlation signal vector  $Y(t)$  is given by

$$R_{YY} = E[Y(t)Y^\dagger(t)] = P_1 \mathbf{G}_{1,k} \mathbf{G}_{1,k}^\dagger + R_{uu_{1,k}},$$

the post-correlation signal vector is

$$R_{\tilde{Y}\tilde{Y}_{1,k}} = \frac{1}{T_c} E[\tilde{Y}_{1,k}^m \tilde{Y}_{1,k}^{m\dagger}] = N_c P_1 \mathbf{G}_{1,k} \mathbf{G}_{1,k}^\dagger + R_{uu_{1,k}},$$

and interference-plus-noise covariance is

$$R_{uu_{1,k}} = \sum_{\ell=1, \ell \neq k}^{L_1} P_1 \mathbf{G}_{1,\ell} \mathbf{G}_{1,\ell}^\dagger + \sum_{i=2}^n \sum_{\ell=1}^{L_i} P_i \mathbf{G}_{i,\ell} \mathbf{G}_{i,\ell}^\dagger + \sigma_n^2 \mathbf{I}.$$

To estimate the channel vector  $\mathbf{G}_{1,k}$ , we solve the generalized eigenvalue problem corresponding to the largest eigenvalue of the Hermitian positive-definite matrix pencil  $R_{\tilde{Y}\tilde{Y}_{1,k}} = \lambda R_{YY}$  [86]. In other words, we solve for the generalized eigenvalue to estimate  $\mathbf{G}_{1,k}$

$$R_{\tilde{Y}\tilde{Y}_{1,k}} \mathbf{G}_{1,k} = \lambda R_{YY} \mathbf{G}_{1,k}.$$

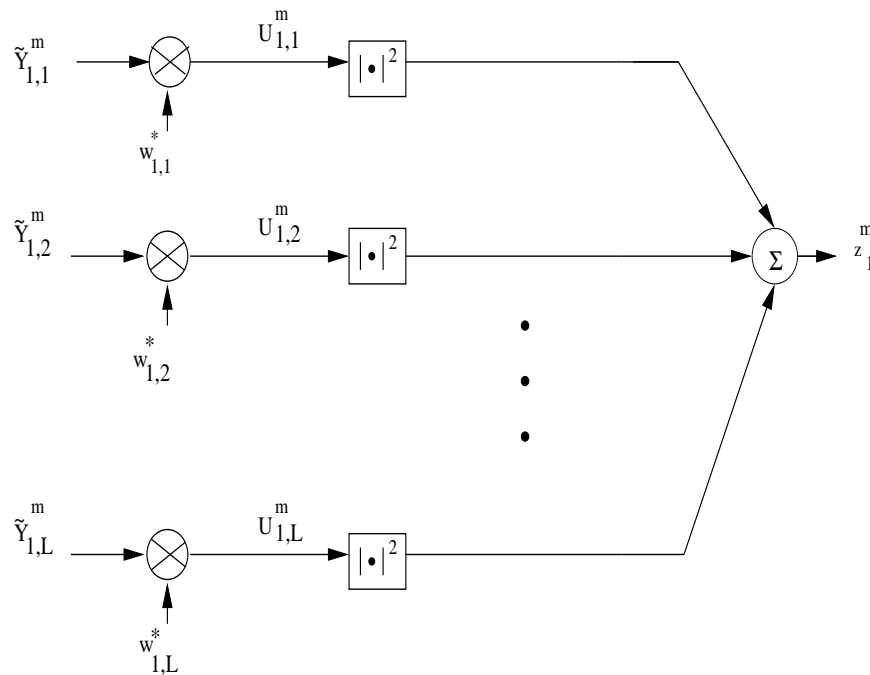


Figure 3.5: Beamforming and noncoherent RAKE

The code-filtering approach used to estimate the channel vector  $\mathbf{G}_{1,k}$  and the optimum weights  $w_{1,k}$  is given in [60].

Once the  $\mathbf{G}_{1,k}$  and  $w_{1,k}$  have been estimated, the signal can be combined using the RAKE receiver (see Fig. 3.5) which non-coherently combines the  $L_1$  multipaths. The output is then given by

$$z_1^m = \sum_{k=1}^{L_1} z_{1,k}^m = \sum_{k=1}^{L_1} |w_{1,k}^\dagger \tilde{Y}_{1,k}^m|^2 \quad m = 1, \dots, M. \quad (3.9)$$

The symbol transmitted by the 1<sup>st</sup> user is now obtained by a hard decision [1] on the output of non-coherent RAKE:

$$\hat{h} = \arg \max_{m=1, \dots, M} z_1^m. \quad (3.10)$$

### 3.4.3 BER Analysis

The optimum weight of the beamformer that maximizes the signal-to-interference-plus-noise ratio (SINR) is given by [47]

$$w_{1,k} = \xi R_{uu_{1,k}}^{-1} \mathbf{G}_{1,k}. \quad (3.11)$$

Assuming that the MAI is spatially and temporally white ( $R_{uu_{1,k}} = \sigma \mathbf{I}$ ) and  $\sigma^2 = \sigma_I^2 + \sigma_n^2$ , we can write the optimum beamforming weight of the first user as

$$w_{1,k} = \xi \mathbf{G}_{1,k}$$

where  $\xi$  is an arbitrary constant that does not change the beamformer output SINR. Hereafter we set  $\xi = 1$ . For simplicity, set  $L = L_i$  for all  $i$  users.

The calculation of the  $m$ -th decision statistic for user 1 is illustrated in Fig. 3.5. Observe that the input to the square-law in the  $k$ -th branch is given by

$$U_{1,k}^m = \begin{cases} A_1 \sqrt{T_w} \mathbf{G}_{1,k}^\dagger \mathbf{G}_{1,k} + w_{1,k}^\dagger u_{1,k}^m & \text{if } m = h \\ w_{1,k}^\dagger u_{1,k}^m & \text{if } m \neq h \end{cases}$$

where  $w_{1,k}^\dagger u_{1,k}^m$  is a zero-mean complex Gaussian random variable with variance  $\sigma^2$ . The decision variables for the first user are then

$$z_1^m = \sum_{\ell=1}^L |U_{1,\ell}^m|^2, \quad m = 1, \dots, M.$$

For  $m = h$ , conditioned on  $A_1$  and  $\mathbf{G}_{1,k}$  [1],  $z_1^m$  has the non-central  $\chi^2$  distribution with  $4L$  degrees of freedom and noncentral parameter [60]

$$\mathcal{E} = P_1 T_w \sum_{\ell=1}^L \mathbf{G}_{1,k}^\dagger \mathbf{G}_{1,k}$$

which is the symbol energy. For the case of  $t_{em} = 3, 6$  and  $m \neq h$ ,  $z_1^m$  has the central  $\chi^2$  distribution with  $4L$  degrees of freedom.

The conditional probability density function (pdf) of  $z_1^m$  given the symbol energy-to-interference-plus-noise ratio  $\gamma_s = \frac{\mathcal{E}}{\sigma^2}$  is therefore

$$f_{z_1^m}(z|\gamma_s) = \begin{cases} \frac{1}{\sigma^2} \left(\frac{z}{\sigma^2 \gamma_s}\right)^{2L-1} e^{-\frac{\gamma_s \sigma^2 + z}{\sigma^2}} I_{2L-1} \left(\sqrt{\frac{4\gamma_s z}{\sigma^2}}\right), & m = h \\ \frac{1}{\sigma^{4L} \Gamma(2L)} z^{2L-1} e^{-z/\sigma^2}, & m \neq h \end{cases}$$

where  $I_L(\cdot)$  is the modified Bessel function of the  $L^{\text{th}}$  order and  $\Gamma(\cdot)$  is the Gamma function [41].

Given the pdfs above, we can now calculate the probability of error. For simplicity, assume without loss of generality that the first Walsh symbol was transmitted, so  $h = 1$ . Then the conditional error probability given  $\gamma_s$  is given by

$$\begin{aligned} P_M(\gamma_s) &= 1 - P_c(\gamma_s) \\ &= 1 - P(z_1^2 < z_1^1, z_1^3 < z_1^1, \dots, z_1^M < z_1^1 | \gamma_s) \\ &= 1 - \int_0^\infty [P(z_1^2 < z | z_1^1 = z)]^{M-1} f_{z_1^1}(z | \gamma_s) dz \end{aligned}$$

where

$$P(z_1^2 < z | z_1^1 = z) = 1 - e^{-\frac{z}{\sigma^2}} \sum_{\ell=0}^{2L-1} \frac{1}{\ell!} \left(\frac{z}{\sigma^2}\right)^\ell.$$

If  $\mathbf{G}_{i,\ell}$  is a zero-mean complex Gaussian random vector, then  $\gamma_s$  has a  $\chi^2$  probability density function (pdf) with  $4L$  degrees of freedom [60]:

$$f_{\gamma_s}(\gamma) = \frac{\gamma^{2L-1}}{(\bar{\gamma})^{2L} (2L-1)!} e^{-\gamma/\bar{\gamma}} \quad (3.12)$$

Averaging over  $f_{\gamma_s}(\gamma)$ , we obtain the unconditional pdf of  $z_1^m$  for  $h = m$

$$\begin{aligned} f_{z_1^m}(z) &= \int_0^\infty f_{z_1^1}(z | \gamma_s) f_{\gamma_s}(\gamma) d\gamma \\ &= \frac{z^{2L-1}}{\sigma^{4L} (1 + \bar{\gamma})^{2L} (2L-1)!} e^{-z/\sigma^2(1+\bar{\gamma})} \end{aligned} \quad (3.13)$$

where  $\bar{\gamma} = \frac{P_1 T_w}{L \sigma^2}$  is the average SINR-per-path-per-antenna.

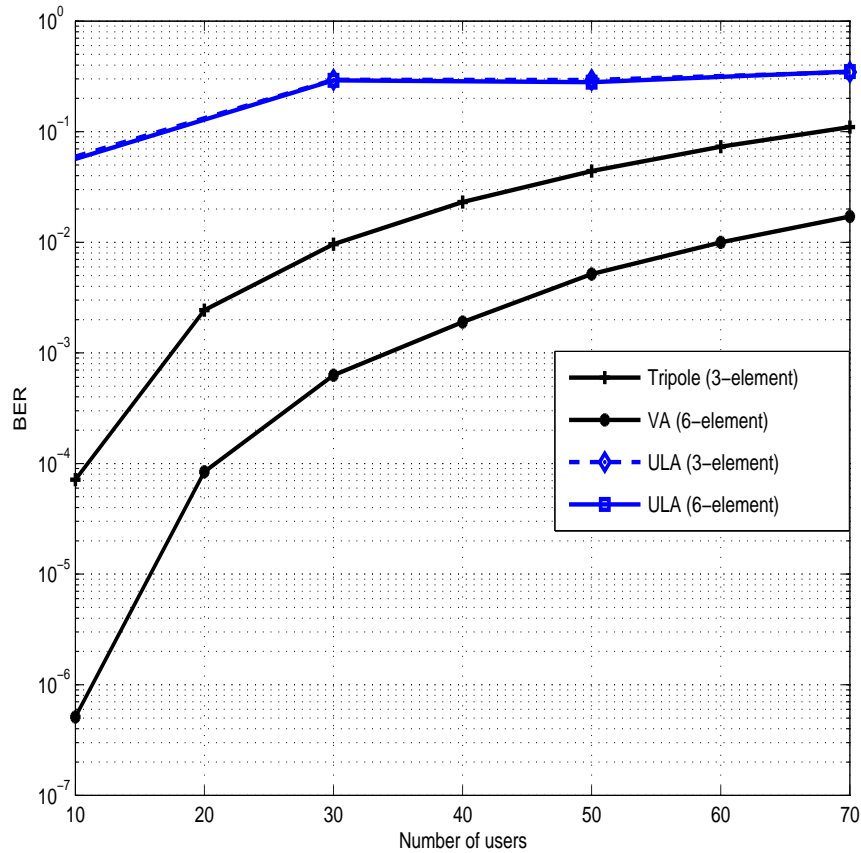


Figure 3.6: BER of 3- and 6-element vector antennas compared with linear antenna arrays with 3 and 6 elements for  $L=3$  multipaths.

Using eq. 3.13, we can write the average symbol-error-probability of  $M$ -ary orthogonal modulation for vector antennas as

$$P_M = 1 - \int_0^\infty \left[ 1 - e^{-\frac{z}{\sigma^2}} \sum_{\ell=0}^{L-1} \frac{1}{\ell!} \left( \frac{z}{\sigma^2} \right)^\ell \right]^{M-1} f_{z_1}(z) dz \quad (3.14)$$

and the bit-error-probability becomes

$$P_b = \frac{2^{J-1}}{2^J - 1} P_M$$

where  $J = \log_2 M$ .

To compare the performance of the vector antenna array to a uniform linear array (ULA), we use the equivalent ULA model presented in eq. 3.7.

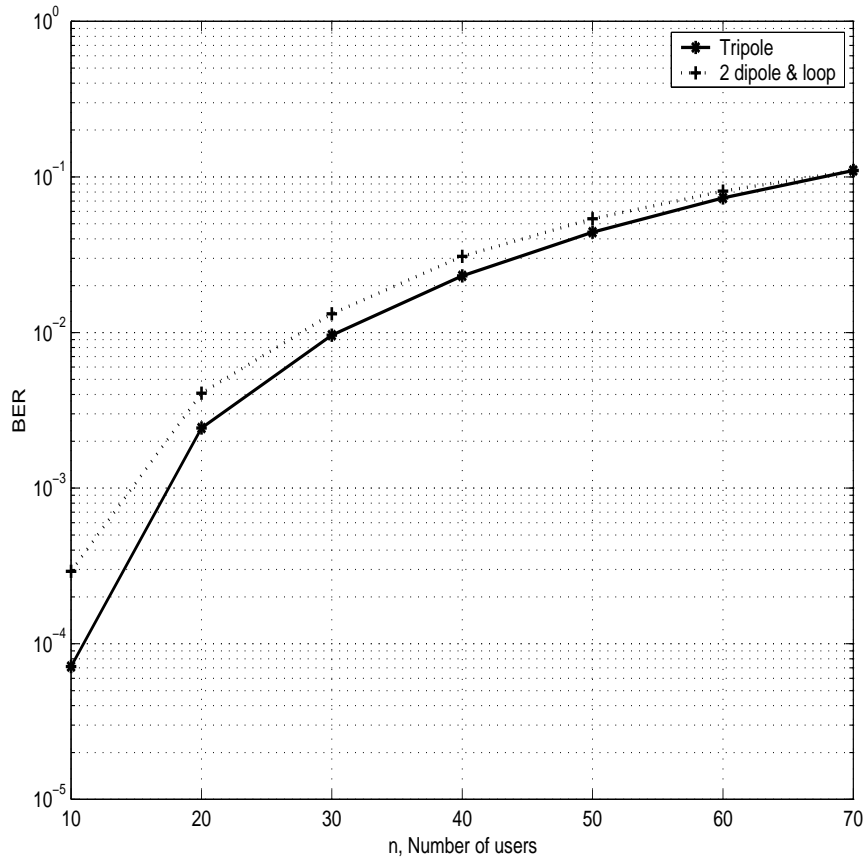


Figure 3.7: BER of the tripole and the 2-dipole and loop vector antenna from [42] for  $L=3$  multipaths.

From Naguib and Paulraj [60], for  $t_{em}$ -element uniform linear array,  $\gamma_s$  has a  $\chi^2$  probability density function (pdf) with  $2L$  degrees of freedom:

$$f_{\gamma_s}(\gamma) = \frac{\gamma^{L-1}}{(\bar{\gamma}t_{em})^L(L-1)!} e^{-\gamma/\bar{\gamma}}. \quad (3.15)$$

Using eq. 3.15, the average symbol-error-probability of  $M$ -ary orthogonal modulation for the ULA is therefore given by

$$P_M^{ULA} = 1 - \int_0^\infty \left[ 1 - e^{-\frac{z}{\sigma^2}} \sum_{\ell=0}^{L-1} \frac{1}{\ell!} \left( \frac{z}{\sigma^2} \right)^\ell \right]^{M-1} f_{z_1}(z) dz.$$

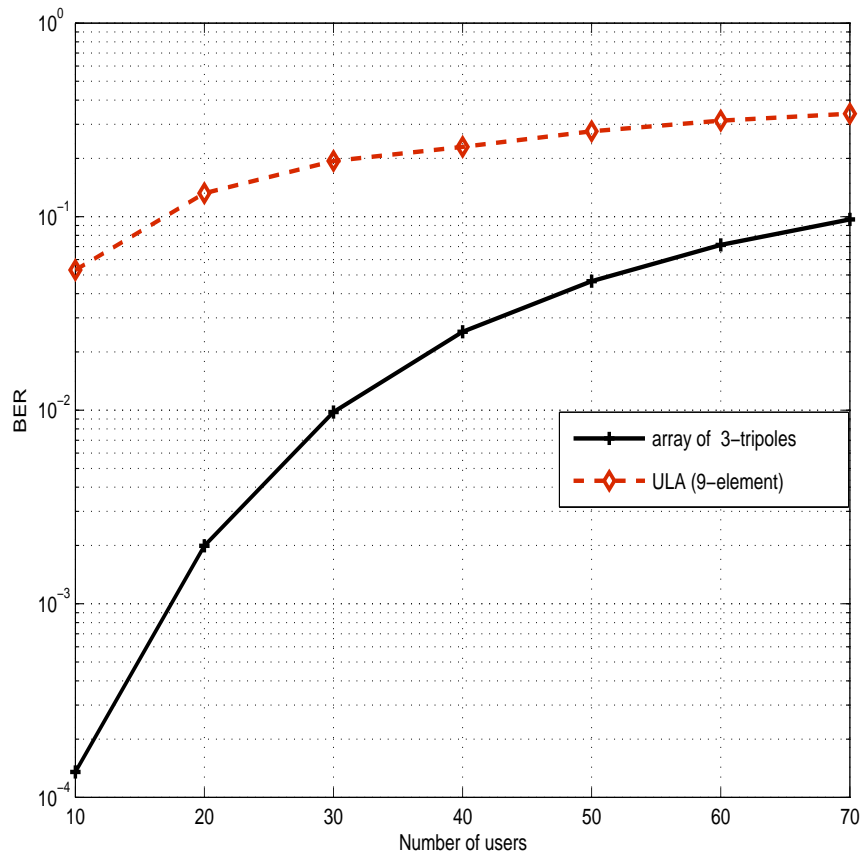


Figure 3.8: BER of a linear array of 3 tripoles and a 9-element ULA for  $L=3$  multipaths.

### 3.4.4 Numerical Results

We now evaluate the performance of the beamformer-RAKE receiver for  $M$ -ary orthogonal modulation system and noncoherent combining described in the previous sections. Each of the desired and interference signals is assigned its own random spreading sequence with a processing gain  $N_c = 256$ . The simulated performance of the beamformer-RAKE receiver for eq. 3.9 and the weight vector given in eq. 3.11 is considered. In these simulations, we consider uniform linear arrays and vector antennas that consist of  $t_{em} = 3, 6$  elements at the receiver. The multipath components of the desired and interference signals are uniformly distributed on a sphere where

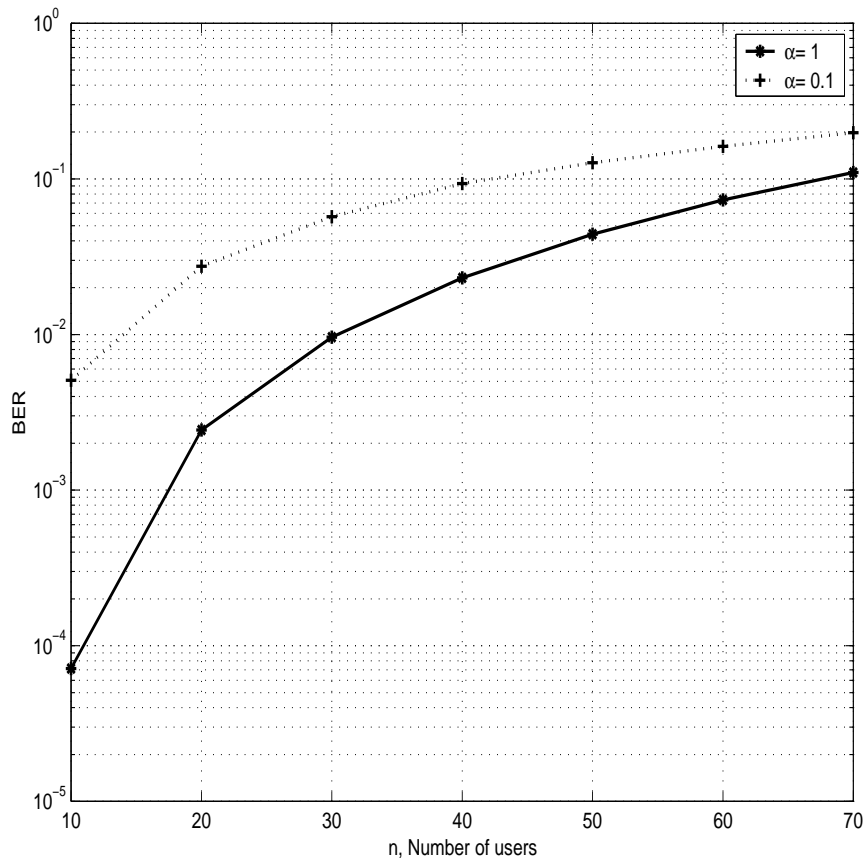


Figure 3.9: BER of tripole antenna for  $\alpha = 0.1$  and  $1$  and  $L=3$  multipaths.

the azimuth angles  $\theta_{i,l}$  and elevation angles  $\varphi_{i,l}$  are as previously described in Section 3.3, and the polarizations  $\mathbf{Z}_{i,l}$  are i.i.d.  $\mathcal{CN}(\mathbf{0}, \mathbf{I})$ . The noise is spatially and temporally Gaussian with covariance  $\sigma^2 \mathbf{I}$ . For all users, we assume equal number of  $L = 3$  multipaths, and that the user's signals arrive with the same power at the base station.

In Fig. 3.6, the performance of vector antennas and linear antenna arrays with the same number of antenna elements ( $t_{em} = 3, 6$ ) is plotted. Note that the tripole antenna outperforms both the  $t_{em}=3,6$  ULAs. Further note that at  $\text{BER}=10^{-3}$  the tripole antenna can accommodate about 17 users while the ULA will accommodate  $< 10$  users. The ability of the tripole antenna to detect 3-electric component increases its

ability to cancel the interference. Further, the 6-element vector antennas outperform both the tripole and ULA. The capacity gain of vector antennas with 6-elements over the tripole antenna is due to the extra components of magnetic field detected.

In Fig. 3.7, we compare two 3-element vector antennas: the tripole antenna and the antenna proposed in [42], which consists of two dipoles and a loop. At  $\text{BER}=10^{-3}$ , the tripole antenna accommodate 17 users while the 2-dipole and loop support only 15 users. For large  $n$ , the geometry of the antenna has little effect and both antenna systems support the same number of users. Once again, the tripole antenna most likely outperforms the antenna from [42] due to the fact that the latter antenna cannot detect same signals that arrive in the plane of the antenna.

In Fig 3.8, we compare a linear array of 3-tripoles spaced a distance of  $\lambda/2$  apart with a 9-element ULA. From the figure, we see that the tripole array significantly outperforms the ULA over the entire range of users considered.

We now consider the impact of the polarization of the received signal on the performance of the tripole antenna. In previous simulations we have taken  $\mathbf{Z}_{i,\ell}$  to be i.i.d.  $\mathcal{CN}(\mathbf{0}, \mathbf{I})$ . We now consider  $\mathcal{CN}(\mathbf{0}, \mathbf{I})$  to be i.i.d.  $\mathcal{CN}(0, \boldsymbol{\Sigma}_{\mathbf{z}})$  where

$$\boldsymbol{\Sigma}_{\mathbf{z}} = \begin{bmatrix} \alpha^2 & 0 \\ 0 & 2 - \alpha^2 \end{bmatrix}.$$

Here  $\alpha$  is a parameter that controls the relative power of the horizontal and vertical components of  $\mathbf{Z}_{i,\ell}$ . When  $\alpha^2 = 0$  or  $2$ , the signal is vertically or horizontally polarized, respectively. When  $\alpha^2 = 1$ , equal power is allocated to both polarizations.

In Fig. 3.9, we consider the performance of a single tripole for the same conditions as in Fig. 3.7 ( $\alpha = 1$ ) compared with the performance of this system for a nearly horizontally polarized received signal  $\alpha = 0.1$ . Note that the performance of the near-linearly polarized system is much worse than that obtained when both polarization have equal energy. This is not surprising, since a linearly polarized signal

is intrinsically less diverse than a signal with two, independent polarizations. We remark here that the performance of the ULA would be far worse than the tripole, since the dipoles in the ULA would not be able to detect the horizontally polarized multipaths.

### 3.5 Conclusions

We have studied multiuser receivers for vector antennas and ULAs for CDMA multipath signals with BPSK modulation and a frequency-selective Rayleigh fading channel. The ST-MMSE and ST-DD receiver with 3-element vector antennas both give comparable performance and demonstrate the ability to exploit the added diversity in  $L = 2, 4, 8$  multipaths. The ST-MMSE with vector antennas also outperforms the ST-MMSE with a ULA for  $L = 2, 4$  multipaths. We further considered an adaptive space-time MMSE receiver based on the LMS algorithm. The adaptive algorithm combined with the tripole antennas captures most of the diversity gain of the channel, but suffers a 1-1.5 dB performance loss compared to the non-adaptive case.

Next we studied the performance of multiuser receivers with vector antennas and ULAs for  $M$ -ary orthogonal modulation systems. Our simulations suggest that the vector antenna outperform the ULAs in all cases in terms of the number of users that can be supported at a given SNR. This gain is due to the fact that vector antennas can detect additional electric and magnetic components in the incident field while ULA can respond to only one polarization. We have also studied the impact of polarization on the performance of vector antennas. We have considered the tripole antenna for two cases: one case is the near-linearly polarized and other case is horizontally and vertically polarized components of the signal. From simulations, the performance of the antenna with two polarization components outperforms the linear

polarization case. These results suggest that linear polarization provides less diversity to interference than an antenna with two equal-energy polarization components.

## Chapter 4

# MIMO Systems based on Vector Antennas

In previous chapters, we considered the impact of vector antennas on the performance of diversity systems in both single-user and multiuser scenarios. In this chapter we investigate the performance of vector antennas for a single-user MIMO system in a multipath environment. The vector antenna considered here is the tripole antenna system, deployed at both the transmitter and receiver. For this system, we consider two MIMO transmission schemes: V-BLAST and channel inversion (CI). The performance of the tripole antenna with i.i.d. fading path gains and empirically measured path gains are compared in terms of the BER. This chapter is organized as follows: In Section 4.1, we give introduction to the V-BLAST algorithm and, in Section 4.1.1, we present the channel model. The simulation results are given in Section 4.1.2. We introduce channel inversion in Section 4.2 and simulation results are given in Section 4.2.1. Finally, we give our conclusions in Section 4.3 .

## 4.1 V-BLAST

Communication systems that exploit multiple antennas at both the transmitter and receiver end are known as multiple-input-multiple-output (MIMO) systems. In rich multipath environments, MIMO systems can achieve a significant higher ergodic capacity than conventional single-antenna systems [78]. One of the first practical MIMO algorithms which was proposed to access these high data rates was the Bell Labs Layered Space-Time (BLAST) algorithm. The first variant of this algorithm, called Diagonal BLAST (D-BLAST), was proposed by Foschini [77] in his seminal 1996 paper. The D-BLAST algorithm divides the data into  $t$  distinct streams equal to the number of transmit antennas. Each stream is then transmitted successively on each of the  $t$  transmit antennas. While D-BLAST can achieve very high data rates, it is also quite complex. Consequently, Wolniansky *et al* [79] have proposed a simplified alternative algorithm known as Vertical BLAST (V-BLAST). In V-BLAST, the data are again divided into  $t$  distinct data streams, but each data stream is now assigned to a fixed transmit antenna. At the receiver, interference cancelation techniques are used to separate the data streams. Note that this requires that the number of receive antennas  $r$  be greater than the number of transmit antennas,  $r \geq t$ .

V-BLAST is considered to be a spatial multiplexing scheme in which substreams of independent data are transmitted over different antennas. Each substream typically has the same constellation at the transmitter. At the receiver, zero-forcing (ZF) or minimum mean-square error (MMSE) receivers are often used to successively detect and cancel each data stream, in a process similar to multiuser detection in CDMA [56] except that a single user is assumed here. In general, V-BLAST detectors either seek to detect the data stream associated with the transmit antenna having the highest SNR (signal-to-noise ratio) in each iteration, or the streams are detected in a fixed deterministic or random order. In [79], Wolniansky *et al* have implemented

a V-BLAST system with  $t = 8$  transmit and  $r = 12$  receive antennas in an indoor environment. Using a zero-forcing detector at the receiver, their results showed that V-BLAST can achieve a spectral efficiency of 20 - 40 bps/Hz at SNRs from 24 dB to 34 dB in a rich scattering environment.

Prior work has considered V-BLAST systems which use uniform linear arrays at the transmitter and receiver. In this chapter we investigate the use of vector antennas that are collocated at one point in space, and which can detect up to six components of the EM field. Previous work by Konanur *et al* [80] has shown that deploying vector antennas at the transmitter and receiver can provide capacity gains comparable to those of ULAs with the same number of antennas. In this work, we will investigate the performance of a V-BLAST system which employs vector antennas at the transmitter and receiver. To calculate performance, we will use empirically measured fading path gains for one tripole antenna transmitting to another in an indoor environment, as reported in [80]. These empirical measurements correspond to the first  $3 \times 3$  measurements for the antenna system in [80]. The bit-error rate for V-BLAST with empirically-measured and i.i.d. channel samples are then compared.

#### 4.1.1 Transmission Algorithm

We consider a MIMO system that consists of a tripole antenna (i.e. three mutually orthogonal electric dipoles) deployed at both the transmitter and receiver. First, we introduce the channel model used in our simulations. Under flat-fading conditions, the received signal can be written as

$$Y = \sqrt{\gamma_t} H \mathbf{b} + N. \quad (4.1)$$

Here  $\gamma_t = \frac{\gamma_r}{t}$ , where  $\gamma_r$  is the signal-to-noise ratio per receive antenna, and  $t = 3$  denotes the number of transmit antennas and  $H = \{h_{ij}\}$  is an  $r \times t$  matrix of complex

fading path gains, the transmitted data  $\mathbf{b} = [b_1, \dots, b_t]^T$ , is an  $t \times 1$  vector of signals chosen from the unit-energy BPSK constellation  $\{+1, -1\}$ , and  $N$  is an  $r \times 1$  vector of complex white Gaussian noise (AWGN) with mean zero and covariance  $\sigma^2 \mathbf{I}$ .

An experimental MIMO system with the three-element antennas considered here was fabricated by Konanur *et al* [80]. A collection of channel measurements for the three were obtained at 2.22 GHz for one tripole transmitting to another in an indoor scattering environment. The total number of channel measurements collected was 46 realizations of  $H$ . In order to use these measurements and compare them with the i.i.d. case, the measurements must be normalized to obtain equal SNR according to the following equation

$$\tilde{H} = \frac{1}{\alpha} H,$$

where  $\alpha$  is the root-mean-squared value of the fading path gains given by

$$\alpha^2 = \frac{1}{t^2} \mathbb{E}\{\text{Tr}[HH^\dagger]\}. \quad (4.2)$$

and  $H^\dagger$  is the conjugate-transpose of  $H$ . Note that in this setting, the number of transmit and receive antennas are equal, therefore we set  $t = r$ .

Using the V-BLAST algorithm, the data are demultiplexed into  $t$  substream for each transmit antenna, which assumed to use the same constellation. The output of the serial-to-parallel conversion is a vector  $\mathbf{b} = [b_{1,m}, \dots, b_{t,m}]$ , where  $b_{i,m}$  is the  $m$ -th symbol of the  $i$ -th substream. At the receiver, a ZF detector is implemented for the substream with maximum SNR. This first detected symbol is then subtracted from the received signal, and the process is repeated until all symbols are detected. This scheme is known as nulling and ordering. The ZF-algorithm is given as follows [79] :

*initialize : (for  $i \leq r$ )*

*$i = 1$*

*$D_i = H^+$*

$$\begin{aligned}
& \text{recursion :} \\
& k_i = \arg \min_j \| (D_i)_j \|^2 \\
& W_{k_i} = (D_i)_{k_i} \\
& y_{k_i} = W_{k_i}^T Y_i \\
& \hat{a}_{k_i} = Q(y_{k_i}) \\
& Y_{i+1} = Y_i - \hat{a}_{k_i} H_{k_i} \\
& D_{i+1} = H_{\bar{k}_i}^+ \\
& i = i + 1
\end{aligned} \tag{4.3}$$

where  $i$  denote the iteration index,  $(D_i)_{k_i}$  is the  $k_i$ -th row of  $D_i$  and the matrix  $H^+$  is the Moore-Penrose Pseudo-inverse of  $H$ . The matrix  $H_{\bar{k}_i}$  is obtained by zeroing columns  $k_1, \dots, k_i$  of  $H$ ,  $Y_i$  is the  $i$ -th column of  $Y$  and  $Q(\cdot)$  denotes the slicing operation which rounds to the nearest value in the signal constellation. (For BPSK,  $Q(y_{k_i}) = \text{sgn}[\text{Re}(y_{k_i})]$ .)

### 4.1.2 Simulation

In this simulation, we use the measured fading path gains obtained in [80] to calculate the performance of the V-BLAST system described in the previous section with tripoles at the transmitter and receiver. The channel measurements are normalized according to eq. 4.2. At the transmitter side, we assume BPSK modulation with the zero-forcing detector described in eq. 4.3 at the receiver.

In Fig. 4.1, the BER of the V-BLAST system calculated with empirically-measured path gains is compared to the theoretical BER of a V-BLAST system with i.i.d.  $\mathcal{CN}(0,1)$  fading path gains. Note that the empirically-measured system is within  $\pm 6$  dB of the theoretical system over the entire range of interest; moreover, the performance of the empirical system improves relative to the i.i.d. case as SNR

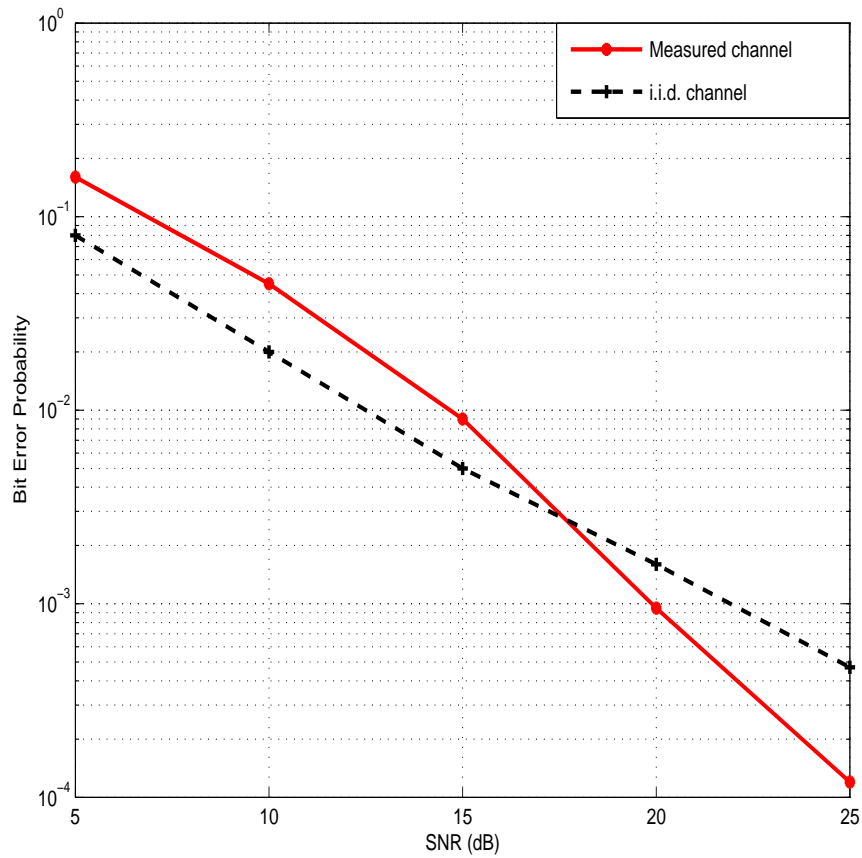


Figure 4.1: Measured and theoretical BER for a V-BLAST system with tripoles at the transmitter and receiver.

increases.

It is important to note that the small number of measurements (46) means that the variation of the BER about the mean plotted in Fig. 4.1 will be relatively large. This is illustrated by Fig. 4.2, where the BERs of the individual channel realizations are plotted together. In principle, these variations suggest that the performance differences observed in Fig. 4.1 may not be statistically significant, and that more measurements need to be collected. In the next section we will use the channel inversion technique [83] to resolve this problem.

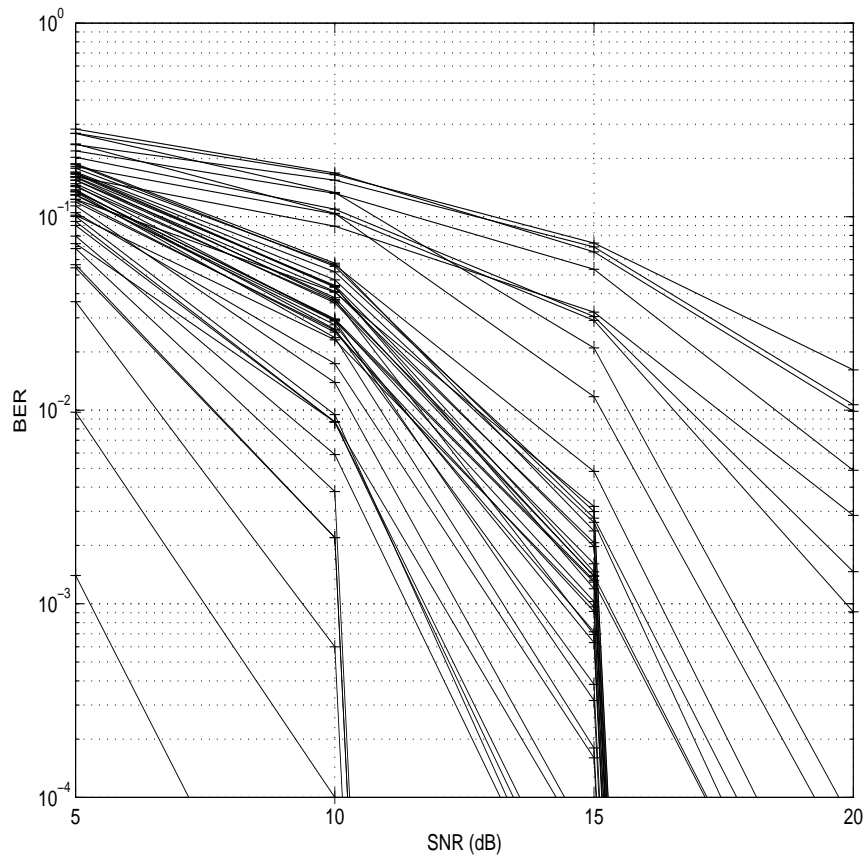


Figure 4.2: Measured BER for a V-BLAST system with tripoles at the transmitter and receiver for all 46 channel realizations.

## 4.2 Channel Inversion

The results of the previous section suggest that the statistical fluctuations of the BER of V-BLAST with empirically-measured channel data are quite large. This is due, in part, to the choice of a fixed data constellations which makes BER highly sensitive to variations in the channel. In this section, we consider an alternative adaptive transmission scheme which adapts the current fading conditions when channel state information (CSI) is available at the transmitter. We consider the channel inversion (CI) technique which invert the fading channels and attain a constant SNR at the receiver. Channel inversion is a simple scheme that use a fixed-rate modulation.

After channel inversion, the channel appears as time-invariant AWGN. The channel inversion for a fading channel and a single-antenna system was studied by Goldsmith *et al* [81]. Since channel inversion compensates for deep fade channel, this results in a capacity penalty. So, when diversity is combined with channel inversion [82] where  $t > r$ , capacity will increase. In [83], CI was studied for MIMO system with flat fading channel and extension to frequency selective channel is investigated by [84]. Most of previous work has considered uniform linear array for channel inversion. In this section we will investigate the impact of vector antenna on the performance of CI in flat fading environment. For antennas implemented at transmitter and receiver sides where ( $t > r$ ), the channel model is the same one given in eq. 4.1 and repeated here

$$Y = \sqrt{\gamma_t} H \mathbf{b} + N.$$

In CI, the channel is inverted by pre-processing of the data

$$\mathbf{b} = H^+ \mathbf{d}, \quad (4.4)$$

where  $H^+$  is the Moore-Penrose pseudo-inverse of  $H$  and  $\mathbf{d}$  is  $r \times 1$  data vector chosen from BPSK constellation transmitted for the i.i.d. Rayleigh fading channel, this scheme's expected transmitted power is given by [83]

$$\mathbb{E}[\mathbf{b}^\dagger \mathbf{b}] = \mathbb{E}[|\mathbf{d}_i|^2] \sum_{i=1}^r \left( \frac{1}{\lambda_i} \right) = \mathbb{E}[|\mathbf{d}_i|^2] \frac{r}{t-r} \quad (4.5)$$

where  $\mathbb{E}[|\mathbf{d}_i|^2]$  is the average power of data bit  $i$  and  $\lambda_i$  for  $i = 1, \dots, r$  are the eigenvalues of  $HH^\dagger$ . When CI is applied at the transmitter, the received signal is given by

$$Y = HH^+ \mathbf{d} + N = \mathbf{d} + N, \quad (4.6)$$

so, the channel is converted to an AWGN channel where the SNR on all channels are equal.

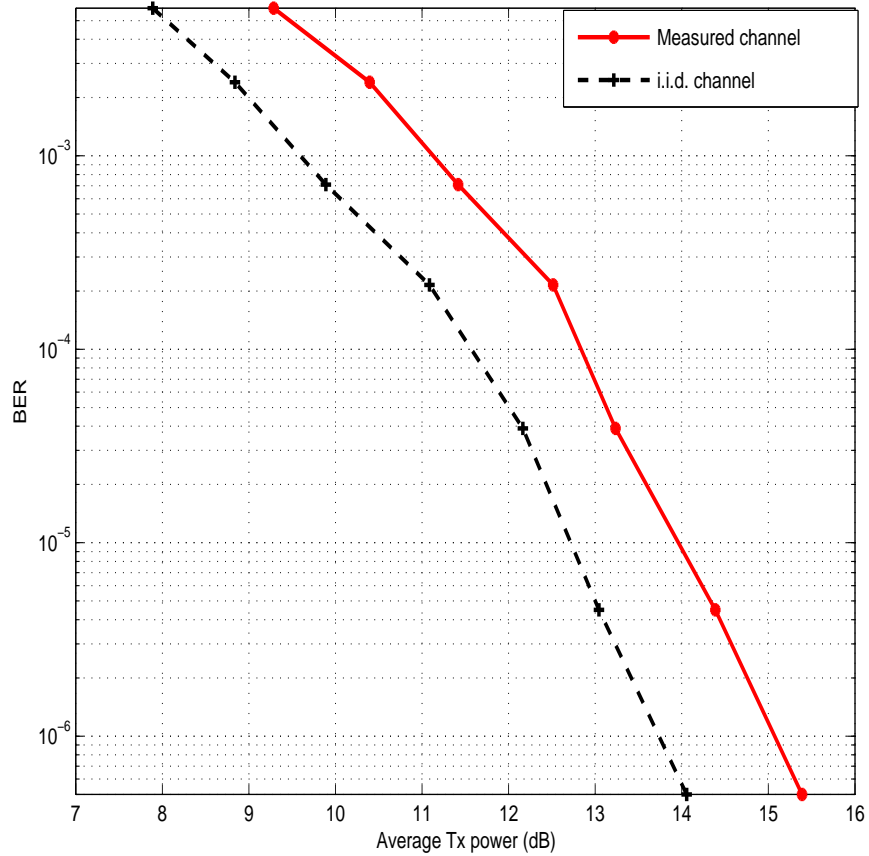


Figure 4.3: Measured and theoretical BER for a BPSK with channel Inversion (CI) for tripole at the transmitter and dual-polarized antenna at receiver.

#### 4.2.1 Simulation

We consider a MIMO system with a single tripole antenna at the transmitter and a dual polarized antenna at the receiver. Channel information is known at the transmitter, an CI is applied at the transmitter to the fading channel matrix  $H$ . Note that we choose  $t > r$  here, so that the expected transmit power in eq. 4.5 is finite. We use eq. 4.4 to invert the channel, then the received signal is given in eq. 4.6. In Fig. 4.3, the average transmitted power in eq. 4.5 is computed and plotted against the BER. Note that the empirically-measured system is within 1-1.5 dB from the i.i.d. channel system. The difference between the two channel systems is nearly 1.5

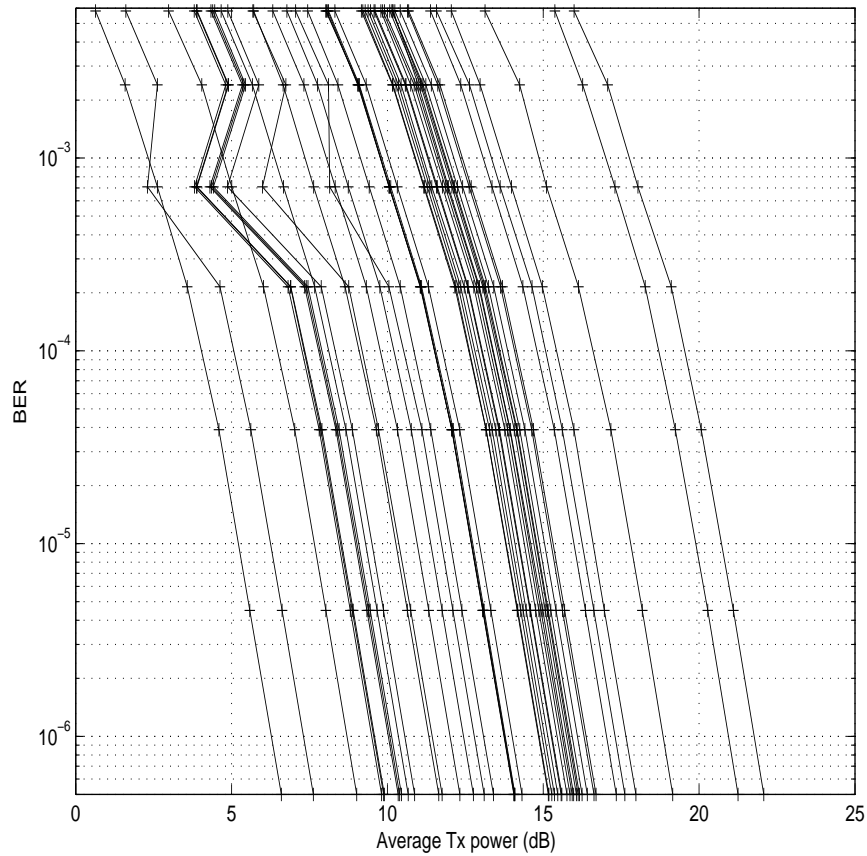


Figure 4.4: Measured and theoretical BER for a Channel Inversion (CI) for tripole at the transmitter and 2-element antenna at receiver.

dB over all the range of SNR. This is further illustrated in Fig. 4.4, where the BER plotted for all realizations are close to the mean plotted in Fig. 4.3. So, the channel inversion was able to compensate for deep fade channels and therefore we attain a stable performance difference in BER between the empirical and theoretical systems.

### 4.3 Conclusions

We have studied the performance of MIMO systems with tripole antennas at the transmitter and tripole or dual-polarized antennas at the receiver. For this system, we have consider the performance of two MIMO transmission algorithms: V-BLAST

and adaptive channel inversion. For both transmission schemes we have evaluated the performance using the empirically-measured fading path gains obtained by Konanur *et al* [80] and, for comparison, the performance predicted by the i.i.d. Rayleigh fading model. For V-BLAST, we find that the empirically-measured system is within  $\pm 6$  dB over the theoretical system over the entire range of interest. While for channel inversion, we find that the empirically-measured system is within 1.5 dB from the theoretical system over the range of SNR. Note that the performance estimates in both cases are based on a small number of channel measurements.

## Chapter 5

# SINR Limitations of Vector Antenna Arrays

In this chapter, we derive the signal-to-interference-plus-noise ratio (SINR) for vector antenna arrays. We consider one user and one interference at the receiver in a frequency-flat Rayleigh fading channel. This SINR expression is a function of the directions-of-arrival (DOAs) of the signal and interference and of the polarization of both signals. We further derive an expression for the beampattern of the vector antenna and compare it, for different DOAs and polarizations, with that of a uniform linear array.

## 5.1 Introduction

Beamforming techniques generally seek to combine the signals from multiple antennas in order to enhance the desired signal and suppress interference from other sources. In some conditions, the desired signal and interference may arrive from similar directions, in which case detection of the desired signal based on direction-of-arrival (DOA) only will yield poor results. In these cases, the desired signal may have a different polarization than the interference, in which case exploiting polarization as well as DOA may enhance the ability of the receiver to reduce the interference relative to the desired signal power.

In a uniform linear array (ULA), the antenna elements are usually dipoles which measure only one component of the electromagnetic field. Such elements do not provide all the information needed to separate signals on the basis of different polarizations. On the other hand, as proposed previously by Nehorai [50], vector antennas can sense multiple polarizations and results in [54] and [55] show that the vector antenna systems can determine DOA and separate signals which scalar arrays can not.

One way to evaluate the performance of beamforming at the receiver is the SINR criterion. The SINR is computed in terms of the parameters of the signal such as the weight vector, DOA and polarization. The derivation of the SINR expression was considered by Compton [85] for the case of a tripole antenna that consist of three mutually-orthogonal dipoles. The impact of polarization (e.g. linear v.s. circular) and direction-of-arrival on the performance of adaptive beamforming was investigated. In Compton's study, the SINR for one user and one interference was considered. Compton's results show that the SINR of the tripole depends on the DOA and polarization of the received signals. When the desired signal approaches linear polarization, the SINR is reduced. If the interference and desired signals have the same DOA and

polarization, SINR approaches is minimized. Other cases of low SINR occur when signals with the same polarization and opposite directions-of-arrival are detected at the receiver.

Nehorai *et al* [53] has studied the performance of the vector antennas that measure all six components of the electromagnetic field. In particular, he derived the minimum-noise-variance beamformer (MV) and an expression for SINR for a system with one user and one interference signal. The impact of the difference between the polarizations of the signals on the SINR of the MV beamformer was examined. These results showed that 6-element vector antennas can achieve a higher SINR than the tripole antenna regardless of the DOAs and polarizations of the received signals. Particularly poor performance occurs for the 6-element antenna when the polarization and the DOA are the same, while for the tripole antenna to have good performance, the polarization and DOA have to be distinct. Nehorai *et al* [53] has also compared the beampattern of vector antennas to that of a ULA. One of the main differences that was noted in [53], was that ULAs and uniform circular arrays (UCA) suffer from grating lobes where as many vector antennas, such as the tripole, do not have such lobes.

In this chapter, we extended the work of Nehorai on the beampatterns of vector antennas to the other types of antennas and flat-fading environments. Previous work has focused on deriving the SINR for one signal and one interference in a non-fading environment. To the best of our knowledge, the beampattern of vector antennas in fading environments has not yet been investigated.

## 5.2 Channel Model

We will consider the minimum-noise-variance beamformer for a vector antenna in a frequency-flat, Rayleigh fading channel. A two-user system is considered, such that one corresponds to the desired signal and other is an interference signal. The transmitted signal for the  $i$ -th user is a complex baseband signal of the form

$$S_i(t) = \sum_{m=1}^M b_i(m)p(t),$$

where  $b_i(m)$  is the sequence of data bits. The received signal is the superposition of both the desired and the interference signal given by

$$Y(t) = A_d \mathbf{G}_d S_d(t) + A_u \mathbf{G}_u S_u(t) + N(t),$$

where the subscripts  $d, u$  denote the desired and interference signal, respectively, and  $A_i$  is the amplitude of signal  $i$ . Here we assume that  $\mathbf{G}_i$  consists of the appropriate  $t_{em}$  ( $1 \leq t_{em} \leq 6$ ) components of  $B(\theta_i, \varphi_i) \mathbf{Z}_i$ , for  $i = d$  or  $u$ , and

$$B(\theta_i, \varphi_i) = \begin{bmatrix} -\sin \theta_i & \cos \theta_i \cos \varphi_i \\ \cos \theta_i & \sin \theta_i \cos \varphi_i \\ 0 & -\sin \varphi_i \\ \cos \theta_i \cos \varphi_i & \sin \theta_i \\ \sin \theta_i \cos \varphi_i & -\cos \theta_i \\ -\sin \varphi_i & 0 \end{bmatrix}$$

is the antenna response (eq. 2.1). The complex vector  $\mathbf{Z}_i$  reflects the change in amplitude, phase, and polarization experienced by the fading path component of the  $i$ -th user. The components of the vector  $\mathbf{Z}_i$  are modeled as i.i.d. zero-mean complex Gaussian random variables and therefore the elements of  $\mathbf{G}_i$  are also zero-mean complex Gaussian random variables. The noise  $N(t)$  is AWGN with mean zero and covariance  $\sigma^2 \mathbf{I}$ .

At the receiver, the output of the beamformer is given by the scalar

$$z_{mv}(t) = \mathbf{W}_d^\dagger Y(t),$$

where  $\mathbf{W}_d$  is the weight vector of the desired signal for the minimum-variance beamformer with a directional constraint given by [53]. This weight vector is the solution to the optimization program

$$\text{Minimize } \mathbf{W}_d^\dagger \mathbf{R}_{YY} \mathbf{W}_d \quad \text{Subject to } \mathbf{W}_d^\dagger \mathbf{G}_d = 1,$$

where the covariance matrix  $\mathbf{R}_{YY}$  is given by

$$\begin{aligned} \mathbf{R}_{YY} &= E\{YY^\dagger\} \\ &= P_d \mathbf{G}_d \mathbf{G}_d^\dagger + P_u \mathbf{G}_u \mathbf{G}_u^\dagger + \sigma^2 \mathbf{I}, \end{aligned}$$

$P_d$  and  $P_u$  are the desired and interference powers, respectively, and  $\sigma^2$  is the noise variance. The optimal solution to this program is given by [53]

$$\mathbf{W}_d = \frac{\mathbf{R}_{YY}^{-1} \mathbf{G}_d}{\mathbf{G}_d^\dagger \mathbf{R}_{YY}^{-1} \mathbf{G}_d}.$$

Proceeding as in [53], we can write the output SINR of MV beamformer as

$$\begin{aligned} SINR &= \frac{P_d \mathbf{W}_d^\dagger \mathbf{G}_d \mathbf{G}_d^\dagger \mathbf{W}_d}{\mathbf{W}_d^\dagger (\mathbf{R}_{YY} - P_d \mathbf{G}_d \mathbf{G}_d^\dagger) \mathbf{W}_d} \\ &= \frac{P_d \mathbf{W}_d^\dagger \mathbf{G}_d \mathbf{G}_d^\dagger \mathbf{W}_d}{\mathbf{W}_d^\dagger (P_u \mathbf{G}_u \mathbf{G}_u^\dagger + \sigma^2 \mathbf{I}) \mathbf{W}_d}. \end{aligned} \quad (5.1)$$

and proceeding as in [87] and [53], we can simplify the SINR expression as

$$\begin{aligned} SINR &= P_d \mathbf{G}_d^\dagger (P_u \mathbf{G}_u \mathbf{G}_u^\dagger + \sigma^2 \mathbf{I})^{-1} \mathbf{G}_d^\dagger \\ &= \gamma_d \left[ \mathbf{G}_d^\dagger \mathbf{G}_d - \frac{\gamma_u |\mathbf{G}_d^\dagger \mathbf{G}_u|^2}{1 + \gamma_u \mathbf{G}_u^\dagger \mathbf{G}_u} \right], \end{aligned} \quad (5.2)$$

where  $\gamma_d = \frac{P_d}{\sigma^2}$  and  $\gamma_u = \frac{P_u}{\sigma^2}$  are the signal-to-noise ratio (SNR) of the desired and interference signals respectively.

For the tripole antenna, we observe from eq. 5.2 that  $\mathbf{G}_d^\dagger \mathbf{G}_d = \mathbf{Z}_d^\dagger \mathbf{Z}_d$  and  $\mathbf{G}_u^\dagger \mathbf{G}_u = \mathbf{Z}_u^\dagger \mathbf{Z}_u$ , so the SINR reduces to

$$SINR_t = \gamma_d \left[ \mathbf{Z}_d^\dagger \mathbf{Z}_d - \frac{\gamma_u |\mathbf{G}_d^\dagger \mathbf{G}_u|^2}{1 + \gamma_u \mathbf{Z}_u^\dagger \mathbf{Z}_u} \right], \quad (5.3)$$

where the subscript  $t$  denote the tripole antenna.

For the six-element vector antenna, we observe from eq. 5.2 that  $\mathbf{G}_d^\dagger \mathbf{G}_d = 2 \mathbf{Z}_d^\dagger \mathbf{Z}_d$  and  $\mathbf{G}_u^\dagger \mathbf{G}_u = 2 \mathbf{Z}_u^\dagger \mathbf{Z}_u$ , so that SINR is

$$SINR_v = \gamma_d \left[ 2 \mathbf{Z}_d^\dagger \mathbf{Z}_d - \frac{\gamma_u |\mathbf{G}_d^\dagger \mathbf{G}_u|^2}{1 + 2 \gamma_u \mathbf{Z}_u^\dagger \mathbf{Z}_u} \right]. \quad (5.4)$$

where the subscript  $v$  denote the 6-element vector antenna.

### 5.3 Beampattern of Certain Vector Antennas

We now study the average beampattern of certain vector antennas when the antenna is steered toward the direction-of-arrival and the polarization of an incident plane wave. We also compare these beampatterns to those of uniform linear arrays (ULA) that respond to only one polarization component. As in [76, 53], we assume there is no noise or interference at the receiver. In [53], Nehorai derived the beampattern (i.e. the normalized response of the vector antenna for an incident plane wave with certain direction and polarization) for a single line-of-sight signal with no fading. For a single path, the beampattern can be written as

$$g_d = \mathbb{E} \left[ |\mathbf{G}_d^\dagger \mathbf{G}_u|^2 / (\mathbf{G}_d^\dagger \mathbf{G}_d) \right], \quad (5.5)$$

where  $\mathbf{G}_d = B(\theta_d, \varphi_d) \mathbf{Z}_d$  and  $\mathbf{G}_u = B(\theta_u, \varphi_u) \mathbf{Z}_d$  are the steering and incident directions, respectively. To simplify our analysis, we set the angles  $\theta_d, \theta_u \in [0, 2\pi]$  and  $\varphi_d = \varphi_u = \pi/2$  so the DOA is measured in terms of  $\theta = [0, 2\pi]$ . The maximum response results when  $\theta_d = \theta_u$ .

## 5.4 Numerical Results

We consider one desired user and one interference signal incident at the receiver. The desired signal and interference arrives with a random polarization state  $\mathbf{Z}_i$  due to multipath fading. In this section, we consider  $\mathbf{Z}_i$  to be i.i.d.  $\mathcal{CN}(0, \mathbf{\Sigma}_z)$  where

$$\mathbf{\Sigma}_z = \begin{bmatrix} \alpha^2 & 0 \\ 0 & 2 - \alpha^2 \end{bmatrix},$$

and  $\alpha$  is a parameter that controls the relative power of the horizontal and vertical components of  $\mathbf{Z}_i$ . In each of the plots below, the SNR of the desired signal is taken to be 0 dB and the SNR of the interference is set at 40 dB. In the following examples, we compare the performance of a different number of vector antenna elements, polarization states, and DOA. We plot the averaged SINR as a function of DOA and polarization. We focus primarily on two vector antennas: the 3-element tripole antenna and a 6-element vector antenna that senses all 6 components of the EM field. The DOA of the signals at the receiver are considered for two cases: The desired and interference signals have the same DOA but different polarizations, and the case when both signals arrive with different DOAs. These DOAs are taken arbitrary from the distribution of the elevation and azimuth angles  $\varphi, \phi$  respectively, as described in Section 3.3 in Chapter 3. In this simulation we plot eqs. 5.3-5.4.

In Fig. 5.1, we plot the expected SINR of the tripole, given in eq. 5.3, and the expected SINR of the 6-element vector antenna in eq. 5.4 as a function of the desired signal polarization  $0 \leq \alpha_d \leq 1$  for a nearly linearly polarized interference  $\alpha_u = 0.1$ . Two propagation conditions are considered: the worst-case scenario in which the desired signal and interference have the same DOAs (upper curves) and the case in which their DOAs are different and randomly chosen. Note that for all  $\alpha_d$  the 6-element antenna outperforms the tripole. Moreover, the performance difference is greatest when equal energy is contained in both the horizontal and vertical components ( $\alpha_d = 1$ ).

Not surprisingly, performance is worst when the desired and undesired signals have similar power in the horizontal and vertical components ( $\alpha_d = 0.1$ ). Note further that the desired signal polarization has a large impact on SINR (2-8 dB).

In Fig. 5.2, we plot the same four curves as in Fig. 5.1, except the interference now has equal power in both the horizontal and vertical polarizations ( $\alpha_u = 1$ ). Once again, the 6-element antenna outperforms the tripole and performance is best for  $\alpha_d = 1$  and worst for  $\alpha_d = 0$ . Note, however, that the impact of  $\alpha_d$  on the SINR is much smaller than in Fig. 5.1 ( $< 2$  dB). This is due to the fact that here the interference has equal energy in both polarizations.

In Fig. 5.3, we again plot the same four curves, now as a function of the interference polarization  $\alpha_u$  for a fixed desired signal polarization of  $\alpha_d = 0.1$ . Once again, we see that SINR differences are greatest when  $\alpha_u$  is small (corresponding to a linearly polarized interference). Moreover, in all cases, performance is best when the interference has equal energy in the two polarizations.

In Fig. 5.4, we plot the same four curves as a function of when  $\alpha_u$  for  $\alpha_d = 1$ . Here the performance is almost independent of  $\alpha_u$  in each case.

In general, from these figures, we conclude that when the desired user has near linear polarization, the SINR is low and highly sensitive to the interference polarization  $\alpha_u$ . On the other hand, when  $\alpha_d = 1$ , the SINR is high and virtually independent of interference polarization.

Finally, in Fig. 5.5 we plot the expected beampattern of the 6-element vector antenna for no interference and  $\alpha_d = 0.1, 0.5, 1$ . This plot shows the beampattern of one path for a signal incident from direction  $(\theta_u, \varphi_u) = (0, \pi/2)$ , where the steering direction is taken to maximize the response of the incident signal. For comparison, the beampattern of a 6-element ULA is plotted in Fig. 5.6. Comparing the two figures, we see that the ULA is subject to many side lobes in comparison to the vector antenna,

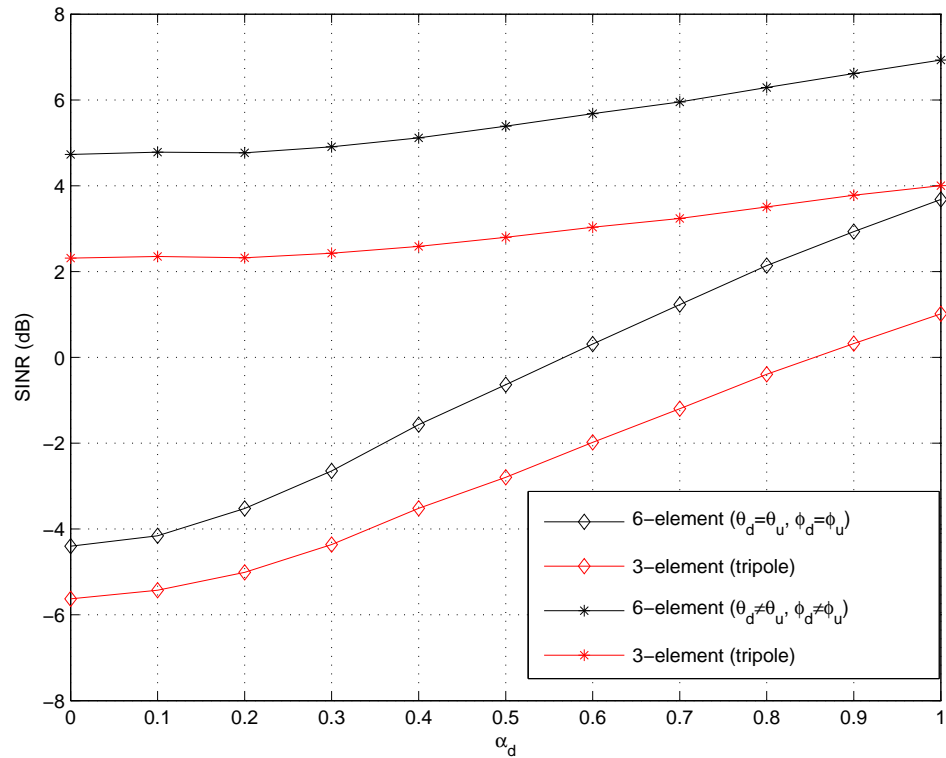


Figure 5.1: The expected SINR as a function of the desired signal polarization,  $0 \leq \alpha_d \leq 1$ , for a nearly linearly polarized interference ( $\alpha_u = 0.1$ ).

and so is less able to detect signals from certain directions.

## 5.5 Conclusions

We have considered the minimum-noise-variance beamforming technique for vector antennas and frequency-flat, Rayleigh fading channels. We considered one user and one interference signal at the receiver. An expression for the SINR was derived as a function of DOA and polarizations of desired signal and interference. Our simulations suggest that the 6-element vector antenna can better suppress interference than a 3-element antenna. Furthermore, when the desired signal has equal energy in both directions, the SINR is less sensitive to interference polarization. Finally, we plotted

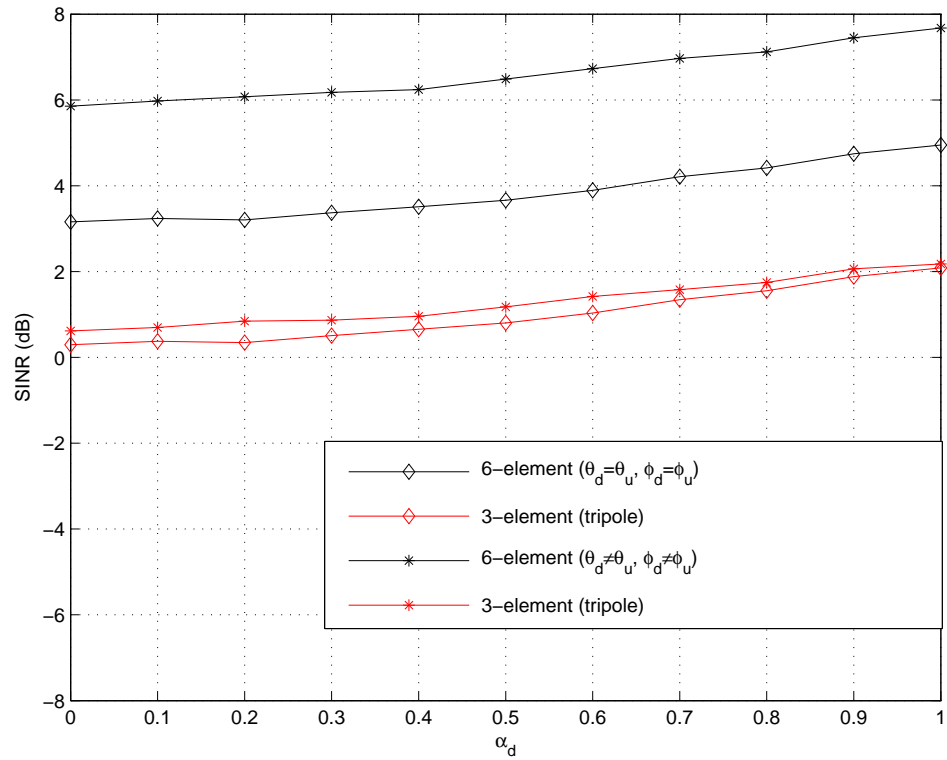


Figure 5.2: The expected SINR as a function of the desired signal polarization,  $0 \leq \alpha_d \leq 1$ , for an interference with equal energy in the horizontal and vertical polarizations ( $\alpha_u = 1$ ).

the beam pattern of a 6-element vector antenna and observed that it suffers from fewer lobes than a conventional ULA.

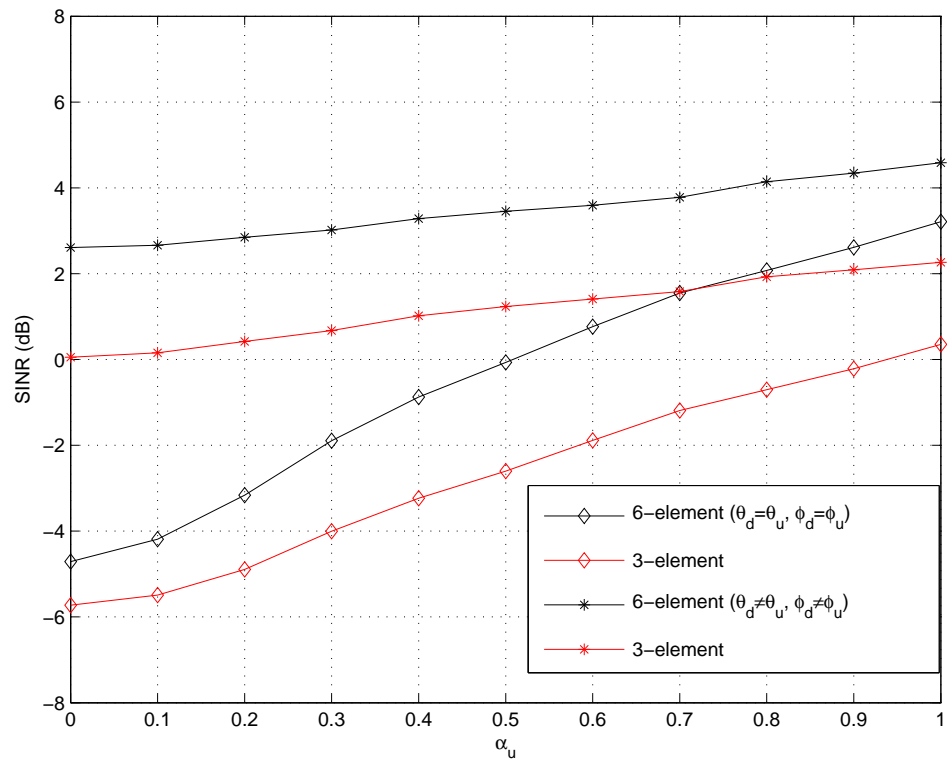


Figure 5.3: The expected SINR as a function of the interference signal polarization,  $0 \leq \alpha_u \leq 1$ , for a nearly linearly polarized desired signal ( $\alpha_d = 0.1$ )

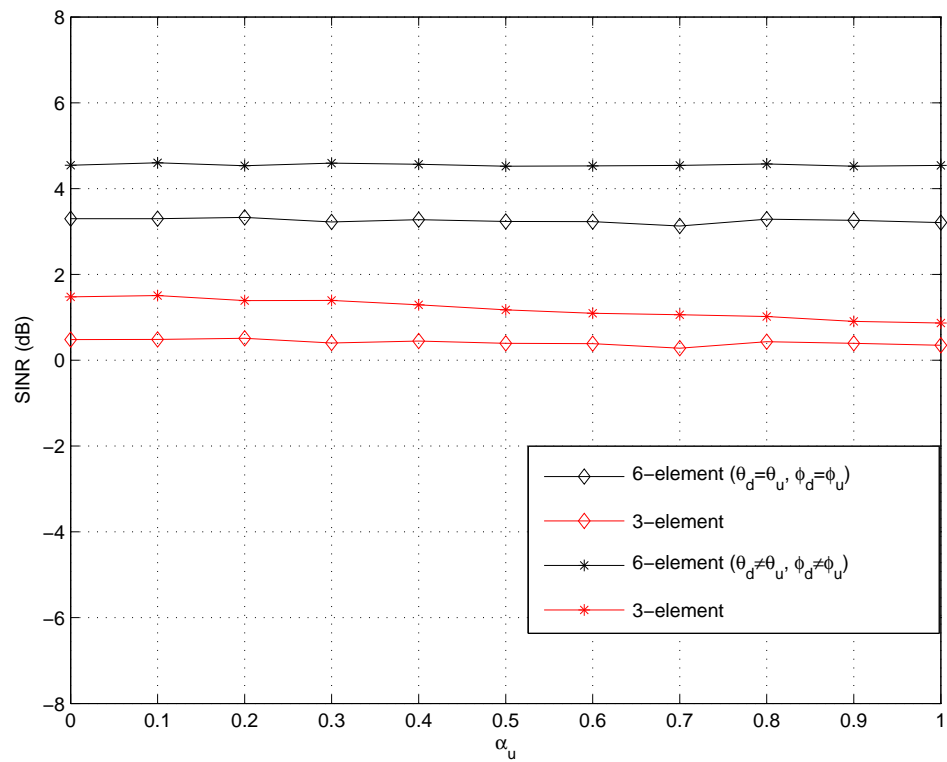


Figure 5.4: The expected SINR as a function of the interference signal polarization,  $0 \leq \alpha_u \leq 1$ , for an desired signal with equal energy in the horizontal and vertical polarizations ( $\alpha_d = 1$ ).

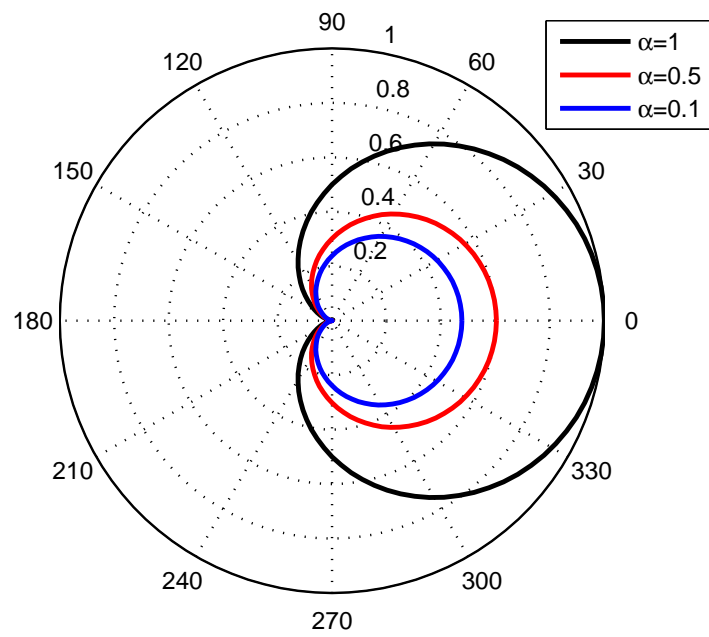


Figure 5.5: Beampattern of the 6-element vector antenna

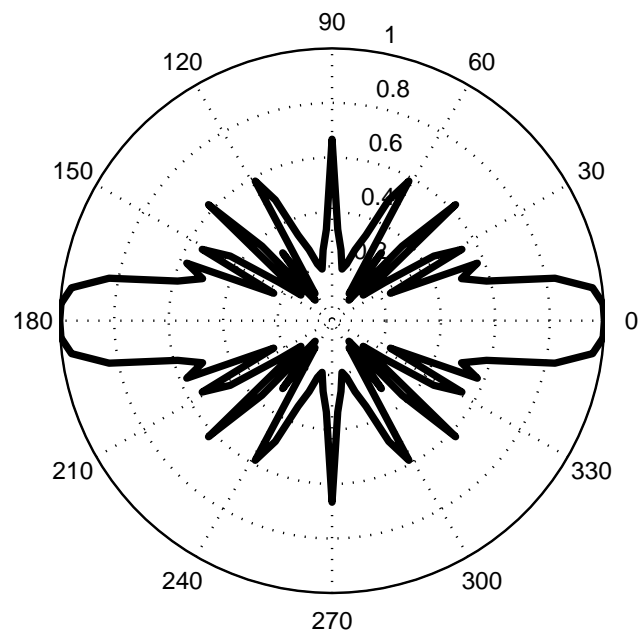


Figure 5.6: Beampattern of the 6-element ULA with spacing  $d = \lambda/2$

## Chapter 6

### Conclusions

In this dissertation we have studied the implementation of vector antennas for CDMA signals in presence of multipath signal propagation. We emphasized on developing vector antenna receivers for single-user and multiuser scenario in frequency-selective Rayleigh fading channel. The vector antenna receivers were compared to uniform linear array (ULA) system having same number of antenna elements.

First we derived a space-time model that describes multipath propagation for single-user system, direct-sequence code-division multiple-access (DS-CDMA). Using this model, we derived maximal-likelihood (ML), minimum mean-square error (MMSE), decorrelator (DD) and matched filter (MF) receivers. The performance of these receivers are measured in terms of BER as a function of SNR. The simulation results show that for fixed number of multipaths and antenna elements, the vector antenna gain in diversity. This diversity gain was illustrated when comparing the tripole antenna which consist of three mutually-orthogonal dipoles and the dual-polarized antenna. The tripole antenna shows a considerable diversity gain than the dual-polarized antenna for fixed number of multipaths. The 6-element vector antenna gain more diversity than the tripole antenna. Furthermore, the tripole antenna

outperforms the two dipole and loop by 0.5-1 dB.

Next, we considered the design of space-time receivers for multiuser system in multipath fading environment. We derived the space-time MMSE, ST-DD and adaptive MMSE. Both the ST-MMSE and ST-DD were able to exploit multipath and gain diversity. We further compared the ST-MMSE for tripole and 3-element ULA. The tripole shows a significant diversity gain for fixed number of multipaths over the ULA. This suggest that the vector antenna responding to the horizontal and linear polarization enabled it to exploit the multipath environment while the ULA respond to only one polarization. We then consider  $M$ -ary orthogonal modulation for data transmission at the mobile and beamformer-RAKE implemented at the base station. Comparing between vector antennas and ULA, the number of users that vector antenna can accommodate is higher than the ULA at given SNR. Then we investigate the impact of polarization for tripole antenna. The parameter  $\alpha$  is set to control the power on the vertical and horizontal polarizations. For near linearly polarization, the tripole antenna accommodate less user than the case of using both polarization components.

For MIMO system, vector antennas are considered for empirically-measured and i.i.d. channel system. We considered the tripole antenna deployed at the transmitter and tripole or dual-polarized antenna at the receiver. Two MIMO schemes are considered: The V-Blast and channel inversion. The BER as function of SNR of the V-BLAST shows that the i.i.d. channel is within  $\pm 6$  dB from the empirical-measurements. For high SNR the empirical-measurements improves over the i.i.d. case. For channel inversion, the difference between the two channel system are within 1.5 dB.

Finally, the derivation of SINR for MV beamforming was considered for different number of vector antenna assuming one desired user and one interference in flat fading

channel. The beampattern for vector antennas as a function of SINR shows that the 6-elements outperform the tripole antenna system. Then we compare the beampattern for 6-element vector antennas and 6-elements ULA. The ULA have many lobes than the vector antenna.

# Bibliography

- [1] J. G. Proakis, *Digital Communications*. 4th ed. New York: McGraw-Hill, 2000.
- [2] Malcom W. Oliphant, "The mobile phone meets the Internet," *IEEE Spectrum*, vol. 36, no. 8, pp. 20-28, Aug. 1999.
- [3] F. G. MacWilliams and N. Sloane, "Pseudo-random sequences and arrays," *Proc. IEEE*, vol. 64, no. 12, pp. 1715-1729, Dec. 1976.
- [4] R. Gold, "Optimal binary sequences for spread spectrum multiplexing," *IEEE Trans. Inform. Theory*, vol. 13, no 4, pp. 619-621, Oct. 1967.
- [5] E. Geraniotis and M. B. Pursley, "Performance of coherent direct-sequence spread-spectrum communications over specular multipath fading channels," *IEEE Trans. Commun.*, vol. 33, pp. 502-508, June 1985.
- [6] H. Xiang, "Binary code-division multiple-access systems operating in multipath fading, noisy channels," *IEEE Trans. Commun.*, vol. 33, no. 1, pp. 775-784, Aug. 1985.
- [7] V. M. Bogachev and I. G. Kiselev, "Optimum combining of signals in space-diversity reception," *Telecommun. Radio Eng.*, vol. 34-35, pp. 83-85, Oct. 1980.
- [8] J. H. Winters, "Optimum combining in digital mobile radio with co-channel interference," *IEEE Trans. Veh. Technol.*, vol. 33, pp. 144-155, Aug. 1984.

- [9] Z. Zvonar and D. Brady, "Suboptimal multiuser detector for frequency-selective Rayleigh fading synchronous CDMA channels," *IEEE Trans. Commun.*, vol. 43, no. 2, pp. 154-157, Feb. 1995.
- [10] H. L. Van Trees, *Detection, Estimation and Modulation Theory*. vol. 1, New York, NY: John Wiley and Sons, 1969.
- [11] R. O. Schmidt, "A signal subspace approach to multiple emitter location and spectral estimation." PhD thesis, Department of Electrical Engineering, Stanford University, Stanford, CA, Nov. 1981.
- [12] B. Ottersten and M. Viberg, "Analysis of subspace fitting based methods for sensor array processing," in *Proc. ICASSP'89*, vol. 4, pp. 2807-2810, May 1989.
- [13] M. Viberg and B. Ottersten, "Sensor array processing based on subspace fitting," *IEEE Trans. Acoustics, Speech and Signal Processing*, vol. 39, no. 5, pp. 1110-1121, May 1991.
- [14] M. Viberg, B. Ottersten and T. Kailath, "Detection and estimation in sensor arrays using weighted subspace fitting," *IEEE Trans. Signal Processing*, vol. 39, pp. 2436-2449, Nov. 1991.
- [15] A. Klouche-Djedid and M. Fujita, "Adaptive array sensor processing applications for mobile telephone communications," *IEEE Trans. Veh. Tech.*, vol. 45, no. 3, pp. 405-416, Aug. 1996.
- [16] B. Widrow, P. E. Mantey, L. J. Griffiths and B. B. Goode, "Adaptive antenna systems," *IEEE Proceedings*, vol. 55, no. 12, pp. 2143-2159, Dec. 1967.
- [17] W. A. Gardner, "Comments on convergence analysis of LMS filters with uncorre-

- lated data,” *IEEE Trans. Acoustics, Speech and Signal Processing*, vol. 34, no. 2, pp. 378-379, Apr. 1986.
- [18] J. B. Foley and F. M. Boland, “A note on the convergence analysis of LMS adaptive filters with Gaussian data,” *IEEE Trans. Acoustics, Speech and Signal Processing*, vol. 36, pp. 1087-1089, Jul. 1988.
- [19] V. Solo, “The limiting behavior of LMS,” *IEEE Trans. Acoustics, Speech and Signal Processing*, vol. 37, no. 7, pp. 1909-1922, Dec. 1989.
- [20] A. Feuer and E. Weinstein, “Convergence analysis of LMS filters with uncorrelated Gaussian data,” *IEEE Trans. Acoust., Speech, Signal Processing*, vol. 33, no. 1, pp. 222-230, Feb. 1985.
- [21] O. L. Frost, III, “An algorithm for linearly constrained adaptive array processing,” *IEEE Proc.*, vol. 60, no. 8, pp. 926-935, Aug. 1972.
- [22] V. Weerackody, “Diversity of the direct-sequence spread spectrum system using multiple transmit antennas,” *Proc. ICC'93*, vol. 3, pp. 1775-1779, Geneva, Switzerland, May 1993.
- [23] P. Balaban and J. Salz, “Optimum diversity combining and equalization in digital data transmission with applications to cellular mobile radio-part I:Theoretical considerations,” *IEEE Trans. Commun.*, vol. 40, no. 5, pp. 885-894, May 1992.
- [24] J. H. Winters, J. Saltz and R. Gitlin, “The capacity of wireless communication systems can be substantially increased by the use of antenna diversity,” in *Proc. Conf. on Information Science and Systems*, vol. 2, Princeton, NJ, pp. 853-858, Mar. 1992.

- [25] R. Y. Chen and C. L. Wang, "On the optimum step size for the adaptive sign and LMS algorithms," *IEEE Trans. Circuits and Systems*, vol. 37, no. 6, pp. 836-840, June 1990.
- [26] R. Nitzberg, "Application of the normalized LMS algorithm to MSLC," *IEEE Trans. Aerospace and Electronic Systems*, vol. 21, pp. 79-91, Jan. 1985.
- [27] N. J. Bershad, "Analysis of the normalized LMS algorithm with Gaussian inputs," *IEEE Trans. Acoustics, Speech and Signal Processing*, vol. 34, no. 4, pp. 793-806, Aug. 1986.
- [28] J. Fernandez, I. R. Corden and M. Barrett, "Adaptive array algorithms for optimal combining in digital mobile communication systems," in *the Proc. 8th Int. Conf. Antennas and Propagation*, vol. 2, pp. 983-986, Edinburgh, Scotland, Apr. 1993.
- [29] Y. Wang and J. R. Cruz, "Adaptive antenna arrays for the reverse link of CDMA cellular communication systems," *Electronics Letters*, vol. 30, no. 13, pp. 1017-1018, June 1994.
- [30] L. C. Andrews, *Special Functions of Mathematics for Engineering*. 2nd ed. New York: McGraw-Hill, 1992.
- [31] G. Raleigh, S. N. Diggavi, A. F. Naguib and A. Paulraj, "Characterization of fast fading vector channels for multi-antenna communication systems," in *Proc. 28th Asilomar Conference on Signals, Systems and Computers*, vol. 2, Pacific Grove, CA, pp. 853-857, Nov. 1994.
- [32] Q. Spencer, M. Rice, B. Jeffs and M. Jensen, "A statistical model for angle of arrival in indoor multipath propagation," in *Proc. IEEE Veh. Tech. Conference*, vol. 3, pp. 1415-1419, May 1997.

- [33] Q. Spencer, M. Rice, B. Jeffs and M. Jensen, "Indoor wideband time/angle of arrival multipath propagation results," in *Proc. IEEE Veh. Tech. Conference*, vol. 3, pp. 1410-1414, May 1997.
- [34] B. Suard, A. F. Naguib, G. Xu and A. Paulraj, "Performance analysis of CDMA mobile communication systems using antenna arrays," in *Proc. Acoustic, Speech and Signal Processing, ICASSP'93*, vol. 4, pp. 153-156, Apr. 1993.
- [35] A. F. Naguib, A. Paulraj and T. Kailath, "Capacity improvement with base-station antenna arrays in cellular CDMA," *IEEE Trans. Veh. Tech.*, vol. 43, no. 3, pp. 691-698, Aug. 1994.
- [36] A. F. Naguib and A. Paulraj, "Performance of CDMA cellular networks with base-station antenna arrays," in *Proc. International Zurich Seminar on Digital Communications*, Zurich, Switzerland, vol. 783, pp. 87-100, Mar. 1994.
- [37] I. E. Telatar, "Capacity of multi-antenna Gaussian channels," *Europ. Tran. Telecommun.*, vol. 10, no. 6, pp. 585-595, Dec. 1999.
- [38] P. C. F. Eggers, J. Toftgaard and A. M. Oprea, "Antennas systems for base station diversity in urban small and micro cells," *IEEE J. Sel. Areas. Commun.*, vol. 11, no. 7, pp. 1046-1057, Sep. 1983.
- [39] R. G. Vaughan, "Polarization diversity in mobile communications," *IEEE Trans. Veh. Technol.*, vol. 39, no. 3, pp. 177-186, Aug. 1990.
- [40] R. U. Nabar, H. Boelcskei, V. Erceg, D. Gesbert and A. J. Paulraj, "Performance of multiantenna signaling techniques in the presence of polarization diversity," *IEEE Trans. Signal Proc.*, vol. 50, no. 10, pp. 2553-2562, Oct. 2002.

- [41] M. R. Andrews, P. P. Mitra and R. deCarvalho, "Tripling the capacity of wireless communications using electromagnetic polarization," *Nature*, vol. 409, no. 6818, pp. 316-318, Jan. 2001.
- [42] A. Konanur, K. Gosalia, S. Krishnamurthy, B. L. Hughes and G. Lazzi, "Investigation of the performance of co-polarized, co-located electric and magnetic dipoles for increasing channel capacity," *IEEE International Symposium on Antennas and Propagation*, vol. 2, pp. 531-534, June 2003.
- [43] R. Price and P. E. Green, "A communication technique for multipath channels," in *Proc. IRE.*, vol. 46, pp. 555-570, Mar. 1958.
- [44] G. L. Turin, "Introduction to spread-spectrum anti-multipath techniques and their application to urban digital radio," *Proc. of the IEEE.*, vol. 68, no. 3, pp. 328-353, Mar. 1980.
- [45] T. P. Krauss, M. D. Zoltowski and G. Leus, "Simple MMSE equalizers for CDMA downlink to restore chip sequence: comparison to zero-forcing and RAKE," *Proc. Acoustics, Speech and Signal Processing (ICASSP '2000)*, vol. 5, pp. 2865-2868, Jun. 2000.
- [46] N. S. Correal and B. D. Woerner, "Evaluation of dual spatial and polarization diversity reception for DS-CDMA multiuser detection," *IEEE International Conference on Universal Personal Communications*, vol. 2, pp. 789-793, Oct. 1998.
- [47] A. F. Naguib, "Adaptive Antennas for CDMA Wireless Networks." PhD thesis, Department of Electrical Engineering, Stanford University, Stanford, CA, Aug. 1996.
- [48] G. D. Forney, "The Viterbi algorithm," *Proc. IEEE*, vol. 61, pp.268-278, Mar. 1973

- [49] R. C. Dixon, *Spread spectrum systems*. New York: Wiley, 1976.
- [50] A. Nehorai and E. Paldi, "Vector-sensor array processing for electromagnetic source localization," *IEEE Trans. Signal Proc.*, vol. 42, no. 2, pp. 376-398, Feb. 1994.
- [51] A. F. Naguib, "Space-time receivers for CDMA multipath signals," *ICC 97 Montreal*, vol. 1, pp. 304-308, June 1997.
- [52] G. Hatke, "Performance analysis of the superCART antenna array," MIT Lincoln Lab, Lexington, MA, Project Rep. AST-22, Mar. 1992.
- [53] A. Nehorai, K. C. Ho and B. Tan, "Minimum-noise-variance beamformer with an electromagnetic vector sensor," *IEEE Trans Signal Proc.*, vol. 47, no. 3, pp. 601-618, Mar. 1999.
- [54] K. C. Ho, K. C. Tan and W. Ser, "An investigation on number of signals whose directions-of-arrival are uniquely determinable with an electromagnetic vector sensor," *Signal Process.*, vol. 47, no. 1, pp. 41-54, Nov. 1995.
- [55] B. T. G. Tan, K. C. Ho and A. Nehorai, "Linear independence of steering vectors of an electromagnetic vector sensor," *IEEE Trans Signal Proc.*, vol. 44, no. 12, pp. 3009-3107, Dec. 1996.
- [56] S. Verdu, *Multuser Detection*. Cambridge, MA: Cambridge University Press, 1988.
- [57] C. B. Papadias and H. Huang, "Linear space time multiuser detection for multipath CDMA channels," *IEEE J. Sel. Areas Commun.*, vol. 19, no. 2, pp. 254-265, Feb. 2001.

- [58] M. Latva-Aho and M. Juntti, "Modified adaptive LMMSE receiver for DS-CDMA systems in fading channels," in *Proc. IEEE Int. Symp. Personal, Indoor and Mobile Radio Communication.*, Helsinki, Finland, vol. 2, pp. 554-558, Sept. 1997.
- [59] M. Latva-Aho, "LMMSE Detection for DS-CDMA systems in fading channels" *IEEE Trans. on Commun.* vol. 48, no. 2, pp. 194-199, Feb. 2000.
- [60] A. F. Naguib and A. Paulraj, "Performance of wireless CDMA with M-ary orthogonal modulation and cell site antenna arrays," *IEEE J. Sel. Areas Commun.*, vol. 14, no. 9, pp. 1770-1783, Dec 1996.
- [61] U. M. Honig and M. L. Honig, "MMSE interference suppression for direct sequence spread-spectrum CDMA," *IEEE Trans. Commun.*, vol. 42, pp. 3178-3188, Dec. 1994.
- [62] L. M. A. Jalloul and M. Holtzman, "Performance analysis of DS/CDMA with noncoherent M-ary orthogonal modulation in multipath fading channels," *IEEE J. Sel. Areas Commun.*, vol. 12, no. 5, pp. 826-870, Sept. 1994.
- [63] D. J. Torrieri, "Performance of direct-sequence systems with long pseudonoise sequences," *IEEE J. Sel. Areas Commun.*, vol. 10, no. 4, pp. 770-781, May 1992.
- [64] M. D. Zoltowski and J. Ramos, "Blind adaptive beamforming for CDMA based PCS/cellular," *Proc. 29th Asilomar Conference on Signals, Systems and Computers*, Pacific Grove, CA, vol. 1, pp. 378-382, Oct. 1995.
- [65] S. Kandala, E. S. Sousa and S. Pasupathy, "Multi-user multi-sensor detectors for CDMA networks," *IEEE Trans. Commun.*, vol. 43 , no. 234, pp. 946-957, Apr. 1995.

- [66] S. Y. Miller and S. C. Schwartz, "Integrated spatial-temporal detectors for asynchronous Gaussian multiple-access channels," *IEEE Trans. Commun.*, vol. 43, no. 234, pp. 396-411, Apr. 1995.
- [67] M. Nagatsuka and R. Kohno, "A spatially and temporally optimal multiuser receiver using an array antenna for DS/CDMA," *IEICE Trans. Commun.*, vol. E78-B, no. 11, pp. 1489-1497, Nov. 1995.
- [68] M. Latva-Aho, "Advanced receivers for wideband CDMA systems." PhD thesis, Department of Electrical Engineering, University Of Oulu, Oulu, Finland, 1998.
- [69] S. Kandala, E. S. Sousa and S. Pasupathy, "Decorrelators for multi-sensor systems in CDMA networks," *European Trans. Telecommun.*, vol. 6, no. 1, pp. 29-40, Feb. 1995.
- [70] U. Madhow and M. L. Honig, "MMSE interference suppression for direct-sequence spread-spectrum CDMA," *IEEE Trans. Commun.*, vol. 42, no. 12, pp. 3178-3188, Dec. 1994.
- [71] X. Wang and H. V. Poor, "Space-time multiuser detection in multipath CDMA channels," *IEEE Trans. Signal Process.*, vol. 47, no. 9, pp. 2356-2374, Sept. 1999.
- [72] S. Krishnamurthy, "Fundamental Limits and Joint Design of Wireless Systems with Vector Antennas." PhD thesis, Department of Electrical Engineering, North Carolina State University, Raleigh, NC, Aug. 2005.
- [73] M. Al-Naser and B. L. Hughes, "Polarimetric vector receivers for CDMA multipath signals," *Proc. of CISS*, Princeton, NJ, pp. 1004-1009, Mar. 2004.
- [74] S. Haykin, Ed., *Adaptive Filter Theory*, 3rd ed. EnglewoodCliffs, NJ: Prentice-Hall, 1996.

- [75] G. A. Deschamps, "Geometrical representation of the polarization of a plane electromagnetic wave," *Proc. IEEE*, vol. 55, pp. 2143-2159, Dec. 1967.
- [76] R. A. Monzingo and T. W. Miller, *Introduction to adaptive arrays*. New York: Wiley, 1980.
- [77] G.J. Foschini, "Layered space-time architecture for wireless communication in a fading environment when using multiple antennas," *Bell Lab Tech. J.*, vol. 1, no. 2, pp. 41-59, Aug. 1996.
- [78] G.J. Foschini and M. J. Gans, "On limits of wireless communications in a fading environment when using multiple antennas," *Wireless Personal Commun.*, vol. 6, no. 3, pp. 311-335, Mar 1998.
- [79] P. W. Wolniansky, G. J. Foschini, G. D. Golden and R. A. Valenzuela, "V-BLAST: an architecture for realizing very high data rates over the rich scattering wireless channel," *Proc. IEEE ISSSE'98*, Pisa, Italy, pp. 295-300, Sept. 1998
- [80] A. Konanur, K. Gosalia, S. Krishnamurthy, B. L. Hughes and G. Lazzi, "Increasing MIMO channel capacity through colocated, copolarized antennas," *IEEE Trans. Microwave Theory and Tech.*, vol. 53, no. 6, pp. 1837-1844, Jun. 2005.
- [81] A. J. Goldsmith and P. P. Varaiya, "Capacity of fading channels with channel side information," *IEEE Trans. Inform. Theory*, vol. 43, no. 6, pp. 1986-1997, Nov. 1997.
- [82] M. S. Alouini and A. J. Goldsmith, "Capacity of Rayleigh fading channels under different adaptive transmission and diversity combining techniques," *IEEE Trans. on Vehicular Technology.*, vol. 48, no. 4, pp. 1165-1181, Jul. 1999.

- [83] V. Jungnickel, T. Haustein, E. Jorswieck, C. Von Helmolt, "On linear pre-processing in multi-antenna systems," *Proc. IEEE Global Telecommunications Conference*, vol. 1, pp. 17-21, Nov. 2002.
- [84] A. Scaglione, P. Stoica, S. Barbarossa, G. B. Giannakis and H. Sampath, "Optimal designs for space-time linear precoders and decoders," *IEEE Trans. on Signal processing*, vol. 50, pp. 1051-1064, May 2002.
- [85] R. T. Compton, Jr., "The tripole antenna: An adaptive array with full polarization flexibility," *IEEE Trans. Antennas Propagat.*, vol. 29, pp. 944-952, Nov. 1981.
- [86] G. H. Golub and C.F.V. Loan, *Matrix Computations*. 2nd ed., Baltimore and London: The John Hopkins University Press, 1989.
- [87] H. Cox, "Resolving power and sensitivity to mismatch of optimum array processes," *J. Acoustical Society of America*, vol. 54, pp. 771-785, Feb. 1973.